MICROFLUIDIC GENERATION OF BIOMATERIAL GRADIENTS FOR CONTROL OF NEURITE OUTGROWTH

By

HARINI SUNDARARAGHAVAN

A Dissertation submitted to the

Graduate School-New Brunswick

Rutgers, The State University and

The Graduate School of Biomedical Sciences

University of Medicine and Dentistry of New Jersey

In partial fulfillment of the requirements

for the degree of

Doctor of Philosophy

Graduate Program in the Department of Biomedical Engineering

Written under the direction of

David Shreiber

and approved by

_____

_____

_____

_____

New Brunswick, New Jersey
October 2008

ABSTRACT OF THE DISSERTATION

MICROFLUIDIC GENERATION OF BIOMATERIAL GRADIENTS FOR CONTROL OF NEURITE OUTGROWTH

By HARINI SUNDARARAGHAVAN

Dissertation Director:

David Shreiber

Abstract

Enhancing and directing axon regeneration through an injury site represents a prime goal for therapies following nerve or spinal cord injury. The objective of this thesis is to develop a system to create durotactic and haptotactic gradients with a biomaterial scaffold for control of neural cell behavior. Gradients of mechanical properties and adhesion are generated in a 3D collagen gel using microfluidics. To spatially control the mechanical properties, gradients of genipin - a naturally occurring, cell-tolerated crosslinking agent - are created in 3D through a fibrillar collagen gel using a simple source-sink network. Durotactic gradients of mechanical properties are evaluated by measuring genipin-induced fluorescence, which we demonstrated can be correlated to the rheological properties of the collagen gel. Neurite growth from chick dorsal root ganglia was assayed in gradients and appropriate controls. Neurite growth was biased down a gradient of stiffness of ~60Pa/mm towards a more compliant region, and neurites were significantly longer in this direction than up the gradient and than in uniform conditions

without crosslinking. Haptotactic gradients are generated by first grafting laminin derived peptides, IKVAV and YIGSR, onto the collagen backbone using 1-ethyl-3-(3-Dimethylaminopropyl) carbodiimide (EDC). Peptide-grafted collagen solutions are mixed with untreated collagen in the network Neurite outgrowth was enhanced in all laminin peptide-grafted collagen gradient conditions compared to the untreated collagen controls. Neurite growth was more responsive to gradients of YIGSR than IKVAV. Enhanced growth was observed in all YIGSR-grafted conditions with the greatest bias in the steepest gradient of (24.7 μg/ml/mm). Enhanced growth was also observed in IKVAV-grafted collagen conditions, but stunted growth occurred in collagen with uniform IKVAV presentation, implying IKVAV may be too 'sticky' for neurite outgrowth at the highest concentration studied. Since both peptides are present on the whole-length laminin molecule, the results suggest that gradients of laminin would be sub-optimal because of the contradiction in the response to the two peptides. These results demonstrate that neurite growth can be enhanced and directed by durotactic and haptotactic gradients, and suggest that including a combination of these gradients in regenerative therapies may accelerate nerve and spinal cord regeneration.

Dedication

To my parents – without your vision, dedication and support, I would never have gotten this far.

Acknowledgements

When I think about how I began my Ph.D. I know that the person I need to thank first is my advisor David Shreiber. When I came to Rutgers, I planned on getting a master's degree and moving on with my life. Without his support I probably would never have switched to the Ph.D. program and though there were definitely times when I thought I regretted that decision, in the end, I know that it was definitely the right choice. Next, I need to thank my co-advisor Bonnie Firestein. Presenting in Bonnie's lab was always helpful for a different perspective and a good time. I also need to thank my committee members: Troy Shinbrot, Noshir Langrana and Helen Buettner.

What made day-to-day graduate school more interesting and sometimes fun is definitely the people at Rutgers. The weird thing about the Shreiber lab is that fellow labmates were not just coworkers but also friends. Infact, my closest friends at Rutgers were my labmates: Jason Maikos, Haling Hao, Chris Gaughan and Gary Monteiro. The initial five of us spent countless happy hours together and even attended Jason's wedding; without friends like these I know graduate school would have been a lot harder. Newer additions to the group, Shirley Masand and Ian Gaudet, have helped make this last year less stressful by always being ready to hangout when I was overwhelmed with lab work and writing. I have to specially thank Gary for his steady support throughout my graduate studies - his encouragement allowed me to get through days when I didn't think I would ever finish.

One of the things that really got me through the years of graduate school was looking forward to trips across the US to see those that are closest to me. The trips I looked forward to the most (other than going home to see my family) were trips to see

my girlfriends. My friends from the University of Michigan (Crazychicas!) and I got together at least once a year for a ‘reunion’ that was always one of the best weekends of the year. Thanks Julie, Mandy, and Sarah for being the best friends a girl could ever hope for. I know you guys will always be there for me and this makes me feel like I can accomplish anything. I also need to thank my friends from high school: Robin, Cheryl, Sarah, and Jen for emails that made every day brighter. There is something really nice about knowing that I can write an email anytime and know that four people will be reading and responding within the hour.

Most importantly, I need to thank my parents, my sister Viji and my brother Vikram. My sister is my very best friend who is always just a phone call away and willing to fly out to see me several times a year. My brother made me work harder by competing with me in every aspect of life and although this has caused many arguments, this has also made both of us accomplish more. My dad is the one who is always on my side; since he is also a Ph.D. it sometimes feels like two against three in my family! My mom is definitely the best mom anyone could ever have; she is the only one who has read everything that I have ever written and I know she is looking forward to reading this thesis.

Table of Contents

Table of Figures

Table of Tables

Chapter 1: Introduction

Spinal cord injury (SCI) affects 253,000 people with 11,000 new injuries annually in the United States [1]. Until recently, SCI was thought to be a permanent, incurable condition. This idea was first challenged in 1980 by Richardson et al. [2], when they showed that neurons from the central nervous system (CNS) can re-grow if in the right environment. SCI is caused by a traumatic blow to the spinal cord and is characterized by damage to the white matter of the spinal cord and a disconnection in neuronal transmission. This leads to loss of motor and sensory function, the gravity of which depends on the location and severity of injury. After injury, a series of events occur that lead to further disruption of neuronal communication. The initial injury causes damage to neuronal cells and a break in the neuronal network. This cellular damage leads to many damaging events including release of excitatory amino acids, influx of cellular calcium, free radical formation and activation of immune response [3, 4]. The body's immune response causes further cell death, secondary tissue deterioration and leads to the formation of a glial scar surrounding the injury site, separating it from the surrounding healthy tissue [5]. This produces a physical and chemical barrier that neurons, even if healthy, cannot cross and therefore the injury cannot repair itself. In addition to glial scar formation, cells that compose the scar express neuron-inhibitory molecules and are known to release factors that hinder neurite growth [6, 7]. This is unlike the environment following peripheral nervous system (PNS) injury, where Schwann cells are known to be aligned, able to direct neurite outgrowth, and are able to express molecules that are favorable for neurite outgrowth [4]. Current studies in treating SCI investigate ways to protect healthy cells from secondary insults, rehabilitate injured cells, and spur

regeneration of axons to ultimately restore lost functions. These studies include biomolecular and cellular therapies [8], guidance therapies [9], and rehabilitation strategies [10]. Since it is known that injured neurons of the CNS are able to re-grow in a better suited microenvironment, therapies should be aimed and masking neuron-inhibitory molecules and factors, and aligning and directing neurites through the injury site, making implantable biomaterials a promising therapy in SCI [8].

This thesis focuses on developing a biomaterial that promotes and directs neurite growth by using durotactic and haptotactic gradients. During development, the body exhibits physical [11] and chemical [12] cues to direct growing axons to form synapses in the nervous system, however, these cues are no longer exhibited after initial connection. In vitro, chemotaxis, the migration of cells in response to soluble factors, and haptotaxis, the migration of cells in response to cellular adhesion sites (insoluble factors), have been studied in an attempt to mirror *in vivo* conditions. More recently, cells have been shown to respond to durotactic properties, or changes in mechanical stiffness [13]. During spinal cord growth and development, growth cones follow guidance cues of attractive and repulsive diffusible factors [14]. In vivo, chemotactic agents are differentially synthesized by cells of the nervous system to provide a temporal and spatial guidance system [15, 16]. However, chemotaxis is difficult to integrate into an engineered biomaterial, since a drug-releasing source would be needed for the chemoattractant. By focusing on the biophysical properties of the biomaterial, we can make properties permanent and immobilized on the biomaterial itself, allowing cells to sense these properties indefinitely. We believe that by incorporating gradients of mechanical properties and adhesion into 3D collagen gels, we will be able to not only promote neurite outgrowth but also directs neurons.

Durotaxis

In the last 10 years it has been show that cells can react to the mechanical properties of the substrate on which they are grown [13, 17, 18], and this response varies based on cell type. One cellular phenomenon that is affected by substrate stiffness is cell migration. Lo et al first found that fibroblast migration depends on whether they are on the soft or stiff region of a polyacrylamide substrate. Fibroblasts that began on the soft side of the gel migrated to the stiff side, however, fibroblasts that began on the stiff side did not cross into the soft region and the term durotaxis was used to describe this phenomena [13]. This behavior is different depending on the type of cell and range of mechanical properties used. Janmey's group found that neurons and astrocytes react differently to the mechanical properties of the substrate. Astrocytes prefer stiff substrates, whereas neurons prefer soft substrates [17]. It is conceivable that there is an optimal mechanical property for neurons, or each cell type, which would lead to the longest neurites, or 'best' migration.

Engler et al. showed that the cytoskeletal organization of muscle cells depends on the stiffness of the substrate on which they are grown with optimal substrate stiffness closest to that of relaxed muscle bundles [19]. A review by Discher et al [18] stressed the importance of substrate stiffness on cellular motility for anchorage dependent cells. Anchorage dependent, contractile cells show an increase in cellular adhesions and a more organized cytoskeleton with increasing stiffness of the substrate on which they are grown. This could be because of the natural environment in which they grow. We know that *in vivo* muscle and skin is much stiffer then the brain and the spinal cord and this could

explain why neurons prefer soft substrates, whereas muscle cells and fibroblasts prefer stiff substrates.

Effect of substrate stiffness has also been studied specifically for neurons. Georges et al. [17] found that cortical neurons show more branched morphology on softer polyacrylamide gels (200 Pa vs 9000 pa). Balgude et al [20] found that in chick dorsal root ganglia (DRG) neurons the rate of neurite extension is higher in softer gels. A study on PC12 cells (a 'neuron-like' cell) found that at very low storage modulus (10 Pa), cells do not show much extension or growth [21]. These studies imply that there is an optimal substrate stiffness for neuronal cells that is between 10 Pa and 200 Pa.

From these studies we see the importance of substrate stiffness on neurite outgrowth. We would expect that neurons prefer a soft substrate for growth and we hypothesize that we can direct and possibly enhance neurite outgrowth using a gradient of mechanical properties from stiff to soft.

Haptotaxis

Besides gradients of soluble factors, cells are also presented adhesion molecules *in vivo* via other cells or extracellular matrix (ECM) molecules [14, 22]. Molecules such as neural cell adhesion molecules (NCAMs) and N-cadherins dictate many cell-cell interactions [23], while ECM molecules such as vitronectin and laminin provide critical guidance cues to the developing nervous system [24,25]. Molecules that are attractive to one cell type may not be to other cells. For example, vitronectin has been shown to strongly attract astrocytes but has little effect on neuronal migration [26]. Conversely, L1 (an NCAM) strongly promotes adhesion of neurons, but has minimal influence on astrocytes in the same culture [27].

Laminin derived peptides, IKVAV and YIGSR, have also been used to increase neuron adhesion and neurite outgrowth [28, 29].

Borkenhagen et al. [29] studied chick DRG growth on 3D agarose gels grafted with YIGSR and YIGSR-scrambled peptides. They found that neurite outgrowth increased for DRGs grown on YIGSR grafted gels as compared to no-peptide and scrambled peptide conditions. Similarly, Schense et al. [30] studied chick DRG outgrowth on RGD grafted fibrin gels and scrambled condition. They found that growth shows a biphasic response, with increased growth in low RGD concentrations when compared to controls, but decreased growth in high RGD concentrations implying high RGD concentration are too 'sticky' to allow for neurite outgrowth. This work has shown that peptides can be important in increasing and directing neurite outgrowth and that there is an optimal concentration of peptide for the most favorable neurite outgrowth.

Though most studies to date have been on neurite outgrowth in discrete samples of varying adhesion, there has been some recent work using 2D and 3D gradients of neuron adhesion sites for neurite outgrowth. Adams et al used a photolinker linked IKVAV peptide system to make 2D gradients of IKVAV on polystyrene [31]. In both steep and shallow gradient cases, neurons preferentially grew 'up the gradient' of IKVAV but once they chose a direction, they showed no indication of growth cone turning. Dolda et al. studied 3D gradients of laminin grafted to agarose gels. Using an *in vivo* rat sciatic nerve model, they show that some regeneration can be produced if laminin gradients are used in conjunction with NGF gradients [32], however, there is little neurite regeneration with laminin gradients alone or isotropic laminin conditions. In all conditions, neurite outgrowth was significantly less then nerve graft controls. *In vitro*,

they showed laminin gradients increase the rate of neurite outgrowth and directed growth ‘up the gradient’ of laminin in ‘shallow’ gradient conditions [33]. We believe neurite outgrowth can be directed by using 3D gradients of IKVAV and YIGSR, where growth can be optimized over laminin gradients by decoupling the effects of whole laminin.

BioMEMS/Microfluidics

Gradient studies are important to gain information on directed cell migration and neurite growth. Over the past 40 years, several methods have been used including the Boyden chamber [34], under-agarose assay [35], and Dunn chamber [36]. Though these studies have been useful, they have one major drawback in that they do not form stable gradients; the gradients change with time due to diffusion. This drawback has led to the development of microfluidic gradient generators. Microfluidics has many advantages including, small reagent volumes, shorter reaction times, and most importantly low Reynolds number flow to allow for controlled mixing of inlet solutions.

Microfluidic gradient generators were first developed in the Whitesides lab [37]. Several chemotactic studies have been done using the Whitesides gradient generator [38-40]. Gradients are made using two inlet channels which are split into three, then four, then five, then six channels and so on. Channels are then brought together to form a single outlet with adjacent stripes of solutions with increasing concentrations from inlet channel one. Initial studies were done using neutrophils and interleukin-8 (IL-8), a chemoattractant for neutrophils, where they found that neutrophils migrate ‘up the gradient’ of IL-8 from 0-50 ng/ml in 90 mins. Wang et al. studied the effects of EGF gradients on MDA-MB-231 breast cancer cells [40]. These studies show the versatility of this technique making it possible to use any combination of cell type and

chemoattractant. Dertinger et al. [41] studied the effects of substrate bound laminin 2D gradients generated by microfluidics on hippocampal neurons and found that neurites extend ‘up the gradient’ of laminin after 24 hours.

In the last 10 years microfluidics has become a more widely used method to develop gradients for cell migration studies. Most commonly, chemotaxis is being studied in 2D, but recent work has been done in 3D microfluidic gradients [42]. Microfluidic devices can be filled with a hydrogel in order to study cell migration and growth in a more natural, 3D environment. Previously, microfluidics devices have been used to study chemotactic gradients and 2D haptotactic gradients but no work has been done in making 3D durotactic or haptotacic gradients. We believe this simple method can be an easy way to find optimal mechanical and adhesive properties for neurite outgrowth. This method promises to be a versatile emerging technology that can be adapted to many different cell/gradient systems.

Summary

A successful approach for spinal cord injury repair will be a combination of many currently investigated strategies. The goal of this thesis is to investigate the use of modified collagen biomaterials, fabricated using microfluidics, for directed and enhanced nerve growth. We study the affect of both stable durotactic gradients and haptotactic gradients. Most current work on the use of modified biomaterials for nerve regeneration has been on discrete samples. Though discrete samples can be used to determine the range of effectiveness of mechanical and adhesive properties, gradients are important for directed growth. We believe that if we know the preference of neurons for a particular

substrate property, we can grow neurites in the direction of their targets. In addition, it is possible to enhance neurite growth through the use of these gradients.

In chapter 2, we present the effects of genipin, a crosslinking agent, on 2 mg/ml collagen gels. Collagen gels were treated with 0, 1, 5, and 10mM collagen and tested using parallel plate rheometry at 2, 4, 6, and 12 hours post treatment. Genipin has the additional effect of fluorescing as it crosslinks and we were able to correlate this fluorescence to the mechanical properties of the gel, developing a non-contact way to measure the mechanical properties of a gel. Gels showed increase in storage modulus and fluorescence as concentration of genipin and duration of exposure increased.

In chapter 3, we develop a microfluidic system that is used to study the effect of gradients of mechanical properties on neurite outgrowth. Our system has a bottom 'cell channel' underneath a gradient 'H-model' device. Gradients of mechanical properties are made using genipin at a concentration 0-1mM for 12 hours and 24 hours; controls are performed with 1-1mM genipin for 12 hours and no-genipin controls. We used this system to study chick DRG neurite growth in gradients of mechanical properties. We found that neurites grow down a gradient of stiffness in both gradient cases. More interestingly, we found that neurite growth in our 0-1mM, 12 hour gradient gels was longer then growth in our control samples implying that gradients are not only directing neurite growth but also enhancing it.

In chapter 4, our microfluidic system is used to study DRG response to adhesion gradients. We studied gradients of both IKVAV and YIGSR which components of laminin and have been shown to direct neurite outgrowth. Gradients are studied in four different slopes created by changing inlet concentrations as well as the length of the

gradient. Gradient experiments are preformed as 0-37 μg peptide/mg collagen (0-100%) and 0-18.5 μg peptide/mg collagen (0-50%) at two different gradient lengths of 3 and 5 mm for both IKVAV and YIGSR. Controls were performed at 100%-100% and 0%-0% (no peptide) at 5mm. In IKVAV experiments we found that neurite outgrowth is increased in all gradient conditions with some directionality in the 0-50%, 5mm condition, which is our shallowest gradient case. In the uniform 100%-100% case we see no increase in neurite outgrowth as compared to the no-peptide control implying that IKVAV-grafted collagen may be too 'sticky' at the highest concentration that we used. In the YIGSR case we see increased neurite outgrowth in all YIGSR-grafted collagen conditions including the 100%-100% uniform conditions. Growth is significantly directed in the 0-50%, 3mm, and 0-100%, 3mm, conditions which are our steepest gradient cases. These results show that neurons can be directed using gradients of IKVAV and YIGSR, however the concentrations at which outgrowth is enhanced and directed is very different; for IKVAV we need a shallow gradient and for YIGSR we need a steep gradient.

In chapter 5 we present the overall discussion and conclusions of this work and future directions. We believe the results from chapter 3 and 4 can be combined to increase and further enhance neurite growth to develop the optimal biomaterial for nerve regeneration. Additionally, a chemotactic gradient, such as a gradient of NGF, could be added to further enhance growth. It is important to note the versatility of the system developed in this project. This system can be extended for any number of cells types and gradients, providing a "limitless" platform for the study of cell migration and neurite growth.

References

1. Willerth, S.M. and S.E. Sakiyama-Elbert, *Approaches to neural tissue engineering using scaffolds for drug delivery.* Adv Drug Deliv Rev, 2007. **59**(4-5): p. 325-38.
2. Richardson, P.M., U.M. McGuinness, and A.J. Aguayo, *Axons from CNS neurons regenerate into PNS grafts.* Nature, 1980. **284**(5753): p. 264-5.
3. Grados-Munro, E.M. and A.E. Fournier, *Myelin-associated inhibitors of axon regeneration.* J Neurosci Res, 2003. **74**(4): p. 479-85.
4. Blits, B., G.J. Boer, and J. Verhaagen, *Pharmacological, cell, and gene therapy strategies to promote spinal cord regeneration.* Cell Transplant, 2002. **11**(6): p. 593-613.
5. Dietrich, W.D., et al., *The role of inflammatory processes in the pathophysiology and treatment of brain and spinal cord trauma.* Acta Neurochir Suppl, 2004. **89**: p. 69-74.
6. Vera-Portocarrero, L.P., et al., *Rapid changes in expression of glutamate transporters after spinal cord injury.* Brain Res, 2002. **927**(1): p. 104-10.
7. Park, E., A.A. Velumian, and M.G. Fehlings, *The role of excitotoxicity in secondary mechanisms of spinal cord injury: a review with an emphasis on the implications for white matter degeneration.* J Neurotrauma, 2004. **21**(6): p. 754-74.
8. Willerth, S.M. and S.E. Sakiyama-Elbert, *Cell therapy for spinal cord regeneration.* Adv Drug Deliv Rev, 2008. **60**(2): p. 263-76.
9. Goldner, J.S., et al., *Neurite bridging across micropatterned grooves.* Biomaterials, 2006. **27**(3): p. 460-72.
10. Behrman, A.L. and S.J. Harkema, *Physical rehabilitation as an agent for recovery after spinal cord injury.* Phys Med Rehabil Clin N Am, 2007. **18**(2): p. 183-202, v.
11. Ito, H., et al., *Haptotactic migration of pancreatic cancer cells induced by bioactive components in bovine liver extract.* J Surg Oncol, 1998. **68**(3): p. 153-8.
12. Rosner, B.I., et al., *Rational design of contact guiding, neurotrophic matrices for peripheral nerve regeneration.* Ann Biomed Eng, 2003. **31**(11): p. 1383-401.
13. Lo, C.M., et al., *Cell movement is guided by the rigidity of the substrate.* Biophys J, 2000. **79**(1): p. 144-52.
14. Gallo, G. and P.C. Letourneau, *Axon guidance: A balance of signals sets axons on the right track.* Curr Biol, 1999. **9**(13): p. R490-2.
15. Campbell, D.S., et al., *Semaphorin 3A elicits stage-dependent collapse, turning, and branching in Xenopus retinal growth cones.* J Neurosci, 2001. **21**(21): p. 8538-47.
16. Legg, A.T. and T.P. O'Connor, *Gradients and growth cone guidance of grasshopper neurons.* J Histochem Cytochem, 2003. **51**(4): p. 445-54.
17. Georges, P.C., et al., *Matrices with compliance comparable to that of brain tissue select neuronal over glial growth in mixed cortical cultures.* Biophys J, 2006. **90**(8): p. 3012-8.

18. Discher, D.E., P. Janmey, and Y.L. Wang, *Tissue cells feel and respond to the stiffness of their substrate.* Science, 2005. **310**(5751): p. 1139-43.
19. Engler, A.J., et al., *Myotubes differentiate optimally on substrates with tissue-like stiffness: pathological implications for soft or stiff microenvironments.* J Cell Biol, 2004. **166**(6): p. 877-87.
20. Balgude, A.P., et al., *Agarose gel stiffness determines rate of DRG neurite extension in 3D cultures.* Biomaterials, 2001. **22**(10): p. 1077-84.
21. Leach, J.B., et al., *Neurite outgrowth and branching of PC12 cells on very soft substrates sharply decreases below a threshold of substrate rigidity.* J Neural Eng, 2007. **4**(2): p. 26-34.
22. Letourneau, P.C., M.L. Condic, and D.M. Snow, *Extracellular matrix and neurite outgrowth.* Curr Opin Genet Dev, 1992. **2**(4): p. 625-34.
23. Edelman, G.M. and F.S. Jones, *Gene regulation of cell adhesion: a key step in neural morphogenesis.* Brain Res Brain Res Rev, 1998. **26**(2-3): p. 337-52.
24. Grimpe, B. and J. Silver, *The extracellular matrix in axon regeneration.* Prog Brain Res, 2002. **137**: p. 333-49.
25. Tucker, R.P., *Abnormal neural crest cell migration after the in vivo knockdown of tenascin-C expression with morpholino antisense oligonucleotides.* Dev Dyn, 2001. **222**(1): p. 115-9.
26. Faber-Elman, A., et al., *Vitronectin overrides a negative effect of TNF-alpha on astrocyte migration.* Faseb J, 1995. **9**(15): p. 1605-13.
27. Webb, K., et al., *Substrate-bound human recombinant L1 selectively promotes neuronal attachment and outgrowth in the presence of astrocytes and fibroblasts.* Biomaterials, 2001. **22**(10): p. 1017-28.
28. Tong, Y.W. and M.S. Shoichet, *Enhancing the neuronal interaction on fluoropolymer surfaces with mixed peptides or spacer group linkers.* Biomaterials, 2001. **22**(10): p. 1029-34.
29. Borkenhagen, M., et al., *Three-dimensional extracellular matrix engineering in the nervous system.* J Biomed Mater Res, 1998. **40**(3): p. 392-400.
30. Schense, J.C. and J.A. Hubbell, *Three-dimensional migration of neurites is mediated by adhesion site density and affinity.* J Biol Chem, 2000. **275**(10): p. 6813-8.
31. Adams, D.N., et al., *Growth cones turn and migrate up an immobilized gradient of the laminin IKVAV peptide.* J Neurobiol, 2005. **62**(1): p. 134-47.
32. Dodla, M.C. and R.V. Bellamkonda, *Differences between the effect of anisotropic and isotropic laminin and nerve growth factor presenting scaffolds on nerve regeneration across long peripheral nerve gaps.* Biomaterials, 2008. **29**(1): p. 33-46.
33. Dodla, M.C. and R.V. Bellamkonda, *Anisotropic scaffolds facilitate enhanced neurite extension in vitro.* J Biomed Mater Res A, 2006. **78**(2): p. 213-21.
34. Boyden, S., *The chemotactic effect of mixtures of antibody and antigen on polymorphonuclear leucocytes.* J Exp Med, 1962. **115**: p. 453-66.
35. Nelson, R.D., P.G. Quie, and R.L. Simmons, *Chemotaxis under agarose: a new and simple method for measuring chemotaxis and spontaneous migration of human polymorphonuclear leukocytes and monocytes.* J Immunol, 1975. **115**(6): p. 1650-6.

36. Zicha, D., G.A. Dunn, and A.F. Brown, *A new direct-viewing chemotaxis chamber.* J Cell Sci, 1991. **99 (Pt 4)**: p. 769-75.
37. Whitesides, G.M., et al., *Soft lithography in biology and biochemistry.* Annu Rev Biomed Eng, 2001. **3**: p. 335-73.
38. Li Jeon, N., et al., *Neutrophil chemotaxis in linear and complex gradients of interleukin-8 formed in a microfabricated device.* Nat Biotechnol, 2002. **20**(8): p. 826-30.
39. Lin, F., et al., *Effective neutrophil chemotaxis is strongly influenced by mean IL-8 concentration.* Biochem Biophys Res Commun, 2004. **319**(2): p. 576-81.
40. Wang, S.J., et al., *Differential effects of EGF gradient profiles on MDA-MB-231 breast cancer cell chemotaxis.* Exp Cell Res, 2004. **300**(1): p. 180-9.
41. Dertinger, S.K., et al., *Gradients of substrate-bound laminin orient axonal specification of neurons.* Proc Natl Acad Sci U S A, 2002. **99**(20): p. 12542-7.
42. Saadi, W., et al., *Generation of stable concentration gradients in 2D and 3D environments using a microfluidic ladder chamber.* Biomed Microdevices, 2007. **9**(5): p. 627-35.

Chapter 2: Genipin-induced changes in collagen gels: correlation of mechanical properties to fluorescence

Abstract

Controlled crosslinking of collagen gels has important applications in cell and tissue mechanics as well as tissue engineering. Genipin is a natural plant extract that has been shown to crosslink biological tissues and to produce color and fluorescence changes upon crosslinking. We have characterized the effects of genipin concentration and incubation duration on the mechanical and fluorigenic properties of type I collagen gels. Gels were exposed to genipin (0, 1, 5, or 10mM) for a defined duration (2, 4, 6, or 12hrs). Mechanical properties were characterized using parallel plate rheometry, while fluorigenic properties were examined with a spectrofluorimetric plate reader and with a standard, inverted epifluorescent microscope. Additionally, Fourier Transform Infrared Spectroscopy (FTIR) was used to characterize and track the crosslinking reaction in real-time (Appendix 2-1). Genipin produced significant concentration- and incubation-dependent increases in the storage modulus, loss modulus, and fluorescence intensity. Storage modulus was strongly correlated to fluorescence exponentially. Minimal cytotoxicity was observed for exposure of L929 fibroblasts cultured within collagen gels to 1mM genipin for 24 hrs, but significant cell death occurred for 5mM and 10mM genipin. We conclude that genipin can be used to stiffen collagen gels in a relatively short time frame, that low concentrations of genipin can be used to crosslink cell-populated collagen gels to affect cell behavior that is influenced by the mechanical properties of the tissue scaffold, and that the degree of crosslinking can be reliably assayed optically via simple fluorescence measurements.

Introduction

It is now clear that in many tissue systems, the mechanostructural properties of the extracellular matrix contribute to the regulation of cellular functions in addition to the mechanical functions of the tissue [1, 2]. To investigate these phenomena, and to properly design bioartificial, tissue-engineered replacements, it is frequently desired to control the mechanical properties of biomaterials. Collagen-based tissue equivalents are of special interest, largely because collagen is a primary mechanostructural element in many connective tissues, including dermis, blood vessels, tendons, and ligaments [3-6]. Additionally, collagen's superior biocompatibility and nearly ubiquitous bioactivity have made it one of the most extensively investigated biomaterial scaffolds for engineering the tissues listed above, and others, including hepatic [7] and neural tissue [8]. It is, therefore, critical to maintain the ability to manipulate the mechanical properties of collagen gels, both to study mechanotransduction and to improve the properties of bioartificial tissues. While the properties of a collagen scaffold can be altered by merely changing the concentration of collagen monomers prior to self-assembly, thereby making a more concentrated gel, most often a crosslinking mechanism is implemented.

A variety of methods exist to crosslink collagen. In vivo, tissues are naturally crosslinked by enzymes such as lysyl oxidase [9, 10] and tranglutaminase [11, 12]. However, use of these enzymes for bulk changes in mechanical properties in cultured tissue mimics is cost prohibitive. Chemical treatments with aldehydes are often used to preserve and stiffen tissues. However, for cell-populated collagen gels (often termed "tissue equivalents"), these treatments are highly toxic. Non-enzymatic glycation has been used to improve the mechanical properties of bioartificial blood vessels in vitro by

including a reducing sugar, such as ribose, in the culture medium [13]. However, the concentrations necessary to achieve sufficient crosslinking to significantly affect the mechanical properties in a timely manner (<1-2 weeks) are toxic, requiring longer incubations at lower concentrations. Irradiation with ultraviolet (UV) light has also been used to crosslink collagen [14], but has limited use in cellular tissues and tissue equivalents because of the potential for UV-mediated DNA degradation. Furthermore, UV light may crosslink thicker tissues non-uniformly. Non-enzymatic nitration, which is linked to many age-associated changes, including alterations in collagen connective tissues consistent with nitrite end-products of nitric oxide, has been shown to increase type I collagen crosslinking and deplete tyrosine residues, and is not immediately cytotoxic [15]. Nitrites can also alter the structure of other proteins and enzymes to affect their regulatory functions [16].

Recently, genipin, a compound extracted from the fruit of the *Gardenia Jasminoides*, has been shown to crosslink cellular and acellular tissues [17-21], as well as biomaterials including gelatin microspheres [22], alginate-chitosan composites [23], and poly(ethylene)-glycol hydrogels [24]. Additionally, results suggest that genipin is cell-tolerated [25]. For these reasons, genipin has been offered as an alternative crosslinking agent for improving the mechanical properties of bioartificial tissues.

Genipin has been found to crosslink gelatin through nucleophilic attack by primary amine groups on lysine and arginine residues on the C3 atom of genipin [26], subsequently embedding a tertiary nitrogen in the six-membered ring in place of an oxygen atom [27]. We expect a similar mechanism for the reaction of collagen and genipin. In addition to crosslinking collagen and increasing mechanical strength,

treatment with genipin, which is blue in crystalline form but produces a clear solution when dissolved in water or saline, has two unique outcomes: (1) following crosslinking with genipin, normally opaque collagen turns blue [28]; and (2) these crosslinks emit fluorescence at 630nm when excited at 590nm [29]. Thus, genipin crosslinking generates a molecular fingerprint that may be probed optically in situ to evaluate the degree of crosslinking and, possibly, the mechanical properties of collagen. Herein, we characterize the effects of genipin exposure on the mechanical properties of acellular collagen gels, and we correlate these properties to fluorescence intensity. We examine the molecular changes during crosslinking with Fourier Transform Infrared Spectroscopy (FTIR) in situ (Appendix 2-1). We also assess the cytotoxic effects of direct exposure of genipin to cells in collagen tissue equivalents. These data provide a valuable blueprint for future studies applying genipin for efficient crosslinking in vitro to evaluate mechanotransduction and to assist in the design of bioartificial tissues for a variety of tissue systems.

Methods

Collagen gels

Type I collagen gels were prepared as previously described [30] by mixing 20 µl 1M Hepes buffer, 140 µl 0.1N NaOH, 100µl of 10X PBS , 60 µl of PBS (Invitrogen, Carlsbad, CA), and 677 µl of 2.0 mg/ml collagen (Elastin Products Company, Owensville, MO) to make a 2.0 mg/ml collagen solution. The collagen solution self-assembles into a gel upon incubation at 37°C. For mechanical testing and fluorescence studies, acellular type I collagen gels were incubated in 0mM, 1mM, 5mM, or 10mM genipin (Challenge Bioproducts Co., Taiwan) in phosphate buffered saline (PBS) for 2, 4, 6, or 12hrs.

Samples were placed on a rocker to ensure adequate diffusion and equilibration of genipin through the gel.

Mechanical testing

Mechanical testing was done using a Rheometrics SR-2000 parallel plate rheometer with a temperature-controlled incubation chamber set to maintain 37°C (TA Instruments, New Castle, DE). A 25mm diameter hole was punched in a 4mm thick layer of poly(dimethyl siloxane) (PDMS). Collagen solution (800μl) was pipetted into the well and transferred to a 37°C incubator to induce self-assembly. Following gel formation, 4.8ml of PBS with a defined concentration of genipin (0, 1, 5, or 10mM) was added to the Petri dish and the dish placed on a rocker to ensure complete mixing. Collagen gels were incubated in genipin for a defined period of time (2, 4, 6, or 12hrs), after which the solution was aspirated, and gels were rinsed generously with PBS. The gels were carefully removed with a spatula and transferred to the bottom plate of the rheometer. The top plate was lowered to a height of 0.8 mm. The dynamic storage and loss moduli of the gel were evaluated at 1% shear strain amplitude at frequencies ranging from 0.1 – 10Hz. Three samples prepared from separate batches of collagen were tested at each combination of genipin concentration/incubation duration. The data were analyzed statistically with ANOVA with genipin concentration and incubation of duration as fixed effects. Significance levels were set at $P < 0.05$.

Fluorescence testing

Changes in fluorescence intensity due to genipin crosslinking were evaluated in gels prepared in a 96-well tissue culture plate. A 40μL aliquot of collagen was pipetted into each well. The plate was incubated at 37°C to induce self-assembly. PBS (240μl) with defined concentrations (0, 1, 5, and 10mM) of genipin was added to each well and the plate placed on a rocker plate to ensure equilibration of genipin throughout the gel. The gels were incubated in genipin for defined durations (2, 4, 6, 12hrs) that matched the conditions from the rheology studies. At the appropriate time point, the genipin solution was removed, and the gels were rinsed extensively with PBS.

Genipin-induced fluorescence was evaluated in two ways. Some plates were transferred to the computer controlled stage of an Olympus IX81 inverted microscope (Olympus, Melville, NY) to evaluate the feasibility of evaluating the fluorescence with standard epifluorescence microscopy for tissue engineering and mechanotransduction applications. An image of the fluorescence intensity of a representative field from each well (generally near the volumetric centroid of the gel) was captured digitally (Hamamatsu ORCA, Hamamatsu City, Japan) (590nm Exc, 630nm Em), and the mean intensity of the field was measured using Olympus Microsuite software (Olympus, Melville, NY). Identical exposure settings were used for all epifluorescent imaging. Each combination of genipin concentration/incubation time was tested in at least triplicate from at least three replicates per condition per experiment. Separate plates were read with a Cytofluor spectrofluorimetric plate reader (Applied Biosystems, Foster City, CA) with 590nm excitation and 645nm emission filters to demonstrate the ability to rapidly screen the degree of crosslinking based on fluorescence.

Cytotoxicity

Cytotoxic effects of genipin were evaluated using Calcein-AM (Invitogen Corp, Eugene, OR) as an indicator of live cells. L929 fibroblasts were uniformly suspended in collagen solution at 50,000 cells/ml. Aliquots of collagen solution (40µl) were then pipetted into individual wells of a 96-well plate, which was transferred to a 37°C incubator to allow the gel to self-assemble. Genipin (0, 1, 5, or 10mM) was added to the media, and the plates were placed on a rocker to facilitate mixing. Gels were incubated in media with genipin for 12 or 24hrs. At the appropriate time point, gels were rinsed in PBS, and 20µl of 8µM Calcein solution was added to each well. Plates were transferred to the computer controlled stage of an Olympus IX81 inverted microscope operating in epifluorescence mode (480nm Exc, 535nm Em). Three representative areas from each well were imaged serially through the thickness of the gel. The images were stacked to project all of the cells through the imaged volume on to one plane, and the cells were counted manually. The number of cells was compared across conditions with ANOVA ($P < 0.05$).

Results

Mechanical testing

Rheological testing with parallel plate rheometry revealed that incubation in genipin increased the storage and loss moduli of acellular collagen gels (Fig. 2-1 and Fig. 2-2, respectively). No shrinkage of the gels was observed with crosslinking (data not shown).

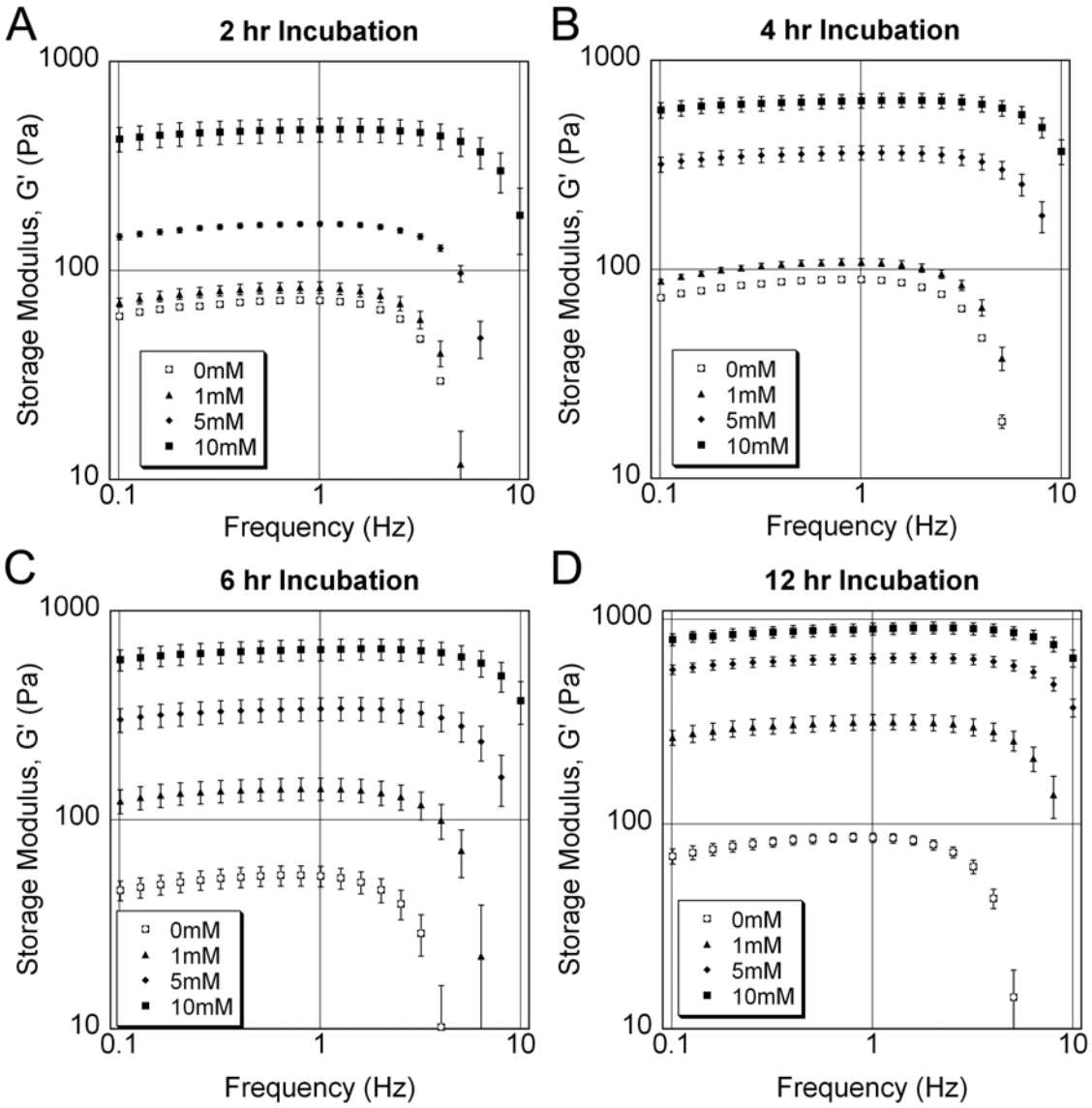

Figure 2- 1: Storage moduli following parallel plate rheometry. (A) 2hr incubation; (B) 4hr incubation; (C) 6hr incubation; (D) 12hr incubation. Samples were subjected to 1% shear strain amplitude over a range of frequencies. Results are average +/- std err. Both genipin concentration and the duration of incubation significantly affected the storage modulus. Storage modulus tended to decline at higher frequencies, which was associated with damage to the gels.

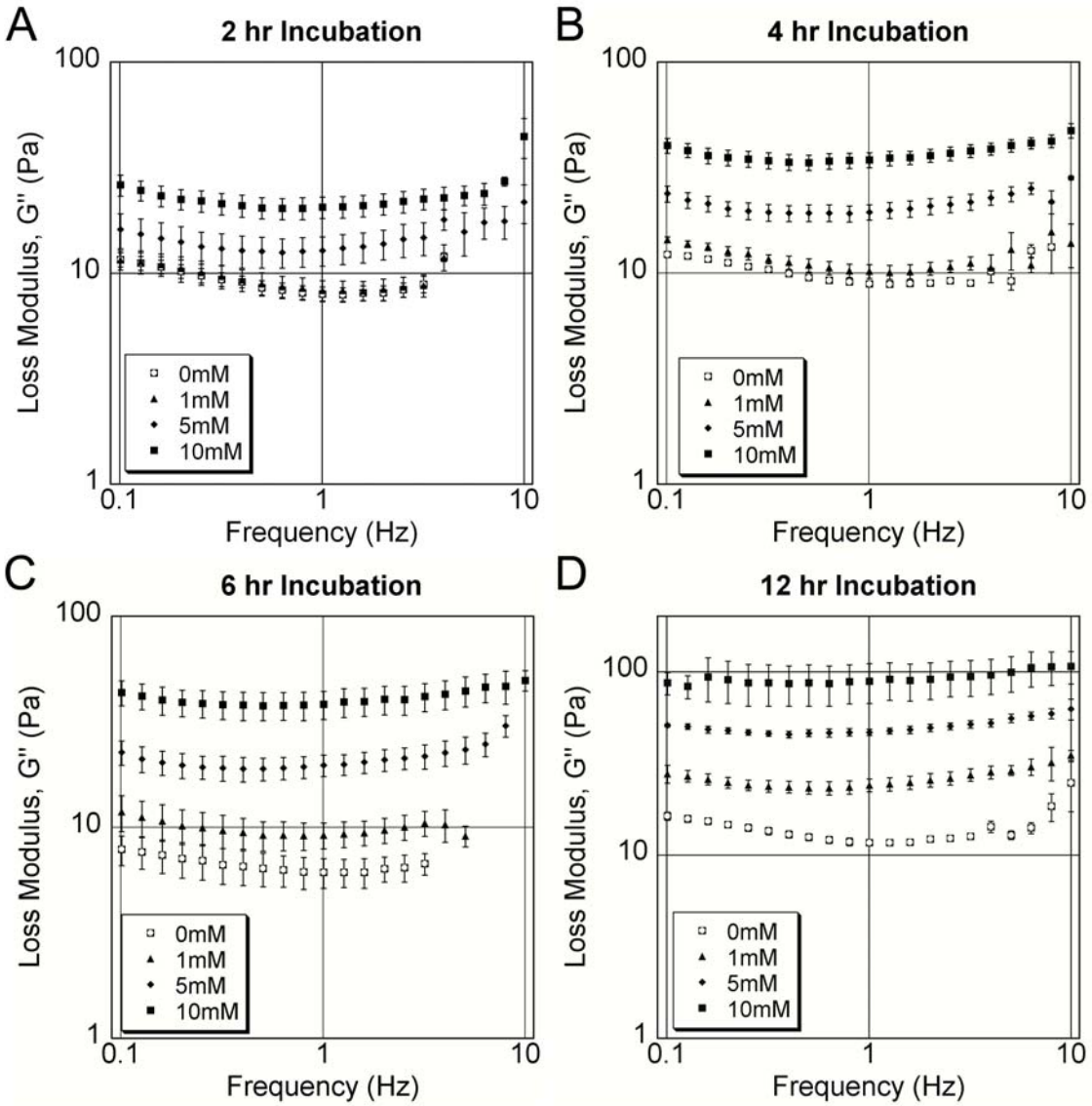

Figure 2- 2: Loss moduli following parallel plate rheometry. (A) 2hr incubation; (B) 4hr incubation; (C) 6hr incubation; (D) 12hr incubation. Results are average +/- std err. Loss modulus tended to decline with frequency and then rise concurrent with the decline in storage modulus at higher frequencies. Both genipin concentration and the duration of incubation significantly affected the storage modulus.

Storage moduli increased gradually with frequency for all conditions, and then dropped off at higher frequencies for many samples. Inspection of gels revealed damage to the samples, which did not occur if experiments were run only at lower frequencies (data not shown), and we assumed that the damage was responsible for the apparent decrease in stiffness. In general, increased crosslinking delayed this damage. Loss modulus decreased gradually with frequency in all conditions, and generally began to increase concurrent with the decrease in storage modulus, which we again attribute to damage to the gel, though the increase in loss modulus was more gradual than the corresponding decrease in storage modulus. Increasing genipin concentration and the duration of incubation also produced significant increases in storage and loss moduli ($P < 0.001$). Cell-induced strain of tissue equivalents, such as the strains produced during cell-mediated gel compaction or cell migration, generally occurs at a low strain rate [31]. We therefore focused on storage moduli at 0.1Hz, which are shown for the different genipin concentrations and incubation durations in Fig. 2-3. Post hoc analysis (Fisher's Least Significant Difference test) revealed significant differences among all pairwise comparisons for the effects of genipin concentration on storage modulus (all $P < 0.001$) and all pairwise comparisons of loss modulus (max $P = 0.046$). For incubation duration, all pairwise comparisons of storage modulus were significantly different (max $P = 0.001$) except 4hrs vs. 6hrs ($P = 0.913$). Similar results were obtained for pairwise comparisons of the effects of duration on loss modulus at 0.1 Hz: all pairwise comparisons were significantly different (max $P = 0.013$), except 4hrs vs. 6hrs ($P = 0.655$). Nearly identical results were observed for comparisons of storage moduli at 2Hz, which represents a loading rate more consistent with functions of many load-bearing tissues. Comparisons of loss moduli at 2Hz showed significant

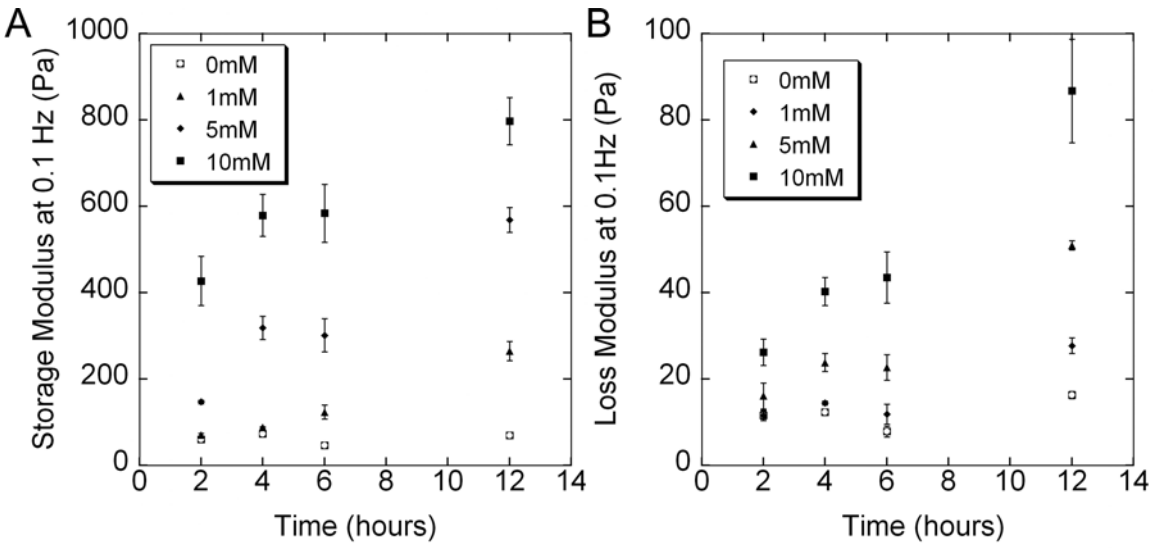

Figure 2- 3 : Average storage moduli (A) and loss moduli (B) (+/- std err) at 1% shear strain amplitude and 0.1 Hz vs. incubation time. Increasing genipin concentration and the duration of incubation in genipin significantly increased the storage and loss moduli of the collagen gels (two-way ANOVA, $P < 0.001$). Fisher's LSD test revealed significant differences among all pairwise comparisons of concentration for storage modulus (all $P < 0.001$) and loss modulus (max $P = 0.046$). For incubation duration, all pairwise comparisons of storage modulus (max $P = 0.001$) and of loss modulus (max $P = 0.013$) were significantly different except 4hrs vs. 6hrs.

differences between all concentrations (max $P = 0.003$) except 0mM vs. 1mM ($P = 0.270$). Loss moduli at 2Hz were significantly different only between 12hrs and each of the other durations (max $P < 0.001$).

Fluorescence testing

Incubation of acellular collagen gels in genipin caused the normally opaque, non-fluorescing gels to turn blue and emit a red fluorescence. The fluorescence intensity of collagen gels was measured in separate samples in parallel to the mechanical testing (Fig. 2-4). Fluorescence intensity measured from digital images captured with epifluorescence microscopy increased significantly with genipin concentration ($P < 0.001$) and incubation duration ($P < 0.001$) (two-way ANOVA). Post-hoc analysis (Fisher's LSD) revealed significant differences among all pairwise combinations of concentration (all $P < 0.001$) and durations (max $P = 0.003$). Similar statistically significant trends were observed in measurements taken spectrofluorimetrically ($P < 0.001$). Post hoc analysis of plate reader fluorescence revealed significant differences (max $P = 0.033$) among all pairwise comparisons of concentrations except 5mM vs. 10mM ($P = 0.199$) and among all pairwise comparisons of duration except 4hrs vs 6hrs ($P = 0.240$). As with any fluorimetric (or colorimetric) optical assay, intensity measurements tended to saturate at high levels of fluorescence for both systems of measurement using a constant exposure setting.

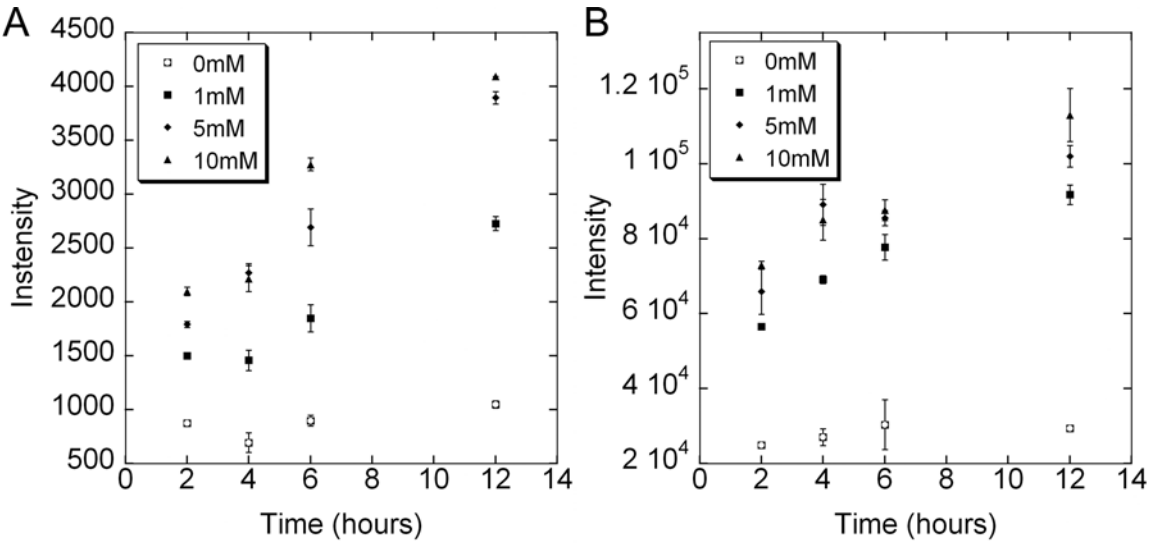

Figure 2- 4: Fluorescence intensity (average +/- std err) of genipin-crosslinked collagen measured using (A) epifluorescent microscopy (590nm excitation, 630nm emission) and (B) spectrofluorimetrically (590nm excitation, 645nm emission). For both, the intensity of fluorescence emission increased significantly with genipin concentration and duration of incubation ($P < 0.001$). Post hoc analysis (Fisher's LSD test) revealed significant differences among all pairwise comparisons of concentrations except 5mM vs. 10mM (max $P = 0.033$) and among all pairwise comparisons of duration except 4hrs vs. 6hrs ($P = 0.240$).

G' = Aexp(B x Intensity)				
Fluorescent Measurement	Frequency	A (+/- std err)	B (+/- std err)	R^2
Microscope	0.1 Hz	22.9 +/- 7.33	3.05e-5 +/- 4.30e-6	0.782
Microscope	2 Hz	24.3 +/- 7.82	3.12e-5 +/- 4.32e-6	0.788
Spectrofluorimeter	0.1 Hz	33.2 +/- 8.36	8.34e-4 +/- 1.1e-4	0.808
Spectrofluorimeter	2 Hz	35.7 +/- 9.11	8.51e-4 +/- 1.1e-4	0.810

Table 2- 1: Results of storage modulus-fluorescent intensity correlations

The concurrent increase in fluorescence intensity with crosslinking presents a unique opportunity to assay the stiffness of the gels optically, if the fluorescence measurement can be appropriately calibrated against a measure of the mechanical properties. The average storage moduli at 0.1Hz and at 2Hz (~largest frequency before a drop-off was observed) were plotted against the average fluorescence intensity at each combination of genipin concentration and duration of incubation (Fig. 2-5). For both fluorescence measurement techniques and both frequencies, stiffness was correlated exponentially to intensity (Table 2-1). The correlation coefficients were nearly identical for 0.1Hz and 2Hz (R^2 = 0.808 and 0.810, respectively, for measurements taken microscopically, and R^2 = 0.782 and 0.788, respectively for measurements taken spectrofluorimetrically). The exponential correlation curves shifted to the left slightly with increasing frequency, consistent with the increase in storage modulus. However, the resulting constants from the correlation were statistically indistinguishable.

Cytotoxicity Data

Most of the previous cytotoxicity studies of genipin had examined cell death following rinsing of genipin-crosslinked tissues or biomaterials prior to addition of cells. For tissue equivalent studies, knowledge of the cytotoxic effects of the genipin solution is required. Cytotoxicity studies using L929 fibroblasts indicated that genipin does cause significant cell death (ANOVA, $P < 0.001$) (Fig. 2-6). However, individual comparisons against the control condition (post hoc analysis – Fisher's LSD test) demonstrated that the adverse effects were limited to exposure 5mM ($P < 0.001$) and 10mM ($P < 0.001$); though lower, cell numbers from samples incubated in 1mM were statistically indistinguishable from controls ($P = 0.26$). The results at 12hrs were consistent with the 24hr results.

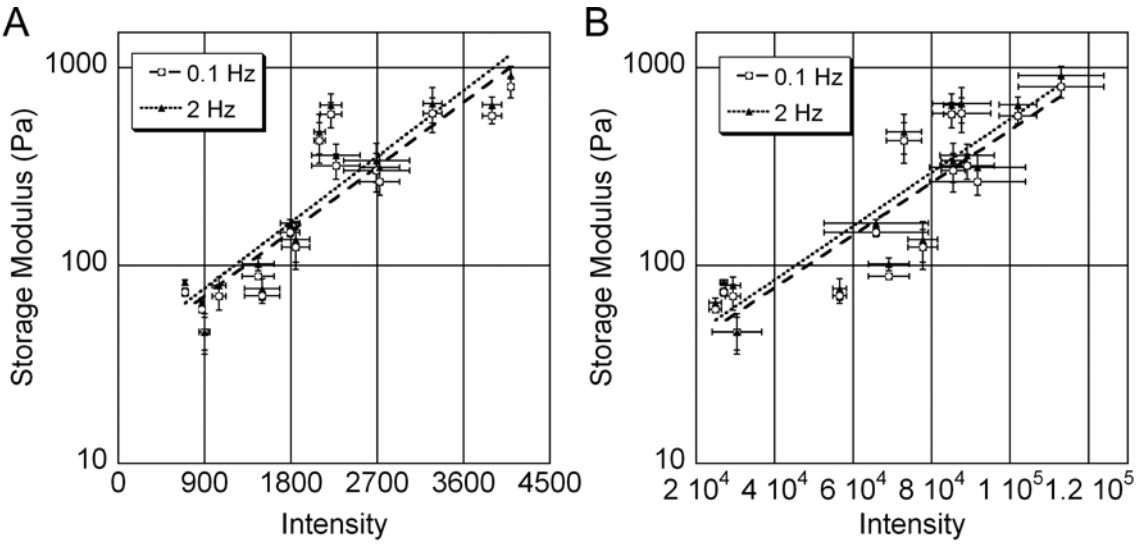

Figure 2- 5: Correlation of average storage modulus (+/- std err) with average fluorescence intensity (+/- std err) measured with epifluorescence microscopy (A) or spectrofluorimetrically (B) for 0.1Hz and 2Hz. In all cases, strong, exponential correlations were observed, indicating that stiffness can be assayed optically following appropriate calibration. Increasing frequency shifted the correlation curve to the left.

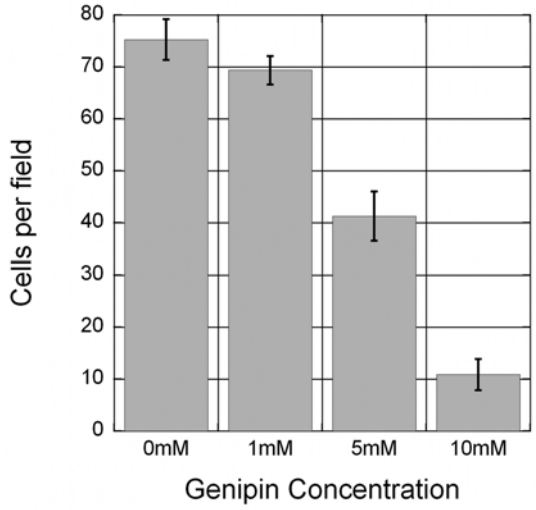

Figure 2- 6: Cytotoxic effects of genipin. L929 fibroblasts entrapped in collagen gels were exposed for 24hrs to culture medium with defined concentrations of genipin immediately upon completion of self-assembly. Live cells were labeled fluorescently with Calcein-AM, and the average number of cells (+/- std err) in a vertical field through the thickness of the gel was determined by manually counting the cells in a stack of several images taken through the height of the gel. Genipin was cytotoxic (ANOVA, $P < 0.001$), but only a small fraction of cells were lost at 1mM, and these results were not statistically different than the 0mM control (Fisher's LSD post hoc test, $P = 0.26$).

Discussion

We have characterized the effects of genipin-induced crosslinking of collagen gels on rheological properties, fluorescence, spectroscopic changes, and cytotoxicity. Rheological measurements were performed at 1% shear strain amplitude over a range of shear rates, which is consistent with previous characterizations of collagen and other biopolymeric gels using similar techniques [32-36]. We found that both the concentration and the duration of incubation in genipin significantly influenced the storage and loss moduli. The storage modulus measurements demonstrated a gradual increase with increasing frequency and were generally consistent with previous reports of collagen rheology [32-35]. Loss modulus showed a gradual decrease with frequency. We further found that genipin-mediated crosslinking produced significant changes in fluorescence that are well-correlated to the stiffness, and that genipin has marked cytotoxic effects at concentrations of 5mM and above. We conclude that genipin-induced crosslinking offers a simple alternative to improve the mechanical properties of tissue constructs, though caution must be taken to preserve cell viability.

We also observed a decline in the storage modulus (and increase in loss modulus) at larger frequencies that we associated with damage to the gel. In previous reports, where this trend was not observed, gels were generally prepared directly on the parallel plates [32-35]. In our case, the lengthy incubations in genipin precluded this possibility, and instead gels were transferred to the rheometer. It is possible that the adhesion to the plates was not as optimal as when gels are directly prepared or that the transfer increased the potential for damage. Nonetheless, the observed decrease in storage modulus was

consistent among samples and, interestingly, the 'failure' properties of the gel improved with increasing concentration and crosslinking duration, indicating that it is a stress-based phenomenon.

Previously, genipin has been used to crosslink biological tissues [21, 37] chitosan-based tissue equivalents [38], and gelatin [39] with genipin concentrations ranging from 1-10mM. In several of these studies, the influence of genipin-mediated crosslinking on cytotoxicity and/or cell viability has been evaluated for different cell types in several different conditions, each in the context of development of a genipin-crosslinked biomaterial [39-41], and relatively low toxicity has been identified following rinsing of the crosslinked tissue. Unlike these studies, we have assessed the cytotoxic effects of genipin on cells directly exposed to controlled concentrations of genipin during crosslinking. We found that exposure to 1mM genipin for 24hrs was mildly cytotoxic to L929 fibroblasts, while exposure to 5mM and 10mM caused significant cell death. Thus, studies involving cellular collagen constructs should be limited to exposure to <= 1mM, while studies with acellular constructs, or at least ones that are initially acellular and rely on cells deposited post-crosslinking to migrate into scaffold, can employ higher concentrations, provided the free genipin is rinsed prior to exposure to cells.

The rheological studies presented herein provide a screening of the effects of genipin on stiffness, but not a direct indication of the utility of the chemical for tissue engineering applications, particularly because we have not yet evaluated the effects of genipin on functional properties of cells. Additionally, the strains and rates used, while consistent with standard parallel plate rheology protocols, are insufficient to assess the utility of genipin for crosslinking bioartificial tissues that routinely experience finite

deformations at accelerated rates. Future studies are aimed at identifying the appropriate timing and incubation durations to optimally influence the mechanical properties of cellular collagen constructs, including mechanical testing to larger strain levels at high rates more appropriate for tissue engineering applications. Previous characterizations with native tissues suggest that such treatments with genipin are plausible and may improve the mechanical properties of the constructs [17, 19, 20].

Beyond providing significantly improved mechanical stiffness of acellular collagen gels, the ability to manipulate the mechanical properties of cellular tissue equivalents on a reasonably short time scale affords the opportunity to study, and potentially exploit, the phenotypic response of cells to changes in mechanical properties within a 3D tissue construct, if it is shown that genipin does not adversely influence cell viability and/or function. The past decade has shown increased focus on quantifying the behavior of cells grown on substrates or in systems of varying compliance, beginning with Pelham and Wang's studies of fibroblast durotaxis using functionalized poly(acrylamide) gels [42]. This system has been adapted to study neural cells [43], endothelial cells [44], and smooth muscle cells [45-47]. In vivo, tissue cells reside within a three dimensional (3D) matrix, which presents a significantly different set of environmental cues than when cells are cultured on a 2D substrate. Quantitative studies of the effects of mechanical properties on cell behavior in 3D, where cells are uniformly distributed throughout the tissue equivalent, rather than seeded on a gel and/or coaxed to invade the gel, have been limited to thin layers of collagen on top of poly(acrylamide) with controlled compliance to indirectly control the stiffness [48]. Genipin can be used to crosslink the 3D tissue equivalents to influence the mechanical properties of the tissue matrix directly, allowing

more complex shapes and boundary conditions to be investigated. For example, culturing cells within collagen gels seeded on poly(acrylamide) membranes naturally mimics a constrained system, where stress is generated at the poly(acrylamide)-collagen boundary as cells exert traction and attempt to contract fibrillar network. However, it has been shown that the accumulation of network stress in a constrained system significantly affects the response of the resident cells [49]. Genipin could be used to stiffen unconstrained, free-floating tissue equivalents as well as constrained ones to distinguish between the influence of the intrinsic mechanical properties of the fibrillar, extracellular matrix network and the mechanostructural properties dictated by the network and its attachments/constraints to external entities.

Genipin also has the added novelty of producing crosslinks that appear blue and fluoresce allowing easy visualization and quantitation of crosslinking. The fluorigenic quality was first identified in forensics research that investigated genipin as a potential fingerprint reagent with increased sensitivity [29]. We hypothesized that the same properties could be used to differentially indicate the degree of crosslinking in collagen gels, which would potentially enable the optical evaluation of mechanical properties. We measured the fluorescence intensity in parallel to mechanical properties in extensively rinsed samples to remove all free genipin, and found strong correlations between the genipin-generated fluorigenic properties and the mechanical properties of the collagen gels using both an epifluorescent microscope and a spectrofluorimetric plate reader. Spectrofluorimetric plate readers have advantages of high throughput and consistent measurement with no lag time between measurements of different samples. The plate reader will also capture the intensity signal through the thickness of the gel. However, only standard plate geometries

can be used for measurement. Epifluorescent imaging is more cumbersome with each sample requiring manual focusing and measurement but could prove useful for samples that do not fit into standard well plate configurations, and for identifying any spatial variance in the degree of crosslinking. Traditional epifluorescent microscopy will also capture a signal through the thickness, but the signal will be strongest at the focal plane, while confocal microscopy could be used to pinpoint the fluorescence changes through the depth of the sample, as well.

The kinetics of the fluorescence changes roughly matched those in stiffness, but the intensity began to saturate at higher levels of crosslinking, leading to the exponential correlation of stiffness with fluorescence. In our experiments, fluorescence intensity was evaluated over a wide range of crosslinking regimens – from no crosslinking solution to incubation in 10mM genipin for 12hrs. To appropriately compare intensity values across this range, constant exposure settings were used for all conditions, and using the same settings necessary to measure low intensity levels at low levels of crosslinking can cause saturation at higher levels of crosslinking. A more sensitive calibration can easily be achieved by optimizing the exposure times for a narrower range of fluorescence.

The strong correlation of genipin-generated fluorescence to mechanical properties allows simple, non-invasive confirmation of mechanical properties for crosslinked gels/equivalents of various geometries that may not be particularly amenable to mechanical characterization to provide measures of within- and between-experiment variabilities. The ability to visualize crosslinks also enables direct observation of spatially varying crosslinking fields, such as defined patterns and gradients, and associated indirect assessment of the spatially varying mechanical properties. In all cases, the thickness of

the actual sample and the ones used to generate a standard curve of fluorescence intensity vs. crosslinking (duration or concentration) must be carefully considered, as a thicker sample (of the same collagen concentration) will generate increased fluorescence; the correlation presented is specifically derived from the samples probed in this study. A separate calibration is necessary for other sample sizes and/or collagen concentrations. Moreover, the introduction of cells and subsequent compaction of the collagen gel will alter the observed fluorescence by increasing fiber density. The fluorescent labeling of collagen via genipin also presents interesting opportunities to observe and measure collagen degradation via lost fluorescence. Thus, while the quantitation of stiffness via fluorescence may be best applied for prescribing and screening initial conditions to evoke specific, stiffness-driven behavior, the fluorigenic potential of genipin may also be used to evaluate matrix remodeling.

References

1. Stoltz, J.F., *Adaptation concept, tissue remodeling, mechanobiology and tissue engineering: a survey.* Biorheology, 2004. **41**(3-4): p. 155-6.
2. Pedersen, J.A. and M.A. Swartz, *Mechanobiology in the third dimension.* Ann Biomed Eng, 2005. **33**(11): p. 1469-90.
3. Silver, F.H., D. DeVore, and L.M. Siperko, *Invited Review: Role of mechanophysiology in aging of ECM: effects of changes in mechanochemical transduction.* J Appl Physiol, 2003. **95**(5): p. 2134-41.
4. Silver, F.H., P.B. Snowhill, and D.J. Foran, *Mechanical behavior of vessel wall: a comparative study of aorta, vena cava, and carotid artery.* Ann Biomed Eng, 2003. **31**(7): p. 793-803.
5. Landis, W.J. and F.H. Silver, *The structure and function of normally mineralizing avian tendons.* Comp Biochem Physiol A Mol Integr Physiol, 2002. **133**(4): p. 1135-57.
6. Silver, F.H., I. Horvath, and D.J. Foran, *Mechanical implications of the domain structure of fiber-forming collagens: comparison of the molecular and fibrillar flexibilities of the alpha1-chains found in types I-III collagen.* J Theor Biol, 2002. **216**(2): p. 243-54.
7. Ranucci, C.S., et al., *Control of hepatocyte function on collagen foams: sizing matrix pores toward selective induction of 2-D and 3-D cellular morphogenesis.* Biomaterials, 2000. **21**(8): p. 783-93.
8. Willits, R.K. and S.L. Skornia, *Effect of collagen gel stiffness on neurite extension.* J Biomater Sci Polym Ed, 2004. **15**(12): p. 1521-31.
9. Casey, M.L. and P.C. MacDonald, *Lysyl oxidase (ras recision gene) expression in human amnion: ontogeny and cellular localization.* J Clin Endocrinol Metab, 1997. **82**(1): p. 167-72.
10. Quaglino, D., et al., *Extracellular matrix modifications in rat tissues of different ages. Correlations between elastin and collagen type I mRNA expression and lysyl-oxidase activity.* Matrix, 1993. **13**(6): p. 481-90.
11. Piacentini, M., et al., *"Tissue" transglutaminase in animal development.* Int J Dev Biol, 2000. **44**(6): p. 655-62.
12. Nurminskaya, M.V., et al., *Transglutaminase factor XIIIA in the cartilage of developing avian long bones.* Dev Dyn, 2002. **223**(1): p. 24-32.
13. Girton, T.S., T.R. Oegema, and R.T. Tranquillo, *Exploiting glycation to stiffen and strengthen tissue equivalents for tissue engineering.* J Biomed Mater Res, 1999. **46**(1): p. 87-92.
14. Wang, X., X. Li, and M.J. Yost, *Microtensile testing of collagen fibril for cardiovascular tissue engineering.* J Biomed Mater Res A, 2005. **74**(2): p. 263-8.
15. Paik, D.C., et al., *The nitrite/collagen reaction: non-enzymatic nitration as a model system for age-related damage.* Connect Tissue Res, 2001. **42**(2): p. 111-22.
16. Drew, B. and C. Leeuwenburgh, *Aging and the role of reactive nitrogen species.* Ann N Y Acad Sci, 2002. **959**: p. 66-81.
17. Chang, Y., et al., *Acellular bovine pericardia with distinct porous structures fixed with genipin as an extracellular matrix.* Tissue Eng, 2004. **10**(5-6): p. 881-92.

18. Liang, H.C., et al., *Effects of crosslinking degree of an acellular biological tissue on its tissue regeneration pattern.* Biomaterials, 2004. **25**(17): p. 3541-52.
19. Sung, H.W., et al., *Stability of a biological tissue fixed with a naturally occurring crosslinking agent (genipin).* J Biomed Mater Res, 2001. **55**(4): p. 538-46.
20. Sung, H.W., et al., *Crosslinking of biological tissues using genipin and/or carbodiimide.* J Biomed Mater Res A, 2003. **64**(3): p. 427-38.
21. Yerramalli, C.S., et al., *The effect of nucleus pulposus crosslinking and glycosaminoglycan degradation on disc mechanical function.* Biomech Model Mechanobiol, 2007. **6**(1-2): p. 13-20.
22. Liang, H.C., et al., *Genipin-crosslinked gelatin microspheres as a drug carrier for intramuscular administration: in vitro and in vivo studies.* J Biomed Mater Res A, 2003. **65**(2): p. 271-82.
23. Chen, S.C., et al., *A novel pH-sensitive hydrogel composed of N,O-carboxymethyl chitosan and alginate cross-linked by genipin for protein drug delivery.* J Control Release, 2004. **96**(2): p. 285-300.
24. Moffat, K.L. and K.G. Marra, *Biodegradable poly(ethylene glycol) hydrogels crosslinked with genipin for tissue engineering applications.* J Biomed Mater Res B Appl Biomater, 2004. **71**(1): p. 181-7.
25. Sung, H.W., et al., *Feasibility study of a natural crosslinking reagent for biological tissue fixation.* J Biomed Mater Res, 1998. **42**(4): p. 560-7.
26. Mi, F.L., *Synthesis and characterization of a novel chitosan-gelatin bioconjugate with fluorescence emission.* Biomacromolecules, 2005. **6**(2): p. 975-87.
27. Sung, H.W., et al., *Mechanical properties of a porcine aortic valve fixed with a naturally occurring crosslinking agent.* Biomaterials, 1999. **20**(19): p. 1759-72.
28. Takami, M. and Y. Suzuki, *Hydrophobic blue pigment formation from phosphatidylgenipin.* J Nutr Sci Vitaminol (Tokyo), 1994. **40**(5): p. 505-9.
29. Almog, J., et al., *Genipin--a novel fingerprint reagent with colorimetric and fluorogenic activity.* J Forensic Sci, 2004. **49**(2): p. 255-7.
30. Enever, P.A., D.I. Shreiber, and R.T. Tranquillo, *A novel implantable collagen gel assay for fibroblast traction and proliferation during wound healing.* J Surg Res, 2002. **105**(2): p. 160-72.
31. Giannone, G., et al., *Periodic lamellipodial contractions correlate with rearward actin waves.* Cell, 2004. **116**(3): p. 431-43.
32. Angele, P., et al., *Influence of different collagen species on physico-chemical properties of crosslinked collagen matrices.* Biomaterials, 2004. **25**(14): p. 2831-41.
33. Forgacs, G., et al., *Assembly of collagen matrices as a phase transition revealed by structural and rheologic studies.* Biophys J, 2003. **84**(2 Pt 1): p. 1272-80.
34. de Paula, M., et al., *Injectable gels of anionic collagen:rhamsan composites for plastic correction: preparation, characterization, and rheological properties.* J Biomed Mater Res B Appl Biomater, 2005. **75**(2): p. 393-9.
35. Knapp, D.M., et al., *Rheology of reconstituted type 1 collagen gel in confined compression.* Journal of Rheology, 1997. **41**(5): p. 971-992.
36. Semler, E.J., C.S. Ranucci, and P.V. Moghe, *Mechanochemical manipulation of hepatocyte aggregation can selectively induce or repress liver-specific function.* Biotechnol Bioeng, 2000. **69**(4): p. 359-69.

37. Huang, L.L., et al., *Biocompatibility study of a biological tissue fixed with a naturally occurring crosslinking reagent.* J Biomed Mater Res, 1998. **42**(4): p. 568-76.
38. Jin, J., M. Song, and D.J. Hourston, *Novel chitosan-based films cross-linked by genipin with improved physical properties.* Biomacromolecules, 2004. **5**(1): p. 162-8.
39. Chang, W.H., et al., *A genipin-crosslinked gelatin membrane as wound-dressing material: in vitro and in vivo studies.* J Biomater Sci Polym Ed, 2003. **14**(5): p. 481-95.
40. Liu, B.S., et al., *In vitro evaluation of degradation and cytotoxicity of a novel composite as a bone substitute.* J Biomed Mater Res A, 2003. **67**(4): p. 1163-9.
41. Mi, F.L., et al., *In vitro evaluation of a chitosan membrane cross-linked with genipin.* J Biomater Sci Polym Ed, 2001. **12**(8): p. 835-50.
42. Pelham, R.J., Jr. and Y.L. Wang, *Cell locomotion and focal adhesions are regulated by the mechanical properties of the substrate.* Biol Bull, 1998. **194**(3): p. 348-9; discussion 349-50.
43. Flanagan, L.A., et al., *Neurite branching on deformable substrates.* Neuroreport, 2002. **13**(18): p. 2411-5.
44. Reinhart-King, C.A., M. Dembo, and D.A. Hammer, *The dynamics and mechanics of endothelial cell spreading.* Biophys J, 2005. **89**(1): p. 676-89.
45. Stamenovic, D., et al., *Experimental tests of the cellular tensegrity hypothesis.* Biorheology, 2003. **40**(1-3): p. 221-5.
46. Tolic-Norrelykke, I.M., et al., *Spatial and temporal traction response in human airway smooth muscle cells.* Am J Physiol Cell Physiol, 2002. **283**(4): p. C1254-66.
47. Engler, A., et al., *Substrate compliance versus ligand density in cell on gel responses.* Biophys J, 2004. **86**(1 Pt 1): p. 617-28.
48. Engler, A.J., et al., *Myotubes differentiate optimally on substrates with tissue-like stiffness: pathological implications for soft or stiff microenvironments.* J Cell Biol, 2004. **166**(6): p. 877-87.
49. Shreiber, D.I., P.A. Enever, and R.T. Tranquillo, *Effects of pdgf-bb on rat dermal fibroblast behavior in mechanically stressed and unstressed collagen and fibrin gels.* Exp Cell Res, 2001. **266**(1): p. 155-66.

Appendix 2-1: FTIR characterization of Genipin-induced changes in collagen gels

Methods:

The reaction between genipin and collagen was monitored in situ using FTIR for up to 4.5 hours in Attenuated Total Reflection (ATR) geometry (Fig. 2A-1). A type I collagen solution was pipetted onto a silicon plate (~1cm x1.5cm) with the longer side beveled at a 45^{o} angle for entry and exit of the IR beam. The plate was sandwiched between two pieces of Teflon® with the top piece hollowed out to contain the collagen. The ATR setup was maintained at 37^{o}C in a nitrogen-purged Magna-IR 760 FTIR Spectrometer (Thermo Electron Corporation, Waltham, MA) to facilitate self-assembly of the collagen. After self-assembly, a solution of 10mM genipin was deposited on top of the collagen and allowed to diffuse into the gel to the silicon-collagen interface. Only the highest concentration of genipin was studied with FTIR to see the most exaggerated response to crosslinking. The infrared beam entered the silicon wafer and was reflected internally (~8x in the top face) creating an evanescent wave that probed a depth of ~2 μm above the surface of the silicon wafer into the collagen gel. Spectra for collagen crosslinked with 10mM genipin for 12hrs (with genipin solution equilibrated throughout the gel as described above), and then rinsed extensively with PBS to remove all free genipin, which represents the most extreme condition characterized rheometrically and fluorimetrically, and the spectra for a pure 10mM genipin solution were similarly acquired. Spectra from untreated type I collagen gels served as the reference for the crosslinked collagen, while the spectrum from water was used as the reference for the genipin solution.

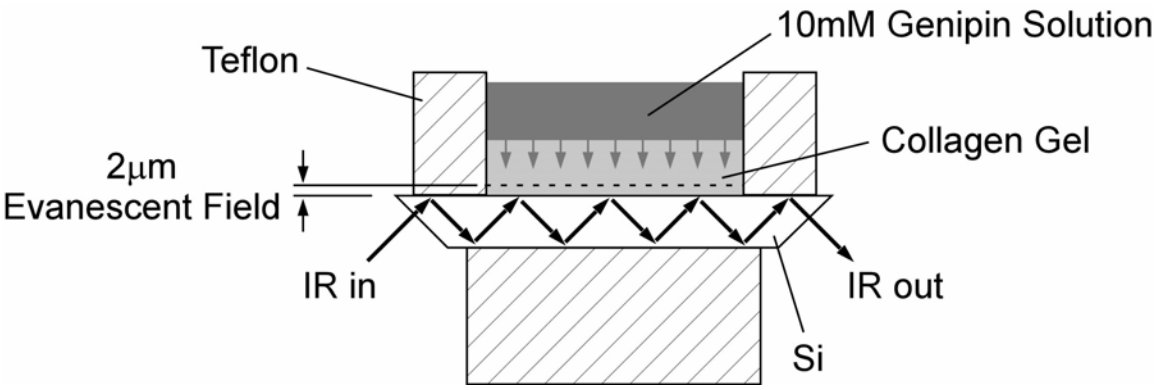

Figure 2A- 1: ATR setup showing genipin deposition for time-resolved study. Genipin solution (10mM) is deposited on top of and diffuses through the collagen gel. A 2μm region of the collagen gel is probed by the IR evanescent field during genipin-mediated crosslinking. The genipin solution (10mM) and collagen crosslinked with genipin for 33 hours are probed in a similar way.

Results:

The FTIR spectra of 10mM genipin, 'fully' genipin-crosslinked collagen (exposure to 10mM genipin for 12hrs and extensively rinsed of free genipin), and collagen during in situ crosslinking with 10mM genipin are presented together in Fig. 2A-2. The spectrum of the genipin solution is dominated by three modes at 990, 1080, and 1635 cm^{-1}, assigned to the ring C-H out-of-plane bend [1], ring C-H in-plane bend [1], and C=C double bond ring stretch modes [1, 2] of the core of the genipin molecule, respectively. The absorption at 1080 cm^{-1} may also include the C-O stretch mode of the primary alcohol on the genipin molecule [1]. Additionally, the C-O-C asymmetric stretch and the CH_3 bend of the methyl ester are observed at 1300 and 1433 cm^{-1}, respectively. The 12hr crosslinked collagen spectrum features these modes, as well as bands at 1104 cm^{-1} and 1370 cm^{-1} that are believed to be vibrational modes related to the formation of new bonds between genipin and the primary amines of lysine, hydroxylysine, or arginine residues in collagen. The band at 1370 cm^{-1} is assigned to the C-N stretch of the tertiary aromatic amine [1, 3] of the crosslinked genipin nitrogen iridoid [4] that is bound covalently to the collagen. The broad, flat appearance of the crosslinking band at 1370 cm^{-1} in the 12hr spectrum is likely due to the flanking of two genipin molecule modes at 1360 and 1395 cm^{-1} (unassigned). The band at 1104 cm^{-1} is assigned to the C-N stretch of the tertiary nitrogen with the adjacent aliphatic carbon atom present in lysine or arginine residues [1, 5]. An absorption near 1104 cm^{-1} is also present in the unreacted genipin molecule as a shoulder to the absorption at 1080 cm^{-1}. It is assigned to the vibrations of both the cyclic

ether and secondary alcohol on the six-membered ring of the genipin molecule. When genipin reacts with collagen, both of these moieties are removed.

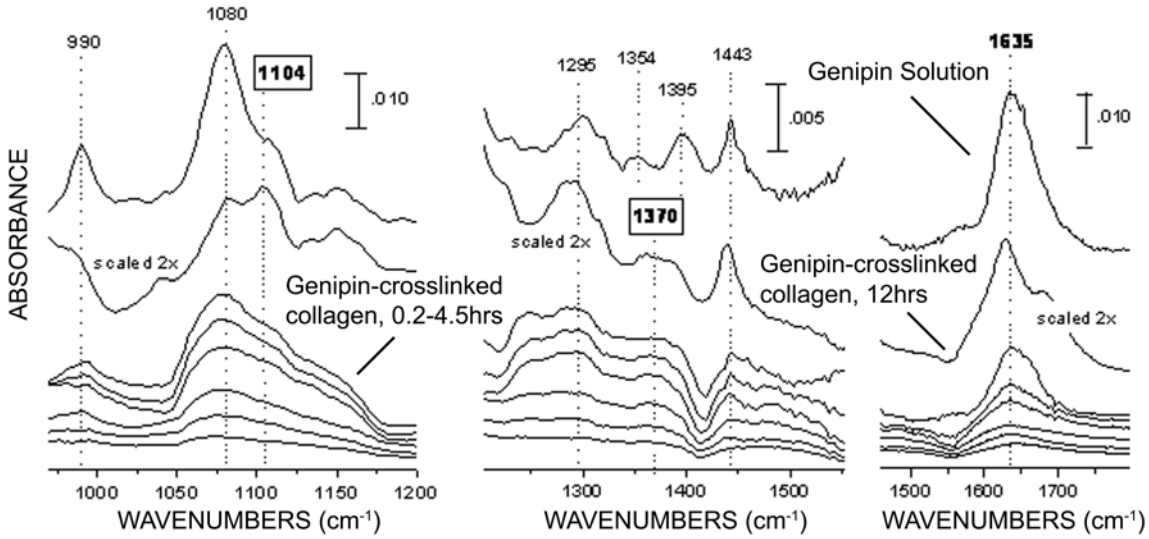

Figure 2A- 2: IR Absorbance spectra of 10mM genipin referenced to a spectrum of pure water (top); collagen after 12 hours of crosslinking with 10mM genipin and extensive rinsing, referenced to a spectrum of uncrosslinked collagen (second from top, scaled 2x) and collagen crosslinked with 10mM genipin *in situ*, 0.2, 0.4, 0.8, 1.7, 3.1, and 4.5 hours after adding genipin, referenced to the initially genipin-free collagen gel (bottom). Several spectral features that are present in the genipin solution alone, and/or the crosslinked and rinsed collagen are seen to evolve during the in situ crosslinking.

Furthermore, the band at 1104 cm^{-1} in the 12hr crosslinked spectrum is significantly stronger than the corresponding band in the spectrum of pure genipin (relative to the band at 1080 cm^{-1}), suggesting that this absorption band is mostly associated with modes formed as a result of crosslinking.

To better identify the origin of features present in the spectrum of 12hr crosslinked collagen, the changes in the collagen spectrum were monitored in situ during the first 4.5hrs of crosslinking (Fig. 2A-2). In this time-resolved experiment, spectral features were expected to increase due to: 1) diffusion of genipin into the region probed by the IR beam (the bottom surface of the collagen gel); and 2) crosslinking of collagen, leading to the appearance of new vibrational modes due to bonds formed during crosslinking. The in situ time-resolved spectra show the growth of several bands that are present in both crosslinked collagen and genipin, such as modes at 990, 1080, 1443, and 1633 cm^{-1}. In addition, the beginning of the growth of a band centered near 1370 cm^{-1} is observed. This feature is only seen in crosslinked collagen. Fig. 2A-3 summarizes the time dependence of several absorbance features. Due to the proximity of the various genipin molecule and crosslinking bands, calculated band areas may include components of smaller bands adjacent to the dominant spectral feature. The 1080 cm^{-1} band area (spanning 1040-1180 cm^{-1}) likely includes the growth of a number of other smaller bands possibly including the crosslinking feature at 1104 cm^{-1}, although it is too small to contribute substantially to band area. The feature at 1370 cm^{-1} is adjacent to genipin bands as stated earlier, and all are included in the area calculation (band complex spanning 1344-1414 cm^{-1}). To facilitate comparisons between trends in band growth,

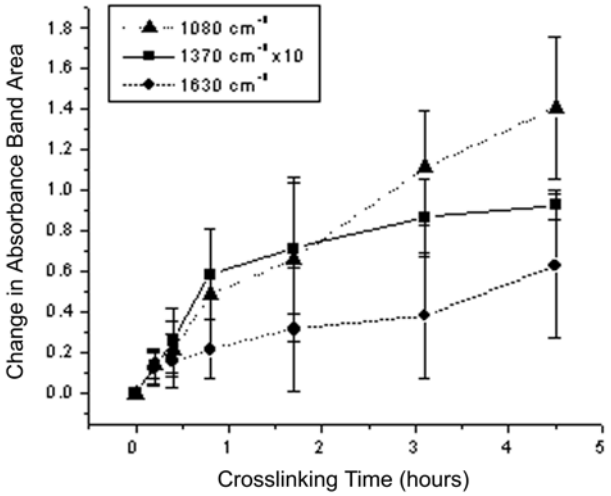

Figure 2A- 3: Changes in absorbance band areas versus crosslinking time for some of the highlighted bands in Figure 2A-2: two genipin bands (triangle, 1080 $cm^{-1}$and circle, 1630 cm^{-1}), and a new genipin-to-collagen crosslinking feature (square, 1370 cm^{-1}). To allow all spectra to be viewed on a common plot, values of smaller band areas were scaled by a constant, as indicated in the inset. Crosslinking time began (at t = 0) when genipin reached the bottom of the collagen gel at the interface with silicon. Error bars combine two sources of errors: 1) baseline selection for area calculations, and 2) reproducibility of runs. End point area values of each band for different runs were normalized to a common value due to variation in absolute absorbance area possibly caused by variation in collagen density among samples.

area absorbance values pf the weaker band at were 1370 cm^{-1} were scaled by a constant (indicated in the inset). Band area growth also differed in absolute value from run to run. Therefore, final in situ values (t = 4.5 hours) of absorbance band areas amongst runs were normalized to a common value for each band, respectively. Similar increasing monotonic trends were observed for change in absorbance of genipin bands at 1080 and 1630 cm^{-1}, however, the growth of the crosslinking band at 1370 cm^{-1} appeared to slow down within several hours. Indeed, the small area of the crosslinking band at 1370 cm^{-1} and its apparent slowing in growth are likely due to the relatively small number of genipin-to-collagen crosslinks in the gel that can form compared with the amount of genipin that diffuses to the region. A description of the modes marked in the spectra of Figure 2A-2 is shown in Fig. 2A-4.

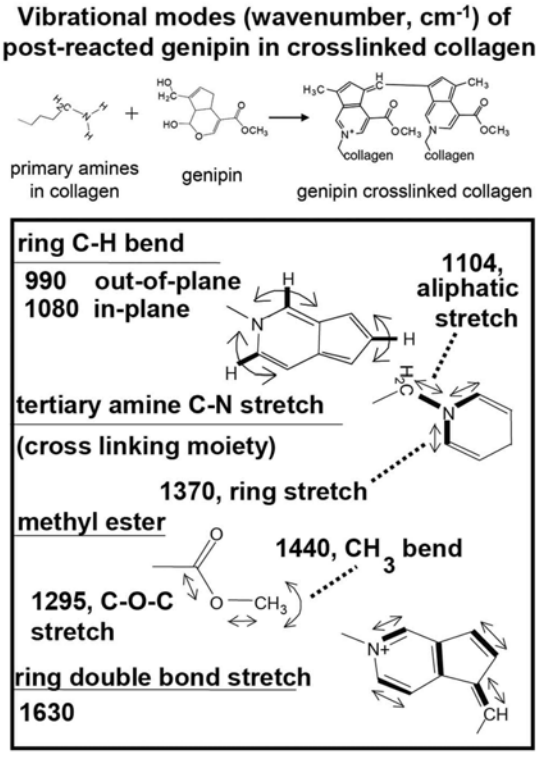

Figure 2A- 4: Description of the modes marked in the spectra of Figure 2A-2.

Discussion:

The colorimetric and fluorimetric properties of the crosslinked collagen are associated with molecular changes produced during crosslinking. In our study, the FTIR spectra include features at 1104 cm^{-1}(C-N stretch) and 1370 cm^{-1} (C-N stretch), that are neither characteristic of genipin nor collagen alone, and are therefore presumably associated with the crosslinked collagen and, perhaps, the color/fluorescence changes. The in situ FTIR demonstrated temporal changes in these features that paralleled the early changes in stiffness and fluorescence at 10mM. However, due to limitations in the FTIR set-up, the in situ spectroscopy could only be performed for ~4.5 hrs before evaporation began to introduce inconsistencies in the results, and a true correlation of stiffness-to-fluorescence-to-spectroscopy was not obtained. Interestingly, Touyama et al. examined the intermediate pigment changes that occur upon reaction of genipin with methylamine. Brownish-red intermediates were associated with 2-methyl-4-carbomethoxy-2-pyrindine derivatives, which had a spectroscopic feature at 1630cm^{-1} [33,55]. We also observed a peak at ~1630cm^{-1} in the rinsed, crosslinked collagen, which is shifted slightly to the left of a corresponding peak at ~1635cm^{-1} in the genipin solution. This shift may be artefactual due to water vibrational peak subtraction and/or due to double bonds, which contribute to the 1630/35 cm^{-1}, being slightly affected due to their proximity to the covalent bonding upon crosslinking and subsequently causing a small 5 cm^{-1} shift for the average of all double bonds.

References:

1. Socrates, G., *Infrared Characteristic Group Frequencies - Tables and Charts.* New York: John Wiley & Sons;, 1994.
2. Touyama, R., et al., *Studies on the Blue Pigments Produced from Genipin and Methylamine .1. Structures of the Brownish-Red Pigments, Intermediates Leading to the Blue Pigments.* Chemical & Pharmaceutical Bulletin, 1994. **42**(3): p. 668-673.
3. Liu, Y.M., et al., *Evaluation of amorphous carbon nitride thin film for magnetic rigid thin film disk by IR spectroscopy.* IEEE Transactions on Magnetics, 1997. **33**(5): p. 3106-3108.
4. Fujikawa, S., Y. Fukui, and K. Kunimasa, *A spontaneous reaction product between genipin and glycine.* Tetrahedron Letters, 1987. **28**(40): p. 4699-4700.
5. Butler, M.F., Y.F. Ng, and P.D.A. Pudney, *Mechanism and kinetics of the crosslinking reaction between biopolymers containing primary amine groups and genipin.* Journal of Polymer Science Part a-Polymer Chemistry, 2003. **41**(24): p. 3941-3953.

Chapter 3: Neurite growth in 3D collagen gels with gradients of mechanical properties

Abstract

We have designed and developed a microfluidic system to study the response of cells to controlled gradients of mechanical stiffness in 3D collagen gels. An 'H'-shaped, source-sink network was filled with a type I collagen solution, which self-assembled into a fibrillar gel. A 1D gradient of genipin – a natural crosslinker that also causes collagen to fluoresce upon crosslinking – was generated in the cross-channel through the 3D collagen gel to create a gradient of crosslinks and stiffness. The gradient of stiffness was observed via fluorescence. A separate, underlying channel in the microfluidic construct allowed the introduction of cells into the gradient. Neurites from chick dorsal root ganglia explants grew significantly longer down the gradient of stiffness than up the gradient and than in control gels not treated with genipin. No changes in cell adhesion, collagen fiber size, or density were observed following crosslinking with genipin, indicating that the primary effect of genipin was on the mechanical properties of the gel. These results demonstrate that (1) the microfluidic system can be used to study durotactic behavior of cells and (2) neurite growth can be directed and enhanced by a gradient of mechanical properties, with the goal of incorporating mechanical gradients into nerve and spinal cord regenerative therapies.

Introduction

The mechanical stiffness of tissue substrates and/or the surrounding network of extracellular matrix has proven to be a crucial regulator of cellular functions [1-3]. Growth and movement of several cell types can be dictated by the substrate/matrix stiffness. Lo and colleagues first reported the preferential movement of fibroblasts with respect to mechanical stiffness and coined the term 'durotaxis' to describe this phenomenon [4]. Since then, quantitative differences in cell motility and process growth have been identified for neurons [5, 6], smooth muscle cells [7], and epithelial cells [8]. In addition, many other phenotypic and functional phenomena have been observed for these and other cells that affect proliferation, differentiation, matrix synthesis and degradation, and traction-mediated events [9].

Directed cell migration is fundamental in many physiologic and pathologic processes such as tissue morphogenesis, wound healing, and tumorigenesis, and is also desired frequently in several tissue engineering applications. Of particular interest is the directed growth of neurites for regeneration of peripheral and central nervous system tissue. During development, axons are guided by attractive and repulsive soluble chemotactic cues and adhesion-based haptotactic cues, as well as contact guidance fields established by glia, aligned ECM proteins, and other axons, all of which are naturally presented in a three dimensional environment. Approaches to regenerating peripheral nerves and spinal cord tissue have attempted to include these directional cues to orient neurite growth [10]. Another parameter, mechanical stiffness, has been shown to significantly affect neurite outgrowth [5, 9], and has been used to enhance growth isotropically by tuning matrix stiffness to entice neurite growth [2], with improved

growth occurring generally on or in more compliant systems. However, gradients of stiffness in a 3D, tissue-like system have not been employed to orient and potentially enhance growth via durotaxis.

Several approaches have been devised to probe the influence of substrate/network stiffness on cellular behavior. Simple techniques involve functionalizing poly(acrylamide) gels of different concentrations and/or crosslinking density with proteins that foster cell attachment [4], or coating these gels with a thin 3D layer of collagen in or on which the cells are cultured [3] to examine the response to uniform presentation of stiffness. Microfabrication techniques have been used to develop more elaborate systems comprising, for example, calibrated, elastomeric microposts of different dimensions, which maintain different bending properties to present a 2D substrate of varying stiffness to the cells [11], or gradients of stiffness generated through photo-initiated crosslinking of a 2D substrate [12].

We have developed a system to generate stable 1D gradients of mechanical properties through a 3D collagen gel. Microfluidic networks are pre-filled with a type I collagen solution, which is allowed to self-assemble. Gradients of genipin, a cell-compatible, fast-acting crosslinking agent [13], are generated through the collagen gel using a source-sink network for a defined period of time to establish a 1D gradient through the 3D gel. Collagen crosslinked with genipin fluoresces at 630nm when excited by light at 590nm [14]. In a previous study, we found that the intensity of the fluorescence correlates well with the degree of crosslinking and storage modulus of the collagen gel [15]. As such, genipin-generated patterns of crosslinks are directly visualized via fluorescence, and interpreted as a gradient of stiffness. We demonstrate the

functionality of these gradients by biasing and enhancing neurite outgrowth from chick dorsal root ganglia (DRGs). Potential effects of genipin-mediated crosslinking on cell adhesion and collagen fiber size and density were examined in separate assays and judged to minimally contribute to the observed neurite growth.

Methods

Microfluidic Networks

A simple, 'H'-shaped, 'source-sink' arrangement was used to generate gradients in a cross channel connecting source-to-sink (Fig 3-1). Channel dimensions for the source-sink network were selected by simulating flow in networks with a computational fluid dynamics package (ESI-CFD Huntsville, AL) to achieve uniform gradients across the width of the cross channel, which showed that the source and sink channels should be at least 2x wider than the cross-channel. Source and sink channels were 500μm wide x 100μm deep and were connected by a 5mm long, 150μm wide, and 100μm deep channel (Fig 3-1A). Microfluidic networks were fabricated using standard photolithography techniques [16] at Bell Labs/Lucent Technologies (Murray Hill, NJ) through a grant from the New Jersey Nanotechnology Consortium. The photomask was printed from an AutoCAD drawing of the network design. A silicon wafer was spin-coated with SU-8 negative photoresist (Microchem, Newton, MA) and baked for 5min at 65°C followed by 10min at 100°C. The photoresist was exposed to UV light through the photomask using a Quintel 2001 CT Mask Alignment/Exposure system. The coated wafer was baked again and immersed in SU-8 developer for 12min to clear un-reacted photoresist and form the final 'master'.

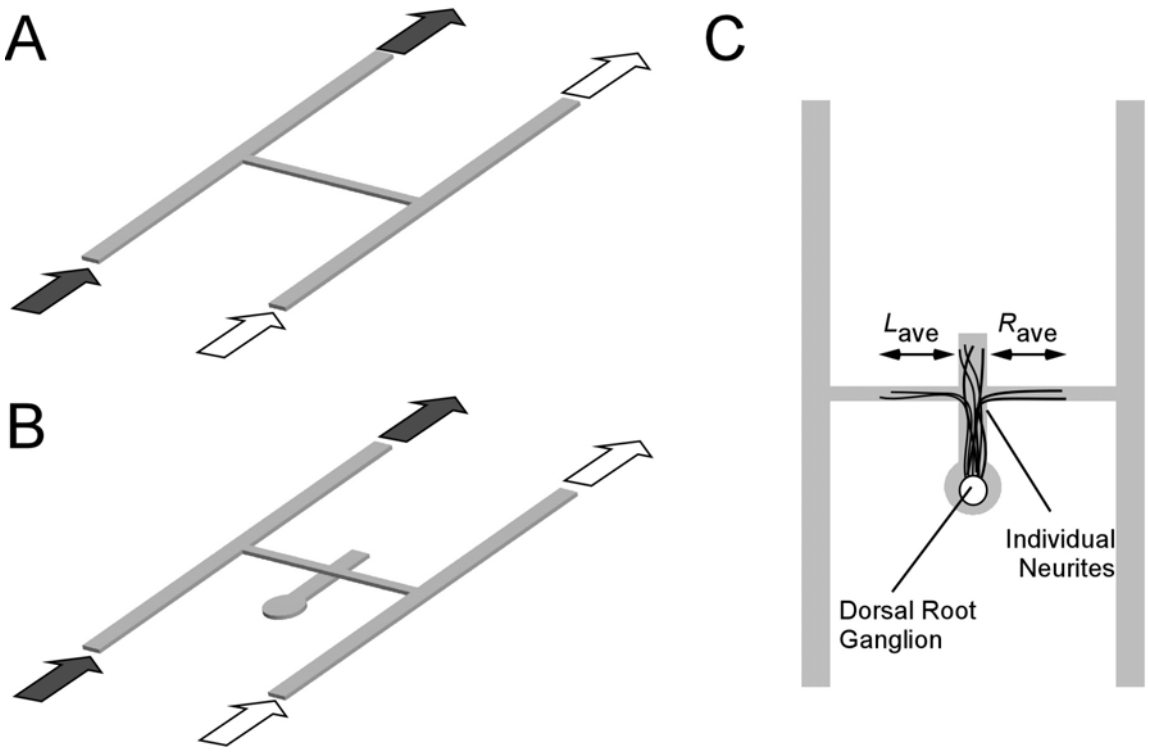

Figure 3- 1: Schematic of 'H'-shaped microfluidics network used to create gradients. (A) After filling the network with collagen solution and allowing the collagen to self-assemble into a gel, a gradient of genipin is created in the cross-channel by supplying culture medium with genipin in the source inlet (dark arrows) and medium alone in the sink channel (white arrows). (B) To introduce cells into the gradient, a second network (facing channel-side up) comprising a straight channel and circular well is filled with collagen and a DRG placed in the well. After self-assembly, the 'H'-network is placed on top of the straight channel, creating a collagen-collagen interface at the intersection. The gradient is then formed in the cross-channel as in (A). (C) Top view of the network shown in (B) with neurite growth drawn in. Neurite growth is quantified by counting the number of processes and the average length of processes that extend from the DRG and grow up and into the cross-channel in the left (*L*) and right (*R*) directions.

A poly(dimethyl siloxane) solution (PDMS; Dow Corning, Midland, MI) was poured over the master and baked overnight at 50°C to produce a negative relief. The PDMS was removed, the design was cut out of the mold, and holes were punched for the inlet and outlet using a blunt 19-gauge syringe. The PDMS and a clean glass slide were plasma treated and bonded together to form the final device. The inlets were connected to a syringe pump (Harvard Apparatus, Cambridge, MA) using polyethylene tubing (Small Parts, Miami Lakes, FL).

Collagen Preparation

Type I collagen solutions were prepared as previously described [17] by mixing 20µl 1M Hepes buffer , 140µl 0.1N NaOH, 100µl 10X PBS , 52µl of PBS (Invitrogen, Carlsbad, CA), and 677µl of a 3.0mg/ml type I collagen solution (Elastin Products Co., Owensville, Missouri) to make a 2.0mg/ml collagen solution. The collagen solution self-assembled into a fibrillar gel upon incubation at 37°C.

Generation of Gradients of Mechanical Properties

The microfluidic networks were first filled uniformly with a type I collagen solution using a syringe pump operating at 0.1ml/min while viewing the network with an upright tissue culture microscope to ensure that the network was filled properly with no bubbles. After inspection, the filled microfluidic network was transferred to a humidified, 37ºC, 5% CO_2 incubator, and the collagen was allowed to self-assemble for at least one hour. The source solution was then changed to culture medium (DMEM + 10% FBS (Atlanta Biologicals, Lawrenceville, GA), 1% glutamine, 1% penicillin/streptomyosin (Sigma, St Louis, MO)) plus a defined concentration of genipin (Challenge Bioproducts Co., Taichung, Taiwan) of either 1mM or 10mM, while the sink solution was changed to

the same medium without genipin. These solutions were flowed gently through the fibrillar gel-filled microfluidic network at 0.3μl/min at 37ºC for 12hrs. To remove the remaining genipin from the network following the desired incubation period, the inlets were switched to medium without genipin. The cross-channel was flushed by actuating only one randomly selected inlet syringe at 0.3μl/min for 3hrs, after which medium was again delivered through both inlets.

Gradient Evaluation

Gradients of genipin-mediated crosslinking were verified by examining the fluorescence intensity emitted by the crosslinked collagen (590nm Exc, 630nm Em), which indirectly verified the pattern of mechanical properties. Our previous study confirmed that fluorescence intensity strongly correlates with the storage modulus measured in shear using parallel plate rheometry for a range of fluorescence intensities generated by crosslinking gels for 2-12hrs with 0-10mM genipin in 24-well plates [15] This calibration was repeated for 0, 0.1, 0.5, and 1mM genipin crosslinked for 12 hrs in single channel microfluidic networks with the same channel depth as used above. Collectively from these studies, the storage modulus in shear at 0.1Hz (the lowest frequency tested) ranges from ~60Pa for untreated collagen to ~360Pa for collagen crosslinked with 1mM genipin and ~800Pa for 10mM genipin for 12hrs of crosslinking. Following rinsing, networks were transferred to a computer controlled stage and imaged using an Olympus IX81 inverted microscope (Olympus, Melville, NY). The fluorescence intensity in the cross-channel was quantified using Olympus Microsuite Image Analysis Software (Olympus, Melville, NY).

Neurite Outgrowth Assay

To evaluate if the changes in stiffness can induce phenotypic changes in cellular behavior, neurite outgrowth from chick DRGs was evaluated in the presence of durotactic gradients. The microfluidic system was modified to include a small well for DRG culture. A second network was generated that comprised a 1mm diameter well connected to a straight 500μm wide and 100μm deep channel (Fig 3-1B). This network was place upside down (channels facing up) on a glass slide and filled with collagen solution. DRGs were isolated from E8 chick embryos (Charles River Laboratories, Willmington, MA), and a single DRG was placed in the collagen-filled circular well. The network was transferred to a 37 ºC incubator to facilitate self-assembly, entrapping the DRG in the collagen gel. The 'source-sink' network was then plasma treated and bonded to the gel-filled underlying network such that the middle of the cross channel of the 'source-sink' intersected with the straight channel of the underlying network approximately 1000μm from the circular well containing the DRG. The top network was filled with collagen solution, which was allowed to gel. Gels were then treated with genipin and rinsed as described above. Gradients of crosslinking were again confirmed by visualizing the gradient of fluorescence.

Networks were transferred to a humidified, 37ºC, 5% CO_2 incubator and perfused with fresh medium (DMEM supplemented with 10% FBS and 100 ng/ml NGF (R&D Systems, Minneapolis, MN)) via gravity flow. DRGs were cultured in the networks for five days to allow neurites to grow through the collagen gel and extend up and into the cross-channel a significant distance, potentially in either direction.

To visualize neurite growth after 5 days in culture, the neurites were stained immunohistochemically in the networks for neurofilament proteins. Inlet solutions were changed to 4% paraformaldehyde for 3 hours to fix the collagen and cells, then changed to a rinse buffer comprising 1% BSA + 0.5% Triton in PBS for 3 hours. Inlet solutions were changed to a 10% goat serum blocking solution in rinse buffer for 4 hours, and then to an anti-neurofilament antibody cocktail of 1:200 α-NF 200 and 1:1000 α-NF 68 (Sigma) overnight. Networks were rinsed for 4 hours, and inlets were switched to a 1:400 dilution of goat anti-mouse Alexa 488 secondary antibody (Molecular Probes/Invitrogen, Eugene, OR) and incubated overnight. Devices were rinsed a final time for 4 hours and then transferred to an inverted epifluorescence microscope for imaging.

Neurite growth was quantified as the number and length of neurites projecting up the stiffness gradient vs. down the stiffness gradient, or in opposite directions for control experiments and uniform crosslinking where no gradient was present. For each device, digital images were taken with a 40X objective at the intersection of the explant and cross-channels and at the end of the individual growth cones. Using Olympus Microsuite Image Analysis Software, the (X,Y) coordinates were recorded for each growth cone and for the channel intersection to determine the distance of growth in the gradient channel (Fig 1C). For a given experiment, one experimental condition (0-1mM for 12hrs, 0-1mM for 24hrs, or 1-1mM for 12hrs) and one control condition (0-0mM) were performed, and in all cases, explants for the paired experiments were from the same chick embryo. Further elements of the data analysis for neurite outgrowth are presented in the *Results* section.

Adhesion Assay

Cell adhesion on collagen gels crosslinked to different degrees with genipin was tested using primary rat dermal fibroblasts as a uniform cell type and with a mixed population of cells harvested from dissociated E8 chick embryo DRGs. DRG explants were suspended in a solution of 0.3% BSA (Sigma), 0.05% trypsin (Sigma) in HBSS (Lonza, Allendale, NJ) for 10 min at 37 ºC, vortexing every 3 min. The sample was centrifuged for 2 min at 2,000 rpm. Cells were resuspended in 1ml media (DMEM supplemented with 10% FBS, 100 ng/ml NGF) and triturated 10 times with a 200 µl pipette tip placed on top of a 1,000 µl pipette tip. Cells were counted using a hemocytometer. Collagen solution (100µl, prepared as above) was pipetted into each well of a 24-well plate. The plate was then incubated at 37ºC for 60min to allow the collagen to self-assemble. The collagen gel in each well was incubated in 600µl genipin solution at 0, 0.5, 1, 5, or 10mM in PBS for 12 hours to allow crosslinking, during which time the plates were on a rocker to ensure rapid equilibration of genipin throughout the gel. The 0.5 mM condition was omitted for experiments with dissociated DRG cells. Each concentration was performed in triplicate in each plate. After 12 hours, the gels were washed three times with PBS. Fibroblasts or dissociated DRG cells (100,000 cells/well) were seeded on top of the gels and allowed to attach for 4 hours. The gels were then washed twice with PBS, and the remaining cells were labeled using Calcein-AM (Invitrogen Carlsbad, CA). Plates were transferred to the computer controlled stage of an Olympus IX81 inverted microscope operating in epifluorescence mode (480nm Exc, 535nm Em). Four images were taken at random per sample and the cells were counted

manually. The adhesion experiment was repeated 3 times, and the average number of attached cells per field compared with ANOVA, with significance levels set at $P < 0.05$.

Fibril size and density assay

To evaluate the effects of the genipin crosslinking regimen on collagen fiber size and density (as an indirect assessment of gel porosity), straight microfluidic channels (500μm wide, 100μm deep, and 1cm long) were bonded to glass coverslips and filled with collagen solution that was spiked with FITC-labeled collagen (10% v/v; Elastin Products), to allow for visualization of fibers. Following self-assembly, inlets were changed to genipin solutions at concentrations of 0, 1, or 10mM for 12 hours. Inlet solutions were then switched to PBS and devices were rinsed for 3 hours. Devices were transferred to a Leica TCS SP2/MP confocal microscope (Leica Microsystems, Exton, PA). Images were taken at 63X with a 2X digital zoom at 488nm excitation with a 500-535nm emission bandpass filter. All image frames underwent two line and frame averaging. Three images were taken at random in each device. Each image was divided into nine equal squares. The average number and diameter of fibers was determined in three of the nine squares with the image analysis software. The analysis was repeated for 3 gels in each condition, and results were compared with ANOVA (significance set at $P < 0.05$).

Results

Gradient characterization

Exposure of fibrillar collagen within microfluidic networks to a gradient of genipin generated a gradient of crosslinks in the collagen, which was observed as a gradient of

fluorescence intensity. The intensity profile in cross-channels was evaluated with image analysis tools (Fig 3-2). A source-sink combination of 10mM-0mM genipin generated a steeper gradient in intensity than a gradient from 1mM-0mM. Uniform presentation of genipin produced uniform increases in intensity compared to 0mM solutions (data not shown). When the underlying explant channel was included for neurite outgrowth experiments, the intensity plot increased at the intersection of the gradient and explant channels but returned to the original linear plot thereafter, indicating that the integrated signal of fluorescence intensity from the thicker collagen gel at the intersection was responsible for the increase, rather than an increase in crosslinking (Fig 3-3). Based on the calibration of fluorescence intensity to storage modulus measured at 0.1Hz and 1% shear strain amplitude, gels treated with 1mM genipin for 12hrs had an average gradient (+/- SEM) of 0.064 +/- 0.005 Pa/μm across the 5-mm long channel. When the exposure time was increased to 24hrs, the gradient increased by ~12% to 0.075 +/- 0.005 Pa/μm.

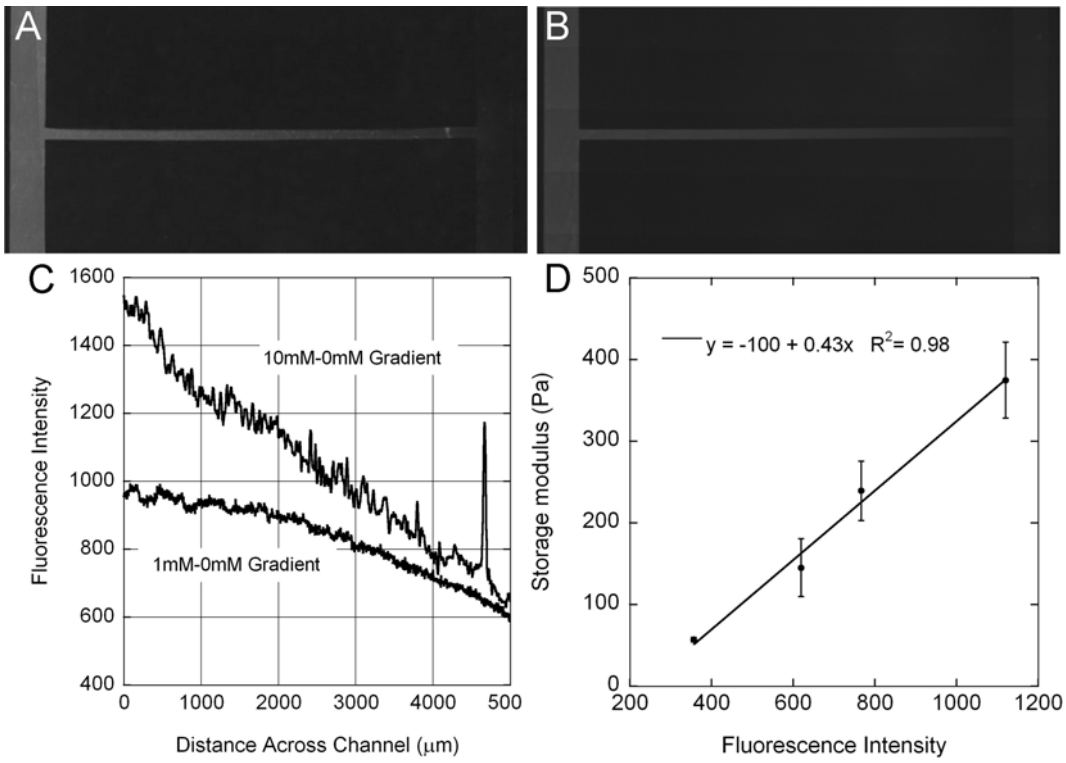

Figure 3- 2: Representative gradients of fluorescence generated by exposure to a gradient of (A) 10mM genipin-0mM genipin or (B) 1mM genipin-0mM genipin for 12hrs. (C) Grayscale intensity values along the cross-channel for the images shown in (A) and (B). (D) The intensity of fluorescence correlates to the stiffness of the gel, as shown in this representative calibration. The gradient of fluorescence is steeped when gels are exposed to a steeper gradient of genipin.

Neurite outgrowth assay

DRG explants were cultured in an underlying channel that intersects at the center of the cross channel and therefore the approximate center of the gradient (e.g. ~170 Pa for gradients generated by 12hr exposure to 0-1mM genipin). In all conditions, several neurites (typically 15-30) grew from the underlying channel into the cross-channel, although most remained in the original channel (Fig 3-4). Those that entered the cross-channel could grow in either direction – either up or down the stiffness gradient, or for control cases, in uniformly untreated or uniformly crosslinked channels. For each experiment, the average length within the cross-channel of the neurites that grew in each of the two directions was calculated. These were then plotted collectively for a given condition on the same set of axes, where the longer length was plotted on the abscissa and the shorter length on the ordinate. The data from each of the four experimental conditions was fit to a line that passed through the origin to evaluate the uniformity of growth. For completely uniform growth, the average lengths should be equal in the two directions, and the best fit line should have a slope of one. Biased growth would result in a shallower slope.

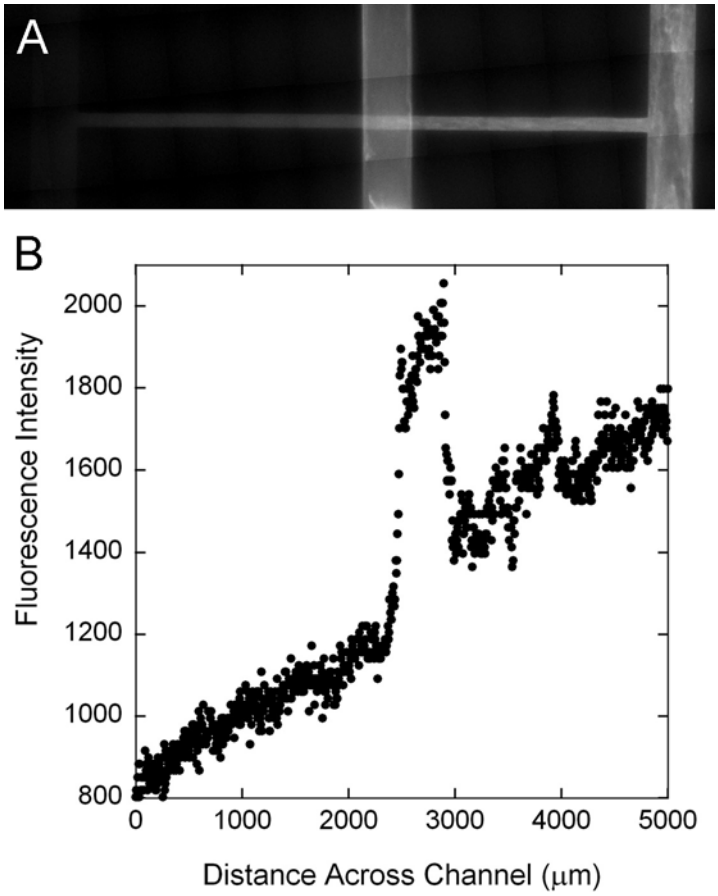

Figure 3- 3: (A) Representative gradient of fluorescence in modified networks with underlying explant generated by a gradient from 0mM (left) to 10mM (right) of genipin for 12hrs. (B) A roughly linear gradient of intensity is observed in the cross-channel, but includes a spike in intensity at the intersection of the two channels, after which intensity returns to the same linear contour. The increase in intensity is due to the integration of fluorescence through the thicker gel at the intersection.

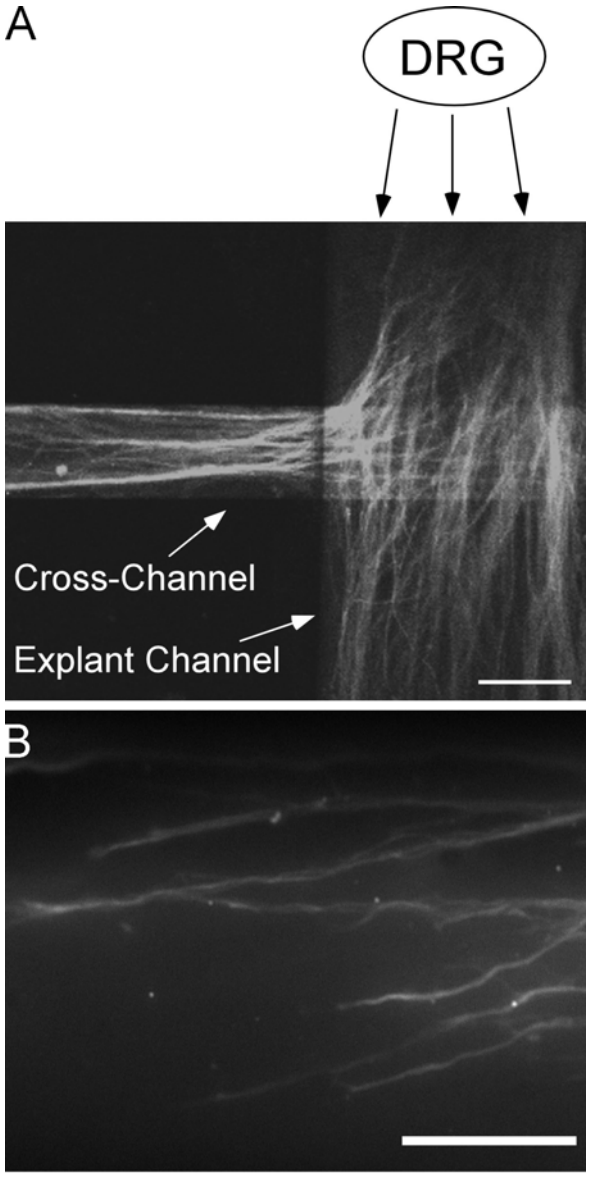

Figure 3- 4: Confocal micrograph of neurite growth in the collagen gel-filled network. A DRG was placed within a collagen gel in the underlying explant channel and cultured for 5 days, at which time the networks were perfused with paraformaldehyde and then stained immunohistochemically for neurofilament proteins. Neurites grew from the DRG and either continued in the explant channel or grew up and into the cross-channel of the overlying 'H'-shaped network. Scale bar: 150μm.

Data from gels exposed to a genipin gradient for 12hrs, 24hrs, and uniform presentation are shown in Fig 3-5. In no case was growth exactly uniform, and all points fell below the line that indicated perfectly symmetric growth. Control experiments were clustered near the ideal line and had slopes (+/- 95% confidence intervals) of 0.89 +/- 0.025 for assays not exposed to genipin, 0.90 +/- 0.059 for assays exposed to 0.5mM genipin uniformly, and0.83 +/- 0.068 for assays exposed to 1mM genipin uniformly. In gradient experiments, the longer length was always in the direction of greater compliance (down the gradient of stiffness). The slopes of the lines fitted through the 0-1mM gradient experimental points and the origin were 0.45 +/- 0.209 for 12hr exposure and 0.57 +/- 0.230 for 24hr exposure, which were both substantially lower than the slopes of the control experiments and clearly below a slope of one. As a measure of the strength of bias, the ratio of relative growth down the gradient (or in the 'longer' direction for uniform 0.5mM and 1.0mM assays) vs. the relative bias in the controls for that was taken and averaged across all experiments. On average, neurite bias was 2.51 +/- 0.77 times greater for 0-1mM, 12hr exposure and 1.77 +/- 0.24 times greater for 0-1mM, 24hr exposure. For uniform presentation, the average ratios were 1.00 +/- 0.03 for exposure to 0.5mM genipin, and 1.04 +/- 0.05 for exposure to 1.0mM genipin. The experimental conditions and relative growth biases are summarized in Table 3-1.

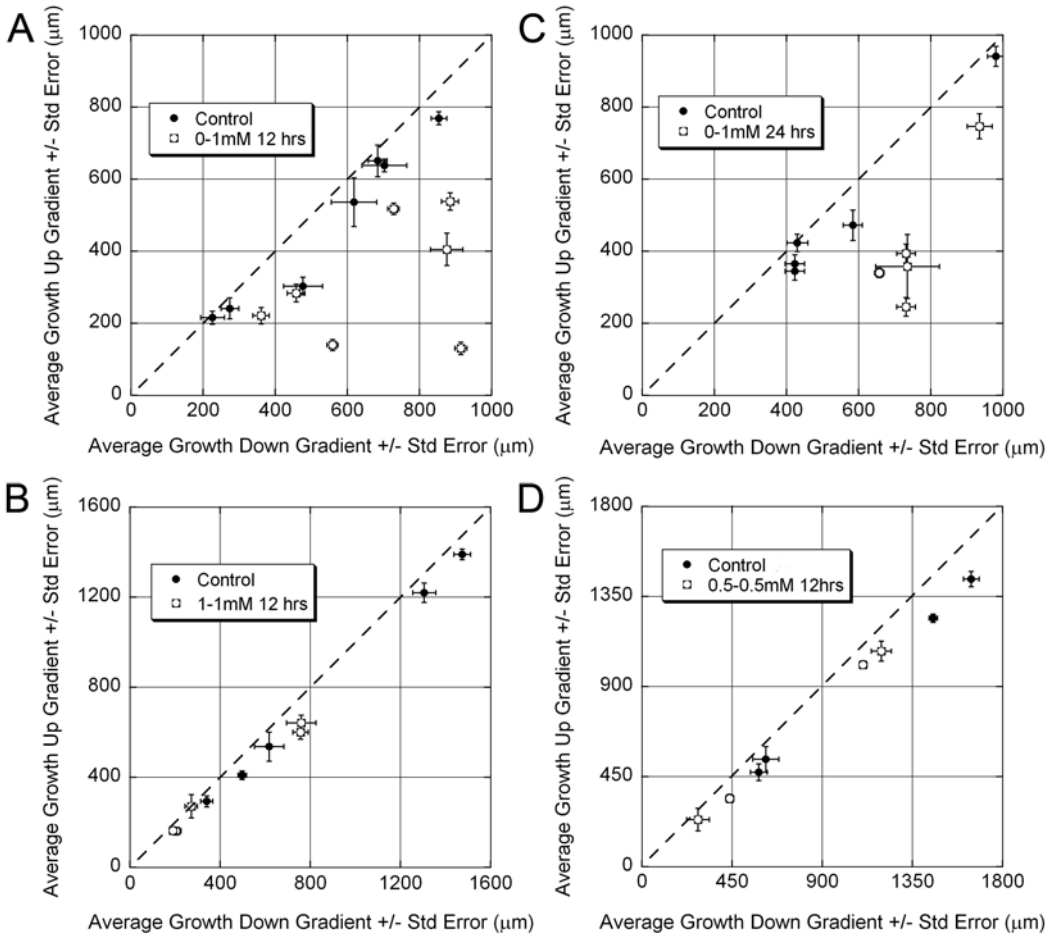

Figure 3- 5: Growth in gradients of stiffness generated by exposing to 0-1mM genipin for 12hrs, 24hrs, and uniform presentation. Each point represents the average growth of neurites in a single network. The longer growth was always expressed as the x-coordinate. Thus, perfectly uniform growth would have a slope of one (dashed line), and biased growth would have a slope less than one. In no case was growth perfectly uniform, though in control experiments, the points fell very close to the dashed line. In gradient experiments, the direction of longer growth was always in the direction of lower stiffness, and these points deviated significantly from the line indicating uniform growth.

Condition	Storage modulus across microfluidic network [a]	n	Relative growth bias [b]
1-0 mM, 12 hour exposure	377 ± 25 – 57 ± 2.8 Pa	7	2.51 ± 0.77
1-0 mM, 24 hour exposure	432 ± 25 – 57 ± 2.8 Pa	5	1.77 ± 0.24
1-1 mM, 12 hour exposure	377 ± 25 – 377 ± 25 Pa	5	1.04 ± 0.05
0.5-0.5 mM, 12 hour exposure	160 ± 28 – 160 ± 28 Pa	5	1.00 ± 0.03

[a] Storage modulus range estimated from calibration of storage modulus measured at 0.1 Hz and 1% shear strain to fluorescence intensity. Results are average ± SE.
[b] Relative growth bias calculated by taking the ratio of growth down : growth up the gradient of stiffness, normalizing by the same ratio from the matched, untreated control experiment, and averaging across all experiments. Results are average ± SE.

Table 3-1: Summary of growth assays.

No statistically significant differences in the number of neurites that extended in the two directions were observed for the untreated control or controls treated with uniform presentation of 0.5mM or 1mM genipin (Fig 3-6). Significantly fewer neurons extended in the 1mM uniform cases than in the untreated controls, but not the 0.5mM uniform controls (P = 0.83). The number of neurites extending down the stiffness gradient was significantly greater than up the gradient for the 0-1mM gradient, 12 hr exposure experiments (P = 0.01); however, this trend was not observed for the experiments treated with a gradient of genipin for 24hrs (P = 1.0).

Significant variability in the magnitude of growth and in the number of neurites was observed in all conditions among different experiments. For example, while always close to uniform, growth in some control experiments was double the growth in other experiments, and the day-to-day trends in growth in the experimental conditions typically paralleled that in the untreated controls. As such, the variability seemed to be linked to an experimental condition – most likely differences in the viability of explants from particular chick embryos. These day-to-day variations were accounted for in the statistical analysis of the length of neurites in gradient and uniform conditions by comparing the length of neurite growth among the control condition, up the gradient of stiffness, and down the gradient of stiffness for the 0-1mM, 12hr exposure experiments with a two-way ANOVA using Type III sum of squares, where the gradient condition was a fixed effect and the day of the experiment was a random effect [17], followed by Scheffe's post hoc test for pairwise comparisons. Average length in gradient experiments is shown in Fig 3-7.

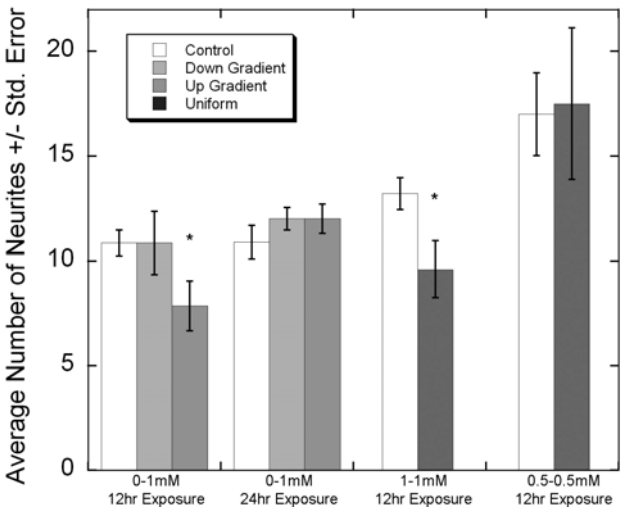

Figure 3- 6: Neurite numbers in experimental cases were compared to matched controls performed on the same day with DRG explants from the same chick. Neurite number was significantly decreased up the gradient of stiffness compared to down the gradient and compared to control cases for 12hr exposure, but not 24hr exposure. Neurite number for uniformly treated 1mM gels was less than matched controls. *, ANOVA followed by Scheffe's post hoc test, $P < 0.05$.

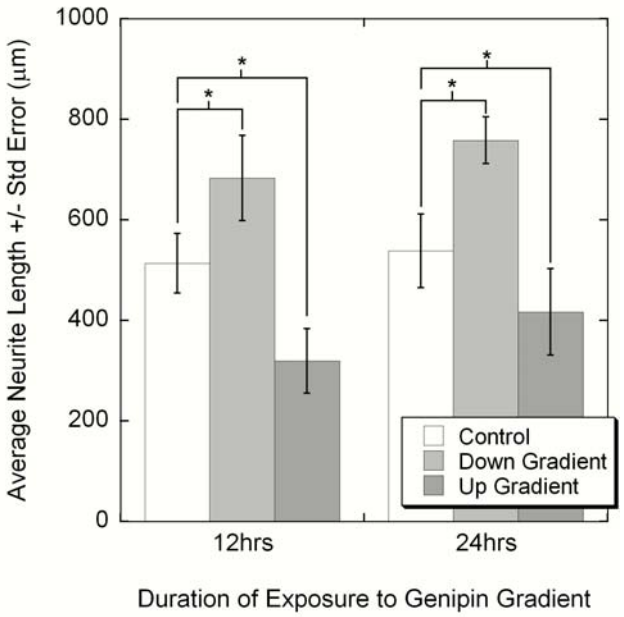

Figure 3- 7: Neurite lengths in gradient cases were compared to matched controls performed on the same day with DRG explants from the same chick. For both 12hr and 24hr treated gels, the average growth down the gradient of stiffness was significantly greater than growth in control, untreated gels, which was greater than growth up the gradient of stiffness. *, two-way ANOVA followed by Scheffe's post hoc test, $P < 0.05$.

The length of neurite growth down the stiffness gradient was significantly greater than growth in the control condition (P = 0.002), and growth in the control was significantly greater than growth up the stiffness gradient (P = 0.001). Similar results were observed in experiments where the gradient was generated with 24hr exposure. Growth down the stiffness gradient was significantly greater than the control growth (P= 0.001), and control growth was greater than growth up the stiffness gradient (P = 0.016). Finally, growth in untreated controls was significantly greater than in gels that were crosslinked with a uniform presentation of 0.5mM for 12hrs (P = 0.38) 1mM genipin for 12hrs (P = 1.4e-5).

Adhesion Assay

The influence of genipin-mediated crosslinking on the adhesion properties of collagen gels was evaluated with a simple detachment assay using dermal fibroblasts as a representative cell that could be uniformly presented. No significant differences were observed in the adhesion of the fibroblasts to collagen gels crosslinked with 1, 5, or 10mM genipin for 12 hours compared to the untreated controls (Fig 3-8A; P = 0.679). The assay was repeated with cells from dissociated DRGs (Fig 3-8B), which represent a mixed population of primarily neurons, Schwann cells, and fibroblasts and again no significant differences in adherent cells were detected (P=0.918). These results indicate that exposure to a gradient of genipin did not introduce significant changes to the adhesion profile presented to cells to influence cell behavior.

Fibril size and density

The influence of genipin-mediated crosslinking on collagen gel fiber morphology was estimated by evaluating the average size and density of collagen fibers in hydrated gels from high magnification epifluorescent images taken with confocal microscopy. Exposure to 1-10mM genipin for 12hrs did not produce any overt changes in fiber morphology or density. No significant differences were observed in the average fibril size (ANOVA, $P = 0.524$) or fibril density ($P = 0.194$; Fig 3-9). These results suggest that the gradient of genipin did not introduce a significant gradient of porosity to influence diffusion or present spatially varying steric hindrance.

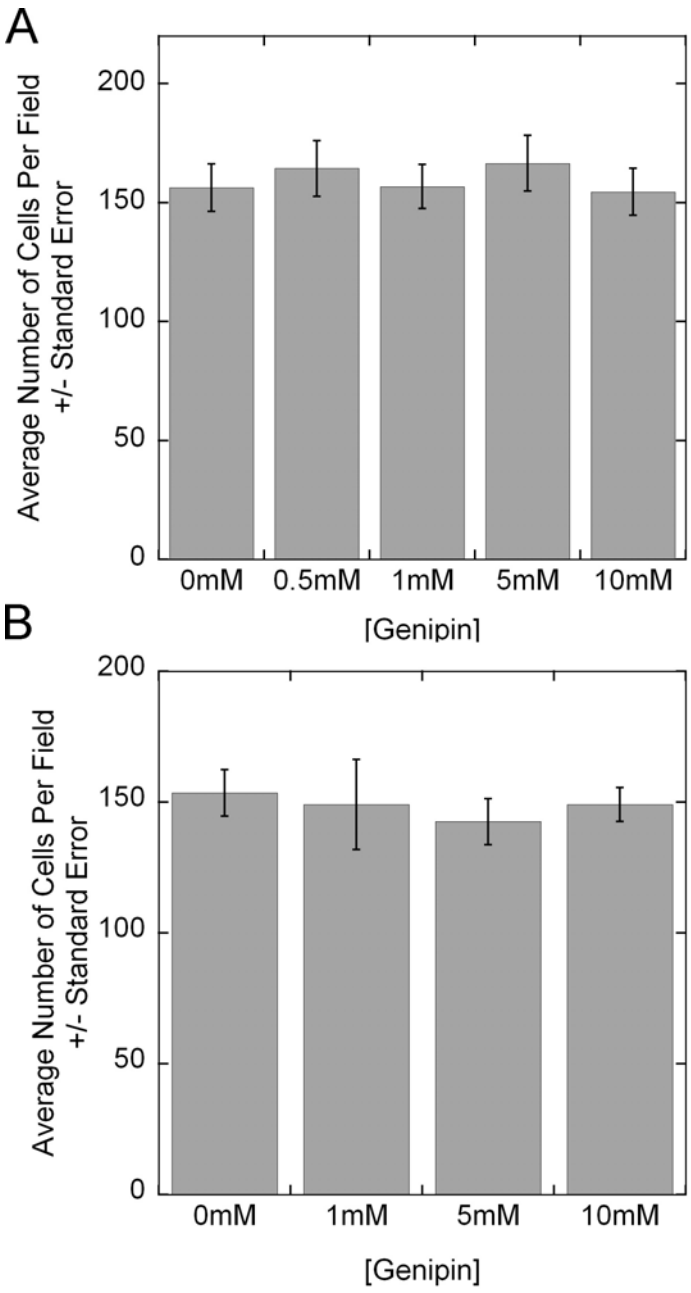

Figure 3- 8: Effects of genipin treatment on cell adhesion. Collagen gels were formed in 24 well plates and crosslinked with defined concentrations of genipin for 12hrs and then rinsed extensively. (A) Rat dermal fibroblasts or (B) cells from dissociated DRG explants were seeded on the gels and allowed to attach for 4hrs. Detached cells were removed with rinsing, and the remaining cells were counted. Fibroblast adhesion to collagen gels treated with 0-10mM genipin for 12hrs did not vary.

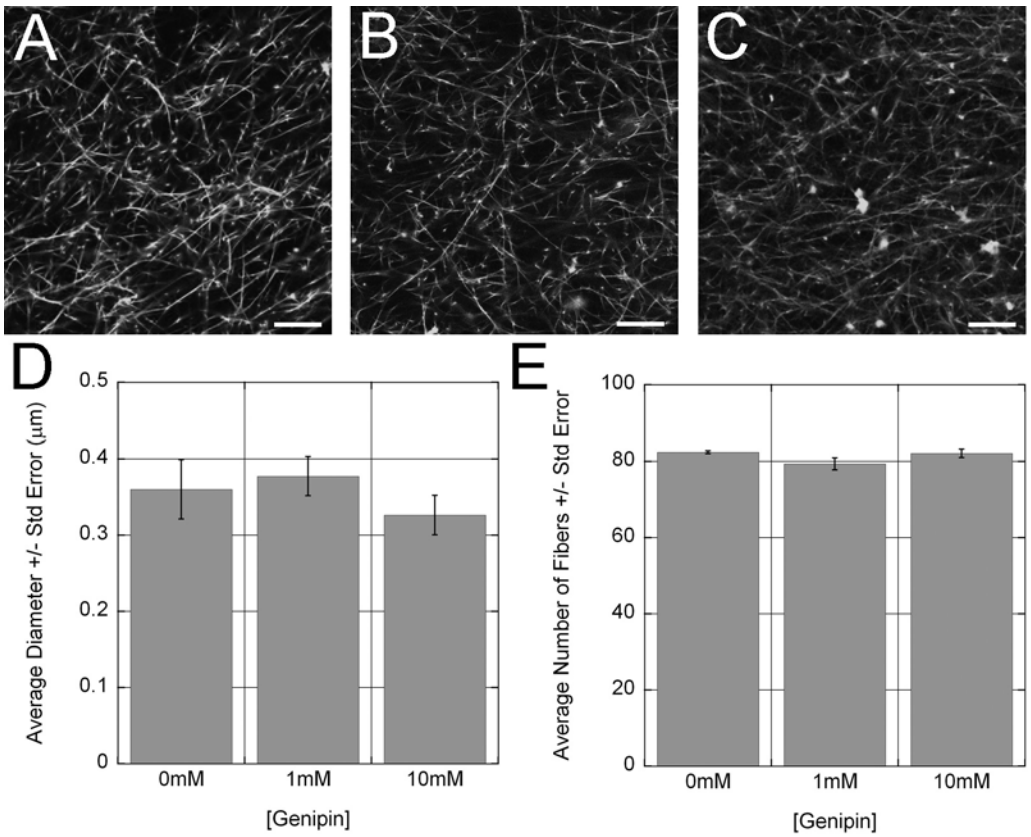

Figure 3- 9: Effects of genipin treatment on collagen fiber morphology. Collagen solutions were spiked with fluorescent collagen, and gels treated with (A) 0mM, (B) 1mM, or (C) 10mM for 12hrs and imaged using confocal microscopy. Images were divided into a 3x3 grid, and the number of fibers and diameter of fibers counted in 3 boxes (the main diagonal). No significant differences were identified in either the fibril size (D) or the number of fibers (E). Scale bar: 10μm.

Discussion

By developing an assay to study the response of cells to spatially varying mechanical properties in a 3D system, we hoped to improve the physiologic relevance of previous studies that demonstrate the importance of substrate mechanical properties in dictating cellular functions, and move towards implementing patterned mechanical properties for tissue engineering applications. Previous studies have demonstrated neuritic preference for compliant substrates [2, 6, 18] but have not shown how neurites respond to spatial changes in tissue or substrate mechanical properties. Using our system, we have shown that neurites preferentially grow down a gradient of stiffness with a 3D collagen gel.

The storage modulus of our gels in the experiments where gradients were formed from 12hrs of exposure to genipin ranges from 57Pa to 375Pa over the 5mm channel, which is a gradient ~0.064 Pa/μm. A typical growth cone is less than 5μm, and it seems remarkable that the growth cone would maintain transducing elements capable of detecting a 0.35 Pa difference in mechanical properties. However, the thin filipodia that protrude from the growth cone and probe the environment can be as long as 50 μm and average ~30 μm in chick DRG neurites [19]. Furthermore, the growth cone itself is merely the leading edge of a much longer neurite that, in this study, grows >1mm within the cross-channel in 5 days. It is possible that the neuron integrates the stiffness information from filopdia and/or contact points along the trajectory of the whole or parts of the neurite to control the rate of growth. Although the length of neurites growing down a steeper gradient of stiffness appeared to be increased with a steeper gradient by ~11% (Fig 9; 24hr vs. 12hr genipin gradient exposure), the differences in the baseline control

response prevented comparisons across these two conditions, and we cannot comment yet on the relationship to gradient steepness.

Rather than driving neurite growth with the gradient, it is also possible that the neurites are merely growing in a 3D environment with an optimal range of mechanical properties. Recent studies have shown that PC12 cells, an immortalized adrenocortical cell that exhibits a neuron-like phenotype when incubated in nerve growth factor, have a biphasic response to stiffness with shorter neurites on gels with a compliance ~10 Pa, and increased growth and branching in gels of a higher compliance from 10^2-10^4 Pa [6]. Other studies show that neurites from primary neurons sense differences between ~200Pa ('soft') and 2kPa ('hard') substrates [9]. Combined with our results, these studies point to the possibility that the optimal stiffness for neurite growth lies between the stiffness at the middle of the cross-channel (e.g. ~150-200Pa for 12hr exposure experiments) and the stiffness at the sink (~60Pa), and that the enhanced growth down the stiffness gradient is because the stiffness of the gel in the control cases is sub-optimal. However, our results following uniform crosslinking with 0.5mM demonstrate that the midpoint stiffness in gradient cases is sub-optimal for growth compared to control conditions, which further indicates that the gradient drives growth.

Genipin as a crosslinking agent

We generated changes in the mechanical properties of collagen gels using a naturally occurring compound, genipin, which we have previously shown to increase stiffness of collagen gels with increasing concentration and genipin exposure times [15]. Genipin has been shown to crosslink cellular and acellular tissues [13, 20-22], as well as biomaterials including gelatin microspheres [23], alginate-chitosan composites [24], and

poly(ethylene)-glycol hydrogels [25], and is increasingly observed in the literature for tissue engineering applications, including nerve regeneration, without adverse affects on cell behavior post-crosslinking. However, we have found the compound to be cytotoxic following direct exposure of cells to >1mM genipin [15], which limited our ability to create gradients with steeper slopes.

Genipin also has the unique feature of causing collagen fibers to fluoresce as it crosslinks, which was particularly beneficial for this study in that it allowed the gradients to be visualized during and after crosslinking as well as to be calibrated to mechanical properties. In principal, however, we have demonstrated the ability to impose a gradient of a soluble factor through a collagen-filled microfluidic network. Thus, any soluble crosslinking agent could be employed, such as aldehyde or enzyme (eg lysyl oxidase and transglutaminase). Moreover, the generation of a gradient of soluble factors also demonstrates that controlled chemotactic gradients can be generated through collagen gels using microfluidics.

Introduction of alternate guidance fields via genipin-mediated crosslinking

In addition to altering the stiffness, genipin may produce other changes in the collagen gel that could also drive or contribute to the biased neurite growth. Specifically, neurite behavior may be affected by direct exposure to genipin. Genipin-mediated crosslinking may produce changes in the adhesion properties of collagen to generate a haptotactic gradient, and/or genipin-mediated crosslinking may alter the porosity of collagen to potentially generate diffusion gradients of nutrients and/or sterically hinder growth.

The cytotoxic effects of higher (>1mM) doses of genipin [15] suggest that genipin may decrease cellular trophism, in general, and neurotrophism, specifically, since the DRG was exposed to genipin during gradient formation. Alternatively, the soluble genipin may act as a chemorepellant. However, the gradient of soluble genipin was maintained for as short as 12hrs, and then the gels were rinsed extensively, well before any neurites reached the cross-channel. If genipin exposure decreased neurite outgrowth from DRGs, we may still expect biased growth away from the genipin source and down the stiffness gradient, but we would also expect that growth to be stunted compared to growth in control conditions, where DRGs were not exposed to genipin or genipin-crosslinked collagen for any period of time. We found that growth was enhanced down the gradient of stiffness compared to untreated controls, which demonstrates that the exposure to genipin or genipin crosslinked gels did not negatively affect neurite growth.

Separate sets of experiments were performed to evaluate the effects of genipin crosslinking on cell adhesion and on fiber density and thickness. We did not observe significant differences in the adhesion of fibroblasts or a mixture of cells from dissociated DRGs seeded on genipin-treated collagen gels vs. control gels, suggesting that haptotactic gradients were not responsible for the observed results. We also did not find significant differences in fibril size or density between control gels and gels treated with genipin, suggesting that neither steric gradients nor nutrient gradients generated by spatially varying porosity were responsible for the observed results. Nutrient gradients may also have been introduced by the simple, source-sink arrangement, which results in stagnant flow and pure diffusive transport in the center of the cross channel when medium is supplied through both of the legs. (This is somewhat ameliorated by having

access to medium at the inlet and outlet of the underlying channel.) This nutrient gradient would be symmetric about the middle of the cross-channel, and would provide an equal driving force up or down the stiffness gradients, or left or right in control conditions. Our results in gradient experiments demonstrated significantly biased growth down the gradient of stiffness, again suggesting that nutrient gradients were not responsible for the observed outgrowth. Collectively, these results indicate that the primary change to the collagen across the gradient channel that affected neurite behavior was in gel stiffness.

The experiments were performed with chick DRG explants, which naturally provide a mixture of tissue cells, including neurons, fibroblasts, and Schwann cells. While neurites were specifically labeled with neurofilament antibodies, we did not attempt to explicitly stain for other cell types. In preliminary experiments, fluorescently labeled phalloidin was used to visualize growth in the networks, and the morphology of the main structures was consistent with neurites, but we cannot discount the possibility that the other cells responded to the stiffness gradient and produced a cellular contact guidance field for the regenerating neurites. It has been shown that fibroblasts prefer to migrate in the direction of increased stiffness [4], which is the opposite of what we have observed for neurite growth, but no data exists for the response of Schwann cells to changes in substrate compliance.

Natural and applied durotactic gradients

The potential to bias and enhance growth with patterns of mechanical properties in 3D gels/scaffolds presents intriguing possibilities for introducing spatial properties into regenerative therapies. For instance, it has been suggested that haptotactic and/or chemotactic gradients could be incorporated into scaffolds for peripheral nerve

regeneration, spinal cord regeneration [6, 10], and re-establishment of neuromuscular junctions to direct axon growth. We now suggest that durotactic gradients could also be included in scaffolds. Durotactic gradients could also be employed in other therapies where directed cell motion is desired, such as wound healing, where re-populating the engineered tissue with host fibroblasts, endothelial cells, and epithelial cells is critical. Durotactic gradients may play a role in natural physiological and pathological processes. For instance, recent studies have demonstrated that the high density pyramidal cellular layers of the postnatal (8-10 day old) rat hippocampus maintain heterogeneous mechanical properties, with the CA3 layer being significantly stiffer than the CA1 layer [26]. At this age, the rat CNS is still undergoing significant developmental changes. In light of our results presented herein, these heterogeneous properties may be important in guiding axons and dendrites for establishing proper neuronal connections, and the properties may change with development to provide dynamic guidance fields.

References

1. Arora, P.D., N. Narani, and C.A. McCulloch, *The compliance of collagen gels regulates transforming growth factor-beta induction of alpha-smooth muscle actin in fibroblasts.* Am J Pathol, 1999. **154**(3): p. 871-82.
2. Balgude, A.P., et al., *Agarose gel stiffness determines rate of DRG neurite extension in 3D cultures.* Biomaterials, 2001. **22**(10): p. 1077-84.
3. Discher, D.E., P. Janmey, and Y.L. Wang, *Tissue cells feel and respond to the stiffness of their substrate.* Science, 2005. **310**(5751): p. 1139-43.
4. Lo, C.M., et al., *Cell movement is guided by the rigidity of the substrate.* Biophys J, 2000. **79**(1): p. 144-52.
5. Flanagan, L.A., et al., *Neurite branching on deformable substrates.* Neuroreport, 2002. **13**(18): p. 2411-5.
6. Leach, J.B., et al., *Neurite outgrowth and branching of PC12 cells on very soft substrates sharply decreases below a threshold of substrate rigidity.* J Neural Eng, 2007. **4**(2): p. 26-34.
7. Peyton, S.R. and A.J. Putnam, *Extracellular matrix rigidity governs smooth muscle cell motility in a biphasic fashion.* J Cell Physiol, 2005. **204**(1): p. 198-209.
8. Saez, A., et al., *Rigidity-driven growth and migration of epithelial cells on microstructured anisotropic substrates.* Proc Natl Acad Sci U S A, 2007. **104**(20): p. 8281-6.
9. Georges, P.C. and P.A. Janmey, *Cell type-specific response to growth on soft materials.* J Appl Physiol, 2005. **98**(4): p. 1547-53.
10. Schmidt, C.E. and J.B. Leach, *Neural tissue engineering: strategies for repair and regeneration.* Annu Rev Biomed Eng, 2003. **5**: p. 293-347.
11. Tan, J.L., et al., *Cells lying on a bed of microneedles: an approach to isolate mechanical force.* Proc Natl Acad Sci U S A, 2003. **100**(4): p. 1484-9.
12. Burdick, J.A., A. Khademhosseini, and R. Langer, *Fabrication of gradient hydrogels using a microfluidics/photopolymerization process.* Langmuir, 2004. **20**(13): p. 5153-6.
13. Sung, H.W., et al., *Crosslinking of biological tissues using genipin and/or carbodiimide.* J Biomed Mater Res A, 2003. **64**(3): p. 427-38.
14. Almog, J., et al., *Genipin--a novel fingerprint reagent with colorimetric and fluorogenic activity.* J Forensic Sci, 2004. **49**(2): p. 255-7.
15. Sundararaghavan, H.G., et al., *Genipin-induced changes in collagen gels: Correlation of mechanical properties to fluorescence.* J Biomed Mater Res A, 2008.
16. Whitesides, G.M., et al., *Soft lithography in biology and biochemistry.* Annu Rev Biomed Eng, 2001. **3**: p. 335-73.
17. Shreiber, D.I., P.A. Enever, and R.T. Tranquillo, *Effects of pdgf-bb on rat dermal fibroblast behavior in mechanically stressed and unstressed collagen and fibrin gels.* Exp Cell Res, 2001. **266**(1): p. 155-66.
18. Fawcett, J.W., R.A. Barker, and S.B. Dunnett, *Dopaminergic neuronal survival and the effects of bFGF in explant, three dimensional and monolayer cultures of embryonic rat ventral mesencephalon.* Exp Brain Res, 1995. **106**(2): p. 275-82.

19. Buettner, H.M., *Nerve growth dynamics. Quantitative models for nerve development and regeneration.* Ann N Y Acad Sci, 1994. **745**: p. 210-21.
20. Liang, H.C., et al., *Effects of crosslinking degree of an acellular biological tissue on its tissue regeneration pattern.* Biomaterials, 2004. **25**(17): p. 3541-52.
21. Sung, H.W., et al., *Stability of a biological tissue fixed with a naturally occurring crosslinking agent (genipin).* J Biomed Mater Res, 2001. **55**(4): p. 538-46.
22. Yerramalli, C.S., et al., *The effect of nucleus pulposus crosslinking and glycosaminoglycan degradation on disc mechanical function.* Biomech Model Mechanobiol, 2007. **6**(1-2): p. 13-20.
23. Liang, H.C., et al., *Genipin-crosslinked gelatin microspheres as a drug carrier for intramuscular administration: in vitro and in vivo studies.* J Biomed Mater Res A, 2003. **65**(2): p. 271-82.
24. Chen, S.C., et al., *A novel pH-sensitive hydrogel composed of N,O-carboxymethyl chitosan and alginate cross-linked by genipin for protein drug delivery.* J Control Release, 2004. **96**(2): p. 285-300.
25. Moffat, K.L. and K.G. Marra, *Biodegradable poly(ethylene glycol) hydrogels crosslinked with genipin for tissue engineering applications.* J Biomed Mater Res B Appl Biomater, 2004. **71**(1): p. 181-7.
26. Elkin, B.S., et al., *Mechanical heterogeneity of the rat hippocampus measured by atomic force microscope indentation.* J Neurotrauma, 2007. **24**(5): p. 812-22.

Chapter 4: Microfluidic generation of adhesion gradients through 3D collagen gels: implications for neural tissue engineering

Introduction:

During development, neurons are directed by gradients of chemoattractants and adhesion sites to find their targets. However, once connections are established and synapses are functional, several of these important directional cues are lost. Even if neurons are influenced to regrow following injury – for instance, by implanting a permissible substrate for neurite outgrowth – they need to be guided across the injury site in order to reconnect and allow for functional recovery. Neurites can be directed by a number of modalities, including contact guidance, chemotaxis, durotaxis, and haptotaxis. Aligned gel fibers, guidance channels, and aligned glial cells have all been used to direct neurites [1-7]. *In vitro*, chemical gradients have been used extensively for neurite direction [8]. However, these systems are difficult to integrate into an *in vivo* system, where complex drug delivery mechanisms are needed for continual chemical cues and therefore, substrate-bound adhesive cues may be a simpler, more 'permanent' way to direct neurite growth, post injury.

The speed and direction of migration of different cell types are strongly correlated to the adhesion type and density present on the substratum. In 2D systems, cell speed depends biphasically on the extracellular-matrix ligand concentration [9] with the highest migration speeds at intermediate ligand concentration (Figure 4-1). If ligand concentration is too low, few adhesions can be made between the cell and the matrix, making cells unable to attach and move on these surfaces. If ligand concentration is too

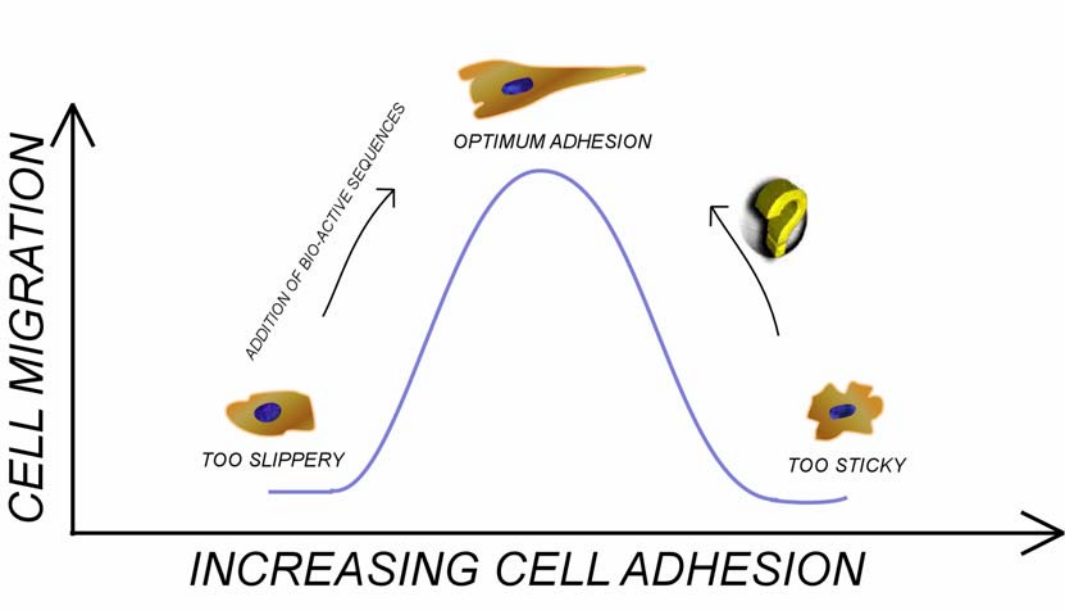

Figure 4- 1: Biphasic curve demonstrating cell migration on surfaces of increasing adhesion. At low concentration of adhesion, cells are unable to attach to the surface and activate sequences to move forward. At high concentrations cells are unable to detach from the surface and move forward.

high, adhesion strength is too high, making cells unable to detach from the substrate in order to migrate. Similarly, adhesion strength is important to neurons because stable formations of adhesive growth cone and filopodial contacts to the substrate are essential for growth cone steering and for neurite growth stimulation [10]. RGD, a ubiquitous cell adhesion peptide has been shown to increase adhesion of a number of different cell types including fibroblasts, smooth muscle cells, and neurons. Neurite outgrowth is affected biphasically by RGD concentration in chick DRG neurons [11]. At a high concentration of RGD, the substrate was found to be 'too sticky' for neurons and neurite growth decreased, but at an 'optimal' intermediate concentration, growth is increased when compared to controls. Though RGD can be used to increase neurite outgrowth, it also increases attachment of various cells types and therefore a more specific protein, laminin, which has been shown *in vivo* to be necessary for growth cone turning [12], can be used to increase neurite outgrowth more specifically [13]. Two peptide regions of the laminin structure are particularly important for neuron adhesion and outgrowth, IKVAV and YIGSR. Over the last 30 years YIGSR and IKVAV have been used in 2D as well as conjugated to 3D hydrogels to increase neuron attachment and neurite outgrowth [14, 15].

Several studies have shown increased neurite outgrowth with YIGSR and IKVAV in 2D [16-18], and some isotropic *in vivo*-like 3D conditions. YIGSR-grafted isotropic 3D gels have been studied with alginate, chitosan and collagen [19-22]. In all cases, YIGSR grafting increased neurite outgrowth over controls and in one case over laminin controls [21]. These studies show that using YIGSR can be an important way to increase neurite outgrowth and make the injury site after SCI more permissible to neurite outgrowth. However, simply increasing neurite outgrowth may not be sufficient for repair

after SCI, since neurons need to be guided to their targets; therefore, directed growth of neurons is an important area of study.

Though much work has been done on discrete samples of varying concentrations of adhesive peptides, little work has been done on directed growth. Photo-immobilized gradients of NGF within poly(2-hydroxyethylmethacylate) [p(HEMA)] gels have been used to guide neurite outgrowth from PC12 cells [23]. In 2D, it has been shown that gradients of IKVAV direct neurite outgrowth in chick dorsal root ganglia (DRG) neurons [18]. 3D gradients of laminin and NGF were studied recently in an *in vivo* model [24]. Regeneration only occurred in experimental conditions where there was both a gradient of NGF and laminin. If either component or both was presented uniformly, they did not obtain regeneration in a sciatic nerve regeneration model. In all cases, this regeneration was lower then in the nerve graft control. Bellamkonda's group has also studied laminin 3D gradients in vitro where they showed that neurites from chick DRG's grow faster up and are more directed in a shallow gradient of laminin as compared to a steep gradient [25].

Our goal is to develop a haptotactic gradients of bioactive peptide – in this cases, IKVAV and YIGSR – within a growth-permitting 3D scaffold. We generate these gradients in type I collagen and study the functionality of these gradients using chick DRGs. Previous work in our lab has demonstrated the functionality of using 1-ethyl-3-(3-Dimethylaminopropyl) carbodiimide (EDC) to couple G<u>RGD</u>S and G<u>RDG</u>S to the collagen backbone in order to modulate cell adhesion [26]. Grafted gels significantly affected adhesion, migration and traction of rat dermal fibroblasts (RDFs) and human smooth muscle cells (SMCs), and did not change mechanical properties or pore size of

collagen gels significantly. Similar methods are employed in this study to conjugate IKVAV and YIGSR to the collagen backbone. Gradients are created in a simple source-sink microfluidic network, and are studied at four different slopes created by either changing inlet concentrations or the length of the cross-channel connecting source-to-sink. Gradient experiments were performed at 0-37 μg peptide/mg collagen (0-100%) and 0-18.5 μg peptide/mg collagen (0-50%) at two different gradient lengths of 3 and 5 mm for both IKVAV and YIGSR. Controls were performed at 100%-100% and 0%-0% (no peptide) at 5mm. Previous work in the lab has demonstrated the Microfluidic systems use of a microfluidic system to study neurite outgrowth in 3D mechanical gradients, and a similar system is used to study neurite response to gradients of IKVAV and YIGSR peptide-grafted collagen.

Methods:

Microfluidic Networks

A simple, 'H'-shaped, 'source-sink' arrangement was used to generate gradients in a cross channel connecting source-to-sink. Source and sink channels were 500μm wide x 100μm deep and were connected by a either a 3mm or 5mm long, 150μm wide, and 100μm deep channel. Microfluidic networks were fabricated using standard photolithography techniques [27] at Bell Labs/Lucent Technologies (Murray Hill, NJ) through a grant from the New Jersey Nanotechnology Consortium. The design was drawn with AutoCAD and a photomask was professionally printed (Cad-Art services, Poway, CA). A silicon wafer was spin-coated with SU-8 negative photoresist (Microchem, Newton, MA) and baked for 5min at 65°C followed by 10min at 100°C. The photoresist was exposed to UV light through the photomask using a Quintel 2001 CT Mask

Alignment/Exposure system. The coated wafer was baked again and immersed in SU-8 developer for 12min to clear un-reacted photoresist and form the final 'master'. A poly(dimethyl siloxane) solution (PDMS; Dow Corning, Midland, MI) was poured over the master and baked overnight at 50°C to produce a negative relief. The PDMS was removed, the design was cut out of the mold, and holes were punched for the inlet and outlet using a blunt 19-gauge syringe. The PDMS and a clean glass slide were plasma treated and bonded together to form the final device. The inlets were connected to a syringe pump (Harvard Apparatus, Cambridge, MA) using polyethylene tubing (Small Parts, Miami Lakes, FL).

Collagen Preparation

Type I collagen solutions were prepared as previously described [28] by mixing 20µl 1M Hepes buffer , 140µl 0.1N NaOH, 100µl 10X PBS , 52µl of PBS (Invitrogen, Carlsbad, CA), and 677µl of a 3.0mg/ml type I collagen solution (Elastin Products, Owensville, Missouri) to make a 2.0mg/ml collagen solution. The collagen solution is kept at 4ºC until use and self-assembled into a fibrillar gel upon incubation at 37°C.

Conjugation of peptides to collagen backbone

A 17-mer peptide sequence, CRARKQASIKVAVSADR, and a 9-mer peptide sequence, CDPGYIGSR, were custom synthesized (Genscript, Piscataway, NJ) and conjugated to the backbone of collagen in suspension. A hetero-bifunctional coupling agent, 1-ethyl-3-(3-Dimethylaminopropyl) carbodiimide (EDC), was used to activate the carboxylic group of the peptide by mixing 1ml of a 1M solution of EDC in MES buffer (pH 2-4) with 1 mg of peptide for ten minutes at 37°C. The peptide-EDC mixture was added to 5ml of a 3mg/ml suspension of type I collagen (Elastin Products, Owensville,

MO) in 0.02N acetic acid. The activated peptide covalently binds to free amines on residues on the collagen backbone via nucleophilic attack. A low pH buffer was used while coupling peptides to avoid self-assembly of collagen fibers. Peptide-EDC-collagen mixtures were incubated on a shaker overnight at 4°C and then dialyzed against 0.02N acetic acid for 12 hours to remove any unconjugated peptide. Dialyzed peptide-grafted collagen was lyophilized at -150°C and 50 mTorr for 12 hours to remove all water. Lyophilized product was re-suspended in 0.02N acetic acid to make a 3mg/ml solution of grafted collagen. Grafting efficiency was evaluated by using a FITC-tagged peptide. FITC-tagged peptides were conjugated to the collagen backbone using the same method described above. Efficiency was determined with a standard curve made by admixing FITC tagged peptide to collagen solution and comparing the fluorescence of the final product to the standard curve.

Neurite Outgrowth Assay

To assay neurite response to haptotactic gradients, the source-sink network was modified to allow introduction of a DRG into the system (Figure 4-2). A second network was generated that comprised a 1mm diameter well connected to a straight 500μm wide and 100μm deep channel. This network was place upside down (channel facing up) on a glass slide and filled with collagen solution. DRGs were isolated from E8 chick embryos (Charles River Laboratories, Willmington, MA), and a single DRG was placed in the collagen-filled circular well. The network was transferred to a 37ºC incubator to facilitate self-assembly, entrapping the DRG in the collagen gel. The ‘source-sink’ network was then plasma treated and bonded to the gel-filled underlying network such that the middle of the cross channel of the 'source-sink' intersected with the straight channel of the

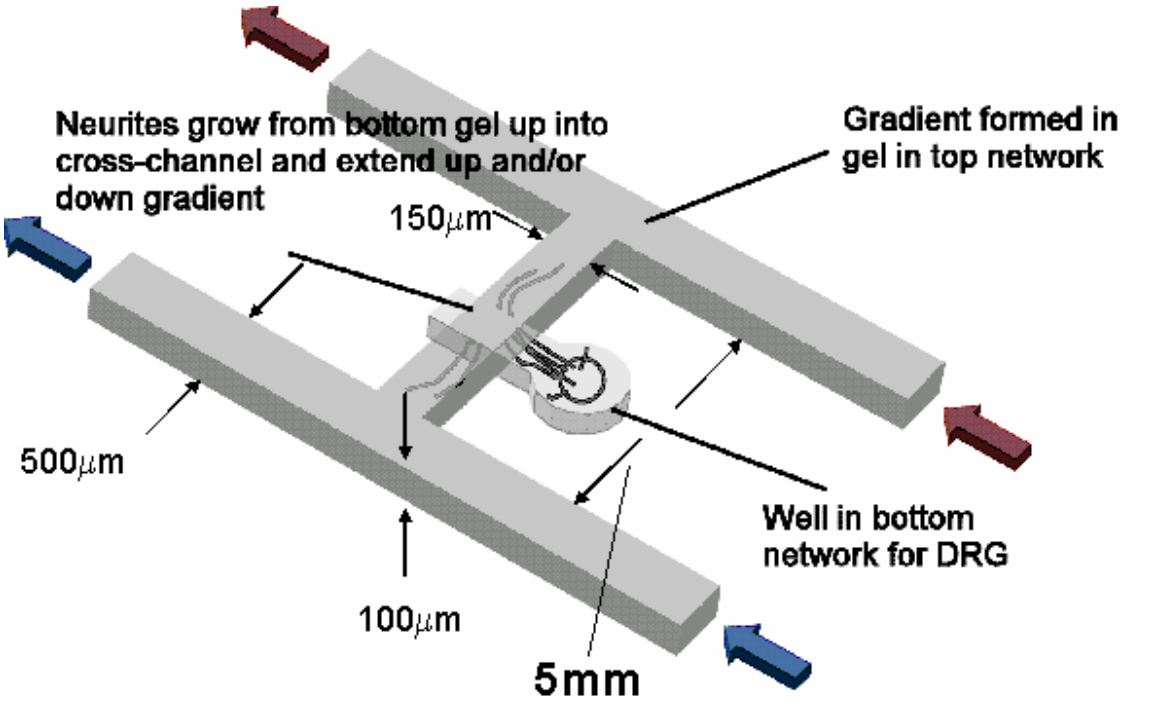

Figure 4- 2: Schematic of the PDMS network. Cells are allowed to grow through the cell channel and into the cross-channel. Projecting neurites then choose to grow up or down the adhesion gradient, or left or right for control conditions.

underlying network approximately 1500μm from the circular well containing the DRG. Peptide grafted collagen was pumped through one leg of the H and native collagen through the other leg to form a gradient through the cross channel. Gradients were visualized by spiking either the peptide-grafted collagen or the native collagen (selected at random) with a FITC-tagged collagen solution.

After filling, networks were transferred to a humidified, 37ºC, 5% CO_2 incubator and perfused with fresh medium (DMEM supplemented with 10% FBS and 100 ng/ml NGF (R&D Systems, Minneapolis, MN)) via gravity flow. DRGs were cultured in the networks for five days to allow neurites to grow through the collagen gel and extend up and into the crosschannel a significant distance, potentially in either direction. For 3mm gradients, neurites grew for 4 days instead of 5 days to prevent neurites from entering the source/sink channel.

To visualize neurite growth, after the culture period, neurites were stained immunohistochemically in the networks for neurofilament proteins. Inlet solutions were changed to 4% paraformaldehyde for 3 hours to fix the collagen and cells, then changed to a rinse buffer comprising 1% BSA + 0.5% Triton in PBS for 3 hours. Inlet solutions were changed to a 10% goat serum blocking solution in rinse buffer for 4 hours, and then to an anti-neurofilament antibody cocktail of 1:200 α-NF 200 and 1:1000 α-NF 68 (Sigma) overnight. Networks were rinsed for 4 hours, and inlets were switched to a 1:400 dilution of goat anti-mouse Alexa 568 secondary antibody (Molecular Probes/Invitrogen, Eugene, OR) and incubated overnight. Devices were rinsed a final time for 4 hours and then transferred to an inverted epifluorescence microscope for imaging.

Neurite growth was quantified as the number and length of neurites projecting up the adhesion gradient vs. down the adhesion gradient, or in opposite directions for control experiments without peptide grafted collagen or with uniform presentation of peptide-grafted collagen, where no gradient was present. For each device, digital images were taken with a 40X objective at the intersection of the explant and cross-channels and at the end of the individual growth cones. Using Olympus Microsuite Image Analysis Software, the (X,Y) coordinates were recorded for each growth cone and for the channel intersection to determine the distance of growth in the gradient channel. For each experiment, at least one adhesion gradient or full adhesion condition and one no-peptide control was done with DRG explants from the same chick embryo. 5mm IKVAV and YIGSR experiments were performed at 100%-0 (14.9 μg/ml/mm – average concentration of 18.5 μg peptide/mg collagen), 50%-0 (7.44 μg/ml/mm– average concentration of 9.25 μg peptide/mg collagen) and uniform, 74.5 μg/ml/mm. The average length of neurites growing in either direction was calculated. For the 3mm length gradient condition, neurites grew for 4 days to prevent neurite growth into source and sink channels. 3mm IKVAV and YIGSR experiments were performed at 100%-0 (24.7 μg/ml/mm– average concentration of 18.5 μg peptide/mg collagen) and 50%-0 (12.4 μg/ml/mm– average concentration of 9.25 μg peptide/mg collagen) and no peptide control (Table 4-1).

	IKVAV / YIGSR		
	Condition	Gradient Concentration (μg peptide/ml collagen/mm)	Average Concentration (μg peptide/mg collagen)
3 mm	100%-0	24.7	18.5
	50%-0	12.4	9.25
5 mm	100%-0	14.9	18.5
	50%-0	7.44	9.25
	100%-100%	Uniform	37

Table 4- 1: Table of all conditions tested for adhesion experiments.

Results:

Peptide conjugation characterization:

To evaluate the efficiency of grafting of peptides to the collagen backbone, the fluorescence of FITC-tagged peptide-grafted collagen was compared to a calibration curve established by serially diluting FITC-tagged peptide grafted collagen solution before removing unbound peptides (through dialysis, lyophilization, and reconstitution). The fluorescence of our final collagen solution was compared to this calibration curve to determine how much of the added peptide is conjugated to the collagen backbone (Figure 4-3). Our typical grafting efficiency was 55-65%. 100% peptide-grafted collagen is ~37 μg peptide/mg collagen or ~74 μg peptide/ml collagen.

Neurite outgrowth assay:

DRG explants from day 8 chick embryos were placed in the cell channel underlying the gradient channel. Gradients were visualized by spiking either the peptide-grafted collagen or the native collagen (selected at random) with a FITC-tagged collagen solution (Figure 4-4). The cell channel intersects the gradient channel at the midpoint of the gradient. Two different gradient channel lengths were studied, 3 and 5 mm. In the 5mm condition, neurites were grown for 5 days before fixing and immunohistochemically staining. Neurites grow down the cell channel and a significant number grow into the crosschannel (Figure 4-5). Those that grow in the cross channel can either grow up or down the gradient (or either direction in the control cases).

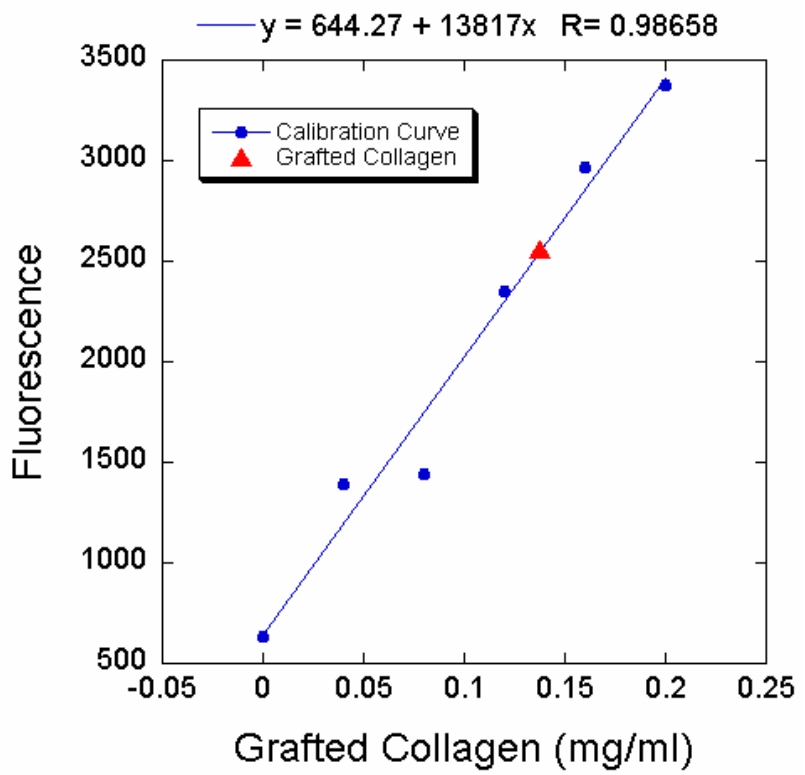

Figure 4-3: Representative calibration curve for calculating grafting efficiency. Calibration curve is created by admixing FITC-tagged peptides with collagen solution. After grafting procedure, peptide grafted collagen is dialyzed against 0.02N acetic acid to remove unbound peptide, lyophilized, and reconstituted in 0.02N acetic acid prior to use. Fluorescence of FITC-tagged peptide grafted collagen is compared to calibration curve to determine efficiency of grafting.

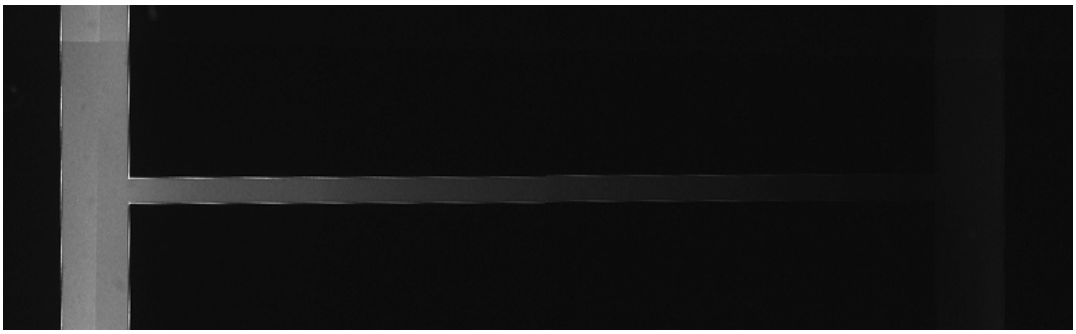

Figure 4- 4: (A) Representative gradient of adhesion in H network visualized by spiking collagen solution on left with 10% FITC-collagen.

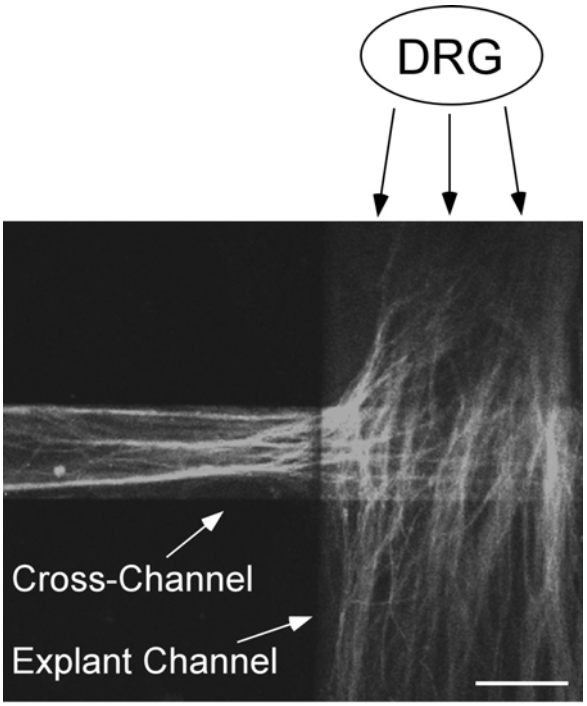

Figure 4- 5: Confocal micrograph of neurite growth in the collagen gel-filled network. A DRG was placed within a collagen gel in the underlying explant channel and cultured for 5 days, at which time the networks were perfused with paraformaldehyde and then stained immunohistochemically for neurofilament proteins. Neurites grew from the DRG and either continued in the explant channel or grew up and into the cross-channel of the overlying 'H'-shaped network. Scale bar: 150μm.

Though similar daily trends are observed between control and experimental conditions, significant variability is possible day to day due to the variability in chicks used. This is accounted for in the statistical analysis by performing a two-way ANOVA where the experimental condition was a fixed effect and day of the experiment was a random effect. Average length up and down the gradient for IKVAV, 5mm experiments and their respective controls are shown Figure 4-6. In this case, 100-0 shows significantly enhanced growth both up and down the gradient of adhesion ($P<0.05$) and the 50-0 case shows enhanced growth though this is not significant (Figure 4-6A). In order to determine directionality of growth, the ratio of growth up the gradient over growth down the gradient is calculated. Significantly directed growth ratios should be greater then one meaning growth is greater up the gradient compared to down the gradient. Growth is most directed in the 50%-0 condition (Figure 4-6B) though this is not significant for IKVAV, 5mm. In the uniform concentration, IKVAV-grafted control case, growth is not enhanced compared to both gradient cases and the control. In the steeper gradients conditions (3mm) growth is significantly enhanced in 50%-0 but growth is not directed in either case (Figure 4-7).

In 5mm YIGSR experiments, growth is significantly enhanced up the gradient of adhesion for both the 100-0 and 50-0 ($P<0.05$) conditions (Figure 4-8A), with some bias up the gradient of peptide in the 100%-0 case (Figure 4-8B). In the uniform concentration, YIGSR-grafted collagen case, growth is significantly increased compared to control conditions and enhanced over gradient conditions, implying that growth may be further enhanced by increasing concentration of peptide. In steeper conditions (3mm) growth is significantly increased in both gradient conditions compared to control (Figure 4-9A) and

significantly directed growth in both the 50%-0 and the 100%-0 conditions (Figure 4-9B) ($P<0.05$).

The number of neurites growing in either direction for all peptide grafted conditions and controls were determined (Figure 4-10,4-11). There was no significant difference in the number of neurites except in the IKVAV 100-0, 3mm case where significantly more neurites grew up the gradient than in the control condition ($P<0.05$).

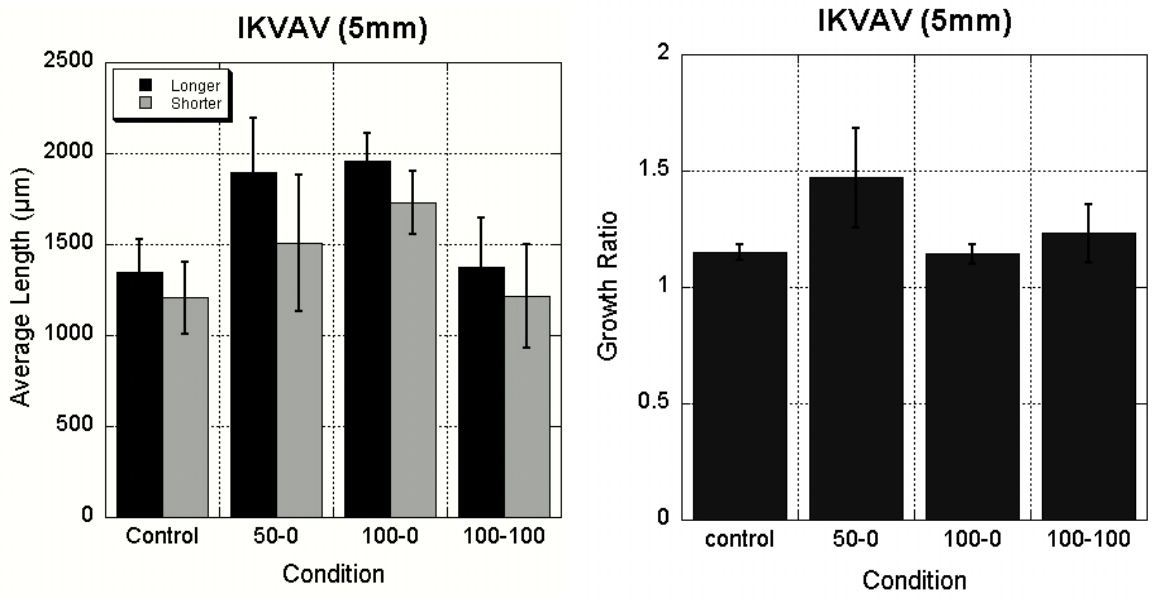

Figure 4- 6: (A) Average length of growth in 'longer' and 'shorter' directions for different conditions of IKVAV grafted collagen. Growth is not increased over controls when the collagen is uniformly grafted with ~37µg IKVAV/mg collagen ('100%'), but is increased in both directions ($P<0.05$). (B) Ratio of growth in 'longer' over growth in 'shorter' directions shows that directional bias is greatest in the shallowest conditions (50-0).

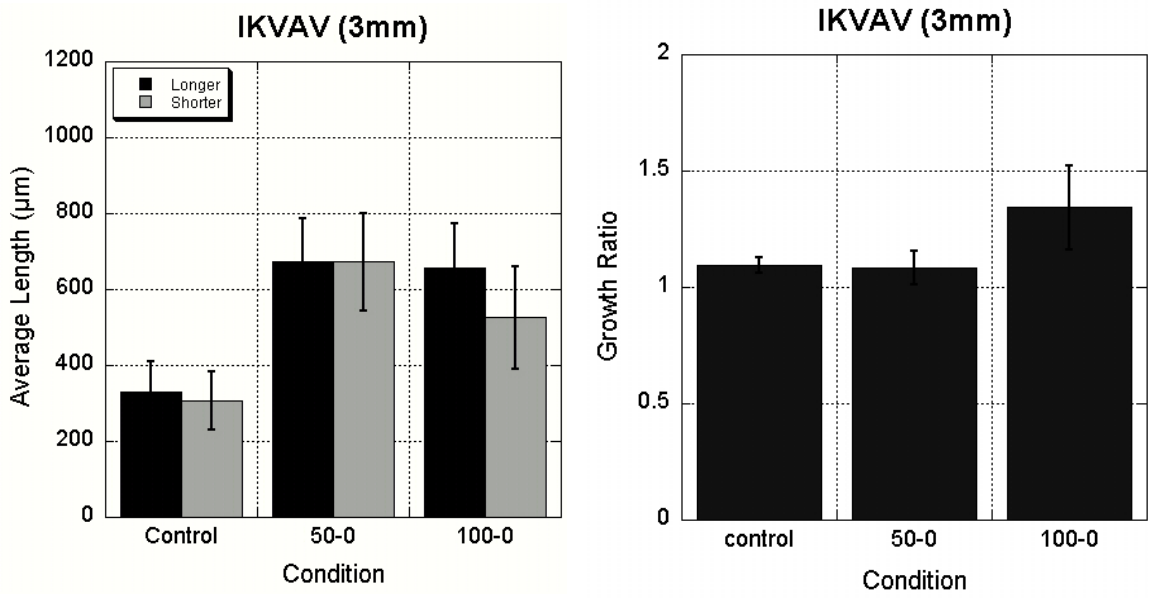

Figure 4- 7: Average length of growth in 'longer' and 'shorter' directions for different conditions of IKVAV grafted collagen at 3mm gradient length. Growth is increased in all IKVAV grafted conditions. (B) Ratio of growth in 'longer' over growth in 'shorter' directions shows that growth is not significantly biased in either gradient condition (50-0, 100-0)

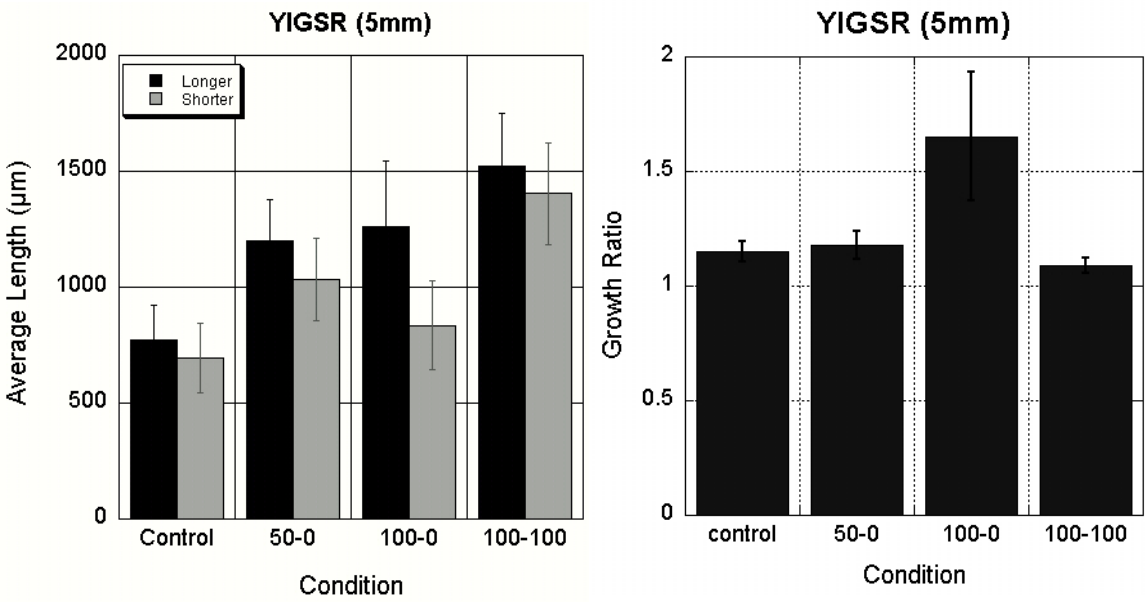

Figure 4- 8: (A) Average length of growth in 'longer' and 'shorter' directions for different conditions of YIGSR grafted collagen. Growth is increased in all YIGSR grafted conditions and is longest in the uniform conditions (100%). (B) Ratio of growth in 'longer' over growth in 'shorter' directions shows that growth is most biased in the steepest gradient condition (100-0)

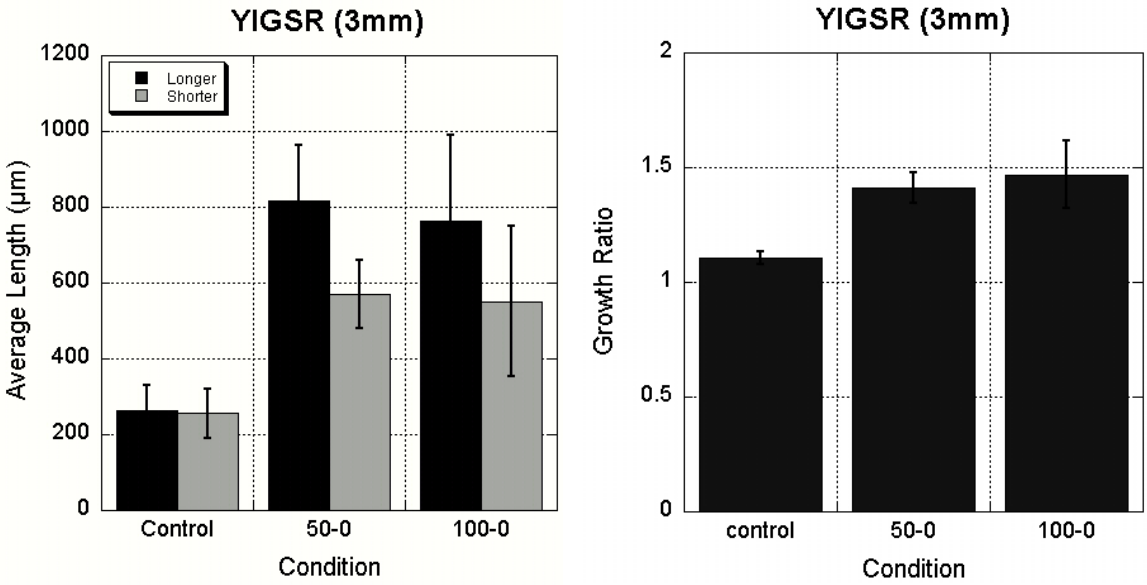

Figure 4- 9: Average length of growth in 'longer' and 'shorter' directions for different conditions of YIGSR grafted collagen at 3mm gradient length. Growth is increased in all YIGSR grafted conditions. (B) Ratio of growth in 'longer' over growth in 'shorter' directions shows that growth is significantly biased in both gradient conditions (50-0, 100-0)

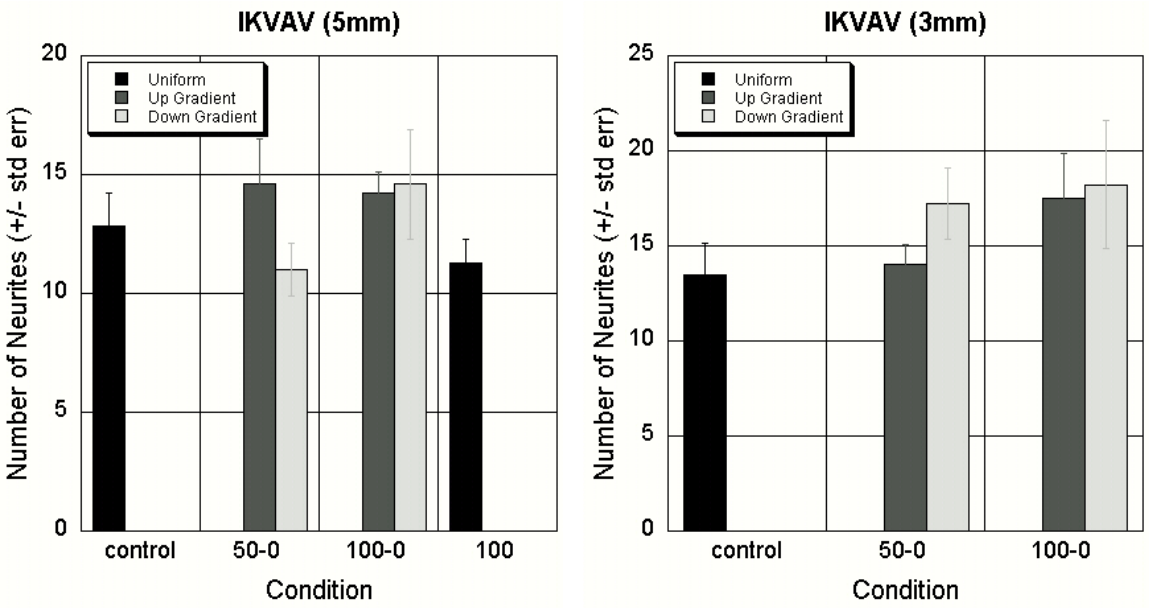

Figure 4- 10: Number of neurites for IKVAV conditions growing up and down the gradient. Number of neurites growing in uniform conditions or up and down the gradient is not significantly different except in the 100-0, 3mm case where significantly more neurites grew up the gradient then the control ($P<0.05$).

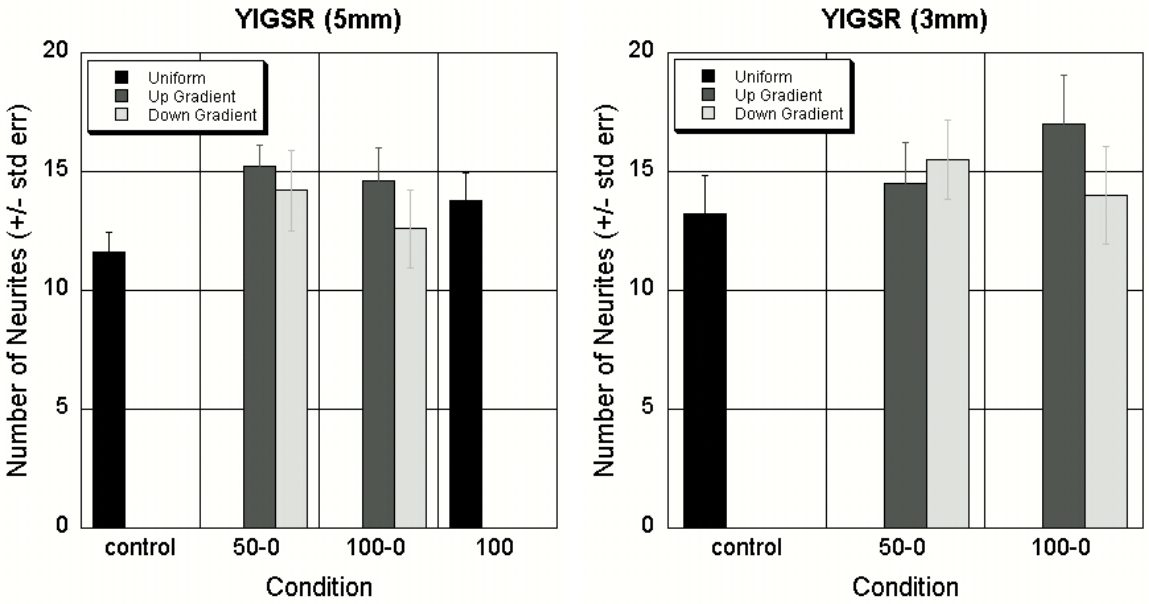

Figure 4- 11: Number of neurites for YIGSR conditions growing up and down the gradient. Number of neurites growing in uniform conditions or up and down the gradient is not significantly different.

Discussion:

We believe, analogous to development, multiple cues will be necessary to direct neurons after spinal cord injury. Given that gradients of laminin have been shown to be important for growth cone turning and guidance *in vivo*, we know adhesion gradients are important for directed growth. We have developed a method to create smooth 3D gradients of IKVAV and YIGSR grafted collagen and tested their functionality in directing neurons using chick DRGs. Most previous work has focused on chemotaxis, which is the use of chemical gradients, and has been shown to influence neurites to grow in a particular direction. In the body, cells differentially synthesize factors to provide chemical cues and in order to incorporate this into a biomaterial we would need a continuous source for the chemoattractant. Rather then developing a complicated system for chemical release, we believe we can use adhesion gradients for directed growth. Adhesion gradients have an important benefit in that they are part of the biomaterial and therefore will provide 'permanent' gradients to direct neurons.

In this study we investigated gradients of IKVAV and YIGSR, which are both neuron-specific peptide regions of laminin [15, 29]. Most work in altering neurite adhesion with IKVAV and YIGSR has been in 2D [17, 29] or isotropic 3D conditions of YIGSR grafted to different materials including collagen, chitosan and alginate [20-22, 29]. Adams et al. [18] looked at substrate bound 2D IKVAV gradients for directing DRG neurites where they first directed neurites to the center of the gradient and then allowed growth cones to choose to grow up or down the gradient of adhesion. They found in steep gradients, most growth cones chose to grow "up the gradient". In more shallow gradients, there is still a bias "up the gradient" but once neurites chose a direction, up or down, they

continue and show no indication of turning to grow “up the gradient”. However, because of the constraint in gradient length, they were not able to look at the final length of neurite outgrowth and found no change in the rate of growth in either direction of the gradient.

Dolda et al. [25] studied gradients of laminin grafted to agarose gels in shallow and steep gradients. DRGs were mixed with the initial agarose gel and therefore, there was little control over where each DRG started in the gradient. Depending on the location of these DRGs they measured neurite growth rate either “up the gradient” or “down the gradient” of laminin and found that in the shallow laminin gradient condition, in their case 0.017 μg/ml/mm, they found a significant difference in growth rate “up the gradient” vs “down the gradient” stating that this would be potentially important in directing neurite outgrowth. However, due to the nature of their study, they were unable to measure growth in both directions from a single DRG or look at the final average length of neurites at the end of their experiment.

In our case, we studied both IKVAV and YIGSR gradients conjugated to collagen in 3D. Neurite were first directed to the center of the gradient and were able to grow either up or down the gradient. We measure the final length of neurites growing in either direction from the same DRG. For both IKVAV and YIGSR, we studied 4 different gradients: 7.44 μg/ml/mm, 14.9 μg/ml/mm, 12.4 μg/ml/mm, 24.7 μg/ml/mm. Though this range is much steeper then previously studied laminin gradients, these concentrations are in the range of those used for YIGSR-grafted collagen gels in isotropic conditions [22] and laminin conjugated agarose gels used *in vivo* [24]. For IKVAV, we find that neurites are most directed in the shallowest gradients, 7.44 μg/ml/mm. In our full IKVAV control,

we find that growth is decreased, implying that at our highest concentration, the IKVAV-grafted collagen is too 'sticky' for neurite outgrowth and on the right side of the biphasic curve (Figure 4-1). If we look at all of our IKVAV experiments together we see that the range we tested displays the biphasic response of IKVAV-grafted collagen to neurites. Neurites entering the gradients channel enter at the midpoint of the gradients which is 0, 9.25, 18.5, or 37 μg peptide/mg collagen for 0, 50%-0, 100%-0 and 100-100% respectively. From our results we see that growth is most increased in the gradient conditions (50%-0, 100%-0) implying that the optimal concentration for IKVAV-grafted collagen is between 9.25-18.5 μg peptide/mg collagen. Native collagen with no added IKVAV is ~37 μg peptide/mg collagen and showed decreased growth as compared to these gradient conditions.

In our YIGSR studies we find that growth enhanced in all YIGSR-grafted conditions, most directed in the steepest condition and longest in the full YIGSR control case. We were unable to compare the average growth in steep gradient conditions with the uniform condition due to the difference in the duration of the experiment for each study. When we compare 3mm gradients to 5mm, we know that the concentration of peptide grafted collagen at the midpoint is the same. The increased directionality of the steeper gradients must be due to the slope of the gradient itself and not because of the starting conditions for neurites in the gradients. We find all YIGSR gradients we tested fall below, or possibly at, the optimal YIGSR-grafted collagen concentration. This is seen by looking the uniform concentration tested at 37 μg peptide/mg, which increased growth over gradient conditions.

Our work confirms that there is a difference in the sensitivity of the response to IKVAV and YIGSR. If we calculate molar concentration we see that the molarity at which YIGSR is active is 0.115 mM, which is almost double the highest concentration we tested for IKVAV (0.06 mM) where IKVAV-grafted collagen concentration was too high for optimal growth. This means that IKVAV is active at a much lower concetration (0.03mM – 0.015mM), that is almost an order of magnitude lower that that needed for YIGSR to be active. Previous work has shown that DRGs are most directed in the shallow gradient of laminin. Laminin has a fixed concentration of IKVAV and YIGSR and these concentrations cannot be changed independently when making a gradient of laminin. If we look at the gradients studied by Dolda et al.[25], they reported that shallow gradients were most effective in directing neurons. When they used gradients of laminin, they are not able to control the concentration of IKVAV and YIGSR they use. If they use a high concentration of laminin, that would mean they are using a high concentration of IKVAV. Based on our experiments, we expect that neurons will not be able to grow in high concentrations of IKVAV and therefore, steep laminin gradients will not be able to direct neurons regardless of the concentration of YIGSR present. Using our system we are able to decouple these two effects and use the optimal concentration for each peptide to make the most favorable substrate for neurite growth and direction.

References

1. Corey, J.M., D.Y. Lin, K.B. Mycek, Q. Chen, S. Samuel, E.L. Feldman, and D.C. Martin, *Aligned electrospun nanofibers specify the direction of dorsal root ganglia neurite growth.* J Biomed Mater Res A, 2007. **83**(3): p. 636-45.
2. Ceballos, D., X. Navarro, N. Dubey, G. Wendelschafer-Crabb, W.R. Kennedy, and R.T. Tranquillo, *Magnetically aligned collagen gel filling a collagen nerve guide improves peripheral nerve regeneration.* Exp Neurol, 1999. **158**(2): p. 290-300.
3. Dubey, N., P.C. Letourneau, and R.T. Tranquillo, *Neuronal contact guidance in magnetically aligned fibrin gels: effect of variation in gel mechano-structural properties.* Biomaterials, 2001. **22**(10): p. 1065-75.
4. Goldner, J.S., J.M. Bruder, G. Li, D. Gazzola, and D. Hoffman-Kim, *Neurite bridging across micropatterned grooves.* Biomaterials, 2006. **27**(3): p. 460-72.
5. Dowell-Mesfin, N.M., M.A. Abdul-Karim, A.M. Turner, S. Schanz, H.G. Craighead, B. Roysam, J.N. Turner, and W. Shain, *Topographically modified surfaces affect orientation and growth of hippocampal neurons.* J Neural Eng, 2004. **1**(2): p. 78-90.
6. Schmalenberg, K.E. and K.E. Uhrich, *Micropatterned polymer substrates control alignment of proliferating Schwann cells to direct neuronal regeneration.* Biomaterials, 2005. **26**(12): p. 1423-30.
7. Thompson, D.M. and H.M. Buettner, *Neurite outgrowth is directed by schwann cell alignment in the absence of other guidance cues.* Ann Biomed Eng, 2006. **34**(1): p. 161-8.
8. Cao, X. and M.S. Shoichet, *Investigating the synergistic effect of combined neurotrophic factor concentration gradients to guide axonal growth.* Neuroscience, 2003. **122**(2): p. 381-9.
9. Palecek, S.P., J.C. Loftus, M.H. Ginsberg, D.A. Lauffenburger, and A.F. Horwitz, *Integrin-ligand binding properties govern cell migration speed through cell-substratum adhesiveness.* Nature, 1997. **385**(6616): p. 537-40.
10. Schmidt, C.E., J. Dai, D.A. Lauffenburger, M.P. Sheetz, and A.F. Horwitz, *Integrin-cytoskeletal interactions in neuronal growth cones.* J Neurosci, 1995. **15**(5 Pt 1): p. 3400-7.
11. Schense, J.C. and J.A. Hubbell, *Three-dimensional migration of neurites is mediated by adhesion site density and affinity.* J Biol Chem, 2000. **275**(10): p. 6813-8.
12. Bonner, J. and T.P. O'Connor, *The permissive cue laminin is essential for growth cone turning in vivo.* J Neurosci, 2001. **21**(24): p. 9782-91.
13. Bellamkonda, R., J.P. Ranieri, and P. Aebischer, *Laminin oligopeptide derivatized agarose gels allow three-dimensional neurite extension in vitro.* J Neurosci Res, 1995. **41**(4): p. 501-9.
14. Ranieri, J.P., R. Bellamkonda, E.J. Bekos, J.A. Gardella, Jr., H.J. Mathieu, L. Ruiz, and P. Aebischer, *Spatial control of neuronal cell attachment and differentiation on covalently patterned laminin oligopeptide substrates.* Int J Dev Neurosci, 1994. **12**(8): p. 725-35.

15. Tashiro, K., G.C. Sephel, B. Weeks, M. Sasaki, G.R. Martin, H.K. Kleinman, and Y. Yamada, *A synthetic peptide containing the IKVAV sequence from the A chain of laminin mediates cell attachment, migration, and neurite outgrowth.* J Biol Chem, 1989. **264**(27): p. 16174-82.
16. Heller, D.A., V. Garga, K.J. Kelleher, T.C. Lee, S. Mahbubani, L.A. Sigworth, T.R. Lee, and M.A. Rea, *Patterned networks of mouse hippocampal neurons on peptide-coated gold surfaces.* Biomaterials, 2005. **26**(8): p. 883-9.
17. Saneinejad, S. and M.S. Shoichet, *Patterned glass surfaces direct cell adhesion and process outgrowth of primary neurons of the central nervous system.* J Biomed Mater Res, 1998. **42**(1): p. 13-9.
18. Adams, D.N., E.Y. Kao, C.L. Hypolite, M.D. Distefano, W.S. Hu, and P.C. Letourneau, *Growth cones turn and migrate up an immobilized gradient of the laminin IKVAV peptide.* J Neurobiol, 2005. **62**(1): p. 134-47.
19. Yu, X., G.P. Dillon, and R.B. Bellamkonda, *A laminin and nerve growth factor-laden three-dimensional scaffold for enhanced neurite extension.* Tissue Eng, 1999. **5**(4): p. 291-304.
20. Itoh, S., I. Yamaguchi, M. Suzuki, S. Ichinose, K. Takakuda, H. Kobayashi, K. Shinomiya, and J. Tanaka, *Hydroxyapatite-coated tendon chitosan tubes with adsorbed laminin peptides facilitate nerve regeneration in vivo.* Brain Res, 2003. **993**(1-2): p. 111-23.
21. Dhoot, N.O., C.A. Tobias, I. Fischer, and M.A. Wheatley, *Peptide-modified alginate surfaces as a growth permissive substrate for neurite outgrowth.* J Biomed Mater Res A, 2004. **71**(2): p. 191-200.
22. Duan, X., C. McLaughlin, M. Griffith, and H. Sheardown, *Biofunctionalization of collagen for improved biological response: scaffolds for corneal tissue engineering.* Biomaterials, 2007. **28**(1): p. 78-88.
23. Kapur, T.A. and M.S. Shoichet, *Immobilized concentration gradients of nerve growth factor guide neurite outgrowth.* J Biomed Mater Res A, 2004. **68**(2): p. 235-43.
24. Dodla, M.C. and R.V. Bellamkonda, *Differences between the effect of anisotropic and isotropic laminin and nerve growth factor presenting scaffolds on nerve regeneration across long peripheral nerve gaps.* Biomaterials, 2008. **29**(1): p. 33-46.
25. Dodla, M.C. and R.V. Bellamkonda, *Anisotropic scaffolds facilitate enhanced neurite extension in vitro.* J Biomed Mater Res A, 2006. **78**(2): p. 213-21.
26. Monteiro, G.A., A.V. Fernandes, H.G. Sundararaghavan, and D.I. Shreiber, *Positively and negatively modulating cell adhesion to type I collagen via peptide grafting.* (in review).
27. Whitesides, G.M., E. Ostuni, S. Takayama, X. Jiang, and D.E. Ingber, *Soft lithography in biology and biochemistry.* Annu Rev Biomed Eng, 2001. **3**: p. 335-73.
28. Shreiber, D.I., P.A. Enever, and R.T. Tranquillo, *Effects of pdgf-bb on rat dermal fibroblast behavior in mechanically stressed and unstressed collagen and fibrin gels.* Exp Cell Res, 2001. **266**(1): p. 155-66.

29. Tong, Y.W. and M.S. Shoichet, *Enhancing the neuronal interaction on fluoropolymer surfaces with mixed peptides or spacer group linkers.* Biomaterials, 2001. **22**(10): p. 1029-34.

Chapter 5: Discussion and Future Work

In the preceding chapters, we have presented a novel technique to evaluate neurite growth in gradients of mechanical properties and adhesion. In chapter 2, we discuss the use of Genipin, a naturally occurring crosslinker, which has been previously used to crosslink chitosan [1], gelatin [2] and poly(ethylene glycol) hydrogels [3] for crosslinking collagen gels. In addition to crosslinking, it fluoresces as it crosslinks and we have shown that mechanical properties can be evaluated through fluorescence measurements. As explained in chapters 3 and 4, we have developed a system that can be used to create gradients of mechanical properties and adhesion sites in 3D collagen hydrogels. Using our system, we are able to find the optimal mechanical properties and concentration of laminin derived peptides YIGSR and IKVAV for neurite outgrowth using a chick dorsal root ganglion (DRG) model system. In evaluating mechanical gradients we found we are able to not only direct neurite growth but also enhance it over fully crosslinked and no crosslink controls. Growth is optimal in gradients of ~375 Pa to ~60 Pa. In our adhesion gradient studies, we find that migration is enhanced in all peptide-grafted collagen gradient conditions compared to the native collagen controls. In the YIGSR case, we see enhanced growth in all YIGSR-grafted conditions with the most increased growth in the full YIGSR condition (~37 μg peptide/mg) implying the optimal concentration for YIGSR-grafted collagen is ≥ 37 μg peptide/mg collagen. For IKVAV, we see enhanced growth in gradient conditions but stunted growth in the full IKVAV-grafted control, implying IKVAV may be too ‘sticky’ for neurite outgrowth at the highest concentration studied. We found the optimal concentration for IKVAV-grafted collagen to be between 9.25-18.5 μg peptide/mg collagen.

The ultimate cure for spinal cord injury (SCI) will likely involve a combination of many currently researched strategies including cell based therapies, drug delivery therapies and biomaterial therapies. A successful therapy must be able to attract a sufficient number of neurons into the bridge material, direct them across the injury site and influence them to grow out of the bridge material and integrate with neurons on the other side. Currently, the most promising approach to SCI repair has been a cell-based tactic where cells are introduced into the injury site to replace the injured cells in the spinal cord and guide neurons across the injury site. These approaches have included adding neural stem cells [4], olfactory ensheathing cells [5], or a Schwann cell bridge [6] with the intention of enticing injured neurons and providing supporting cells for the remyelination of new neurons that are grown [7]. However, in many cases, these systems have either not attracted a sufficient number of neurons, or not allowed neurons to grow out of the bridge material and into the native tissue. In order to make nerve guidance channels more attractive, gradients of soluble or adhesive factors can be used to direct neurons through the bridge material. This could be done by adding drug delivery vehicles commonly used to deliver uniform, steady concentrations of trophic factors such as nerve growth factor (NGF), [8] to the bridge material with chemical factors that attract neurons and/or supporting cells but this would require the development of a precisely placed, compatible controlled-release technology as a source for the chemical factor. We believe that by incorporating 'permanent' gradients of mechanical properties and adhesion into an implantable biomaterial, we can guide neurons across the injury site.

Durotaxis has been a largely overlooked field in cell migration until recently. Previous work with anisotropic mechanical surfaces has shown that fibroblasts prefer

stiff substrates to soft substrates. Work with neurons and astrocytes grown on discrete samples of stiffness have shown that neurons prefer soft substrates, whereas astrocytes prefer stiff substrates. We have been able to further this work by demonstrating that with a gradient of mechanical properties, we are able to not only direct neurons, but also enhance their growth. This shows the importance of substrate properties on cell growth and migration and has several implications for tissue engineering materials. Current research has overlooked the importance of fabricating biomaterials with mechanical properties optimized for the cell type that will integrate into the implant. Mechanical gradients studied in this thesis can be incorporated into materials currently being studied as nerve guidance conduits as a straightforward way to improve integration of an implant with cells surrounding the injury site.

One drawback with our system for making mechanical gradients is the toxicity of genipin. From our experiments, we found that at high concentrations (> 1mM) genipin is toxic. Using our system, the cell channel from which DRGs grow is exposed to genipin during the crosslinking period and this prevents us from trying higher concentrations of genipin. Therefore the maximum gradients we are able to evaluate are an order of magnitude increase in storage modulus across our gradient length. Though we see a bias in neurite growth, we expect that this can be further optimized if we increase the slope of our gradient. One way we are investigating is to increase the slope of the gradient by decreasing the length of our gradient as we did in adhesion experiments. Another way this could be achieved is by either finding a non-toxic way to crosslink collagen or by preventing our cells from being exposed to genipin by blocking the cell channel from the

genipin solution during crosslinking. Current work in the lab is focused on using a non-toxic photocrosslinker to make mechanical gradients of sharper slopes.

In our adhesion experiments, we find that there is a distinction in the concentrations at which YIGSR and IKVAV are most effective and therefore separating these two components from laminin will lead to better direction and growth of neurons. Previous work by Dodla et al showed laminin can be used to direct neurons both *in vivo* and *in vitro* [9, 10]. Using a rat sciatic nerve model, they found that both laminin and NGF gradients were necessary in order to direct neurons across the gap; they get no regeneration with just one component or if either component is uniform. In all cases, this growth is less then in the nerve graft control. *In vitro* experiments showed that a gradient of laminin can be used to direct neurons, with neurites begin most directed in their 'shallow' gradient case. These studies demonstrate that gradients can be very important for directing neurons after injury. We believe that these results can be further enhanced by deconstructing laminin gradients into YIGSR and IKVAV and incorporating mechanical gradients. When using whole laminin as the gradient component, we expect IKVAV to dominate since IKVAV will prevent neurite extension at high concentrations, making shallow gradient most useful for neurite direction, as was found. These results match well with our results using IKVAV gradients. However, we found that YIGSR is most effective in steep gradients. From our studies we see that a higher concentration of YIGSR and lower concentration of IKVAV will be most effective. In our system we are able to take apart these two peptide regions from whole laminin and look at how to make each component most effective. We are also able to do "competing" gradients or YIGSR and IKVAV in order to better understand their effectiveness in directing neurons.

The next logical step for this work would be to combine the currently used gradients and study what properties would lead to the most direction and enhancement of neurite outgrowth. In our case, we find that a 12 hour, 0-1 mM genipin gradient is the best mechanical gradient condition. For the adhesion gradient we found that YIGSR is most favorable at a steep gradient and IKVAV at a shallow gradient. We can combine these two concentrations into one collagen solution to make an optimized adhesion gradient and overlay this gradient with a durotactic gradient. We expect that this would lead to further direction and enhancement of neurite outgrowth. Any peptide can be conjugated to the collagen backbone and used to make a gradient with the system described in this study. In some cases, collagen may be inherently 'too sticky' for cell migration and it has been demonstrated in our lab that adhesion sites can be masked by conjugating scrambled peptides. The versatility of this system allows for many different gradient conditions to be studied along with chemical gradients to improve growth and direction.

It would seem that once optimal gradients are identified, gradient gels can be used as implant material for nerve regeneration models. However, at this time we are not able to remove gradient gels from their PDMS channels. Gradients gels are very small in size (150 μm x 5mm x 100μm) and even if they can be removed, would have to be scaled up for use as a nerve growth conduit. We are investigating ways to remove our gels from the PDMS channel but often the gels are torn during the removal since they do not preferentially bind to either glass or PDMS. If we can determine a way to remove gradient gels, gels can be stacked to make larger nerve guidance conduit with favorable properties for nerve regeneration. It may be more useful to establish a method for

fabricating large scale gradients for use in implant materials. However, the properties that we learn from these experiments can be very important in order to determine future experiment in directed nerve growth and optimal conditions for neurons. Additionally, due to the micron scale of our experiments, we are able to determine optimal gradient properties in an efficient, cost-effective manner and test a variety of conditions which, once optimized, can be scaled up for implant experiments.

Perhaps the most useful result in the previous chapters is a system for making 3D gradients. 3D environments are important in cellular studies because of their similarity to *in vivo* conditions; cells can be stimulated in all directions instead of just the surface on which they are attached. Most studies of cell migration in gradients have been in 2D systems with chemical factors. Though chemical factors can be useful in directing cells, they are not stable and will be lost once all chemicals have dissipated. Therefore, having permanent biomaterial gradients that are a part of the 3D structure of the biomaterial used will be very valuable. This system is versatile and can be used with an unlimited combination of mechanical, adhesive and chemical gradients including competing gradient conditions.

One of our current limitations is single cell viability in our system which has prevented us from doing experiments with other cell types. When using single cells or dissociated neurons, we remove the cell channel and replace it with a glass slide; however, when we tried this with rat dermal fibroblasts, we found that the cells do not survive. We believe this is caused by a lack of nutrient diffusion and waste exchange and therefore current work explores methods to replace the glass slide with a porous membrane material that will allow access to media. Once we increase our cell survival,

we hope to use this system to study other cell types in gradients of mechanical and adhesive properties including fibroblasts, smooth muscle cells, astrocytes, and embryonic stem cells for various applications including wound healing and directed stem cell differentiation. An ongoing project in the lab is on directed differentiation of embryonic stem cells (ESC) using material properties. Discrete samples of collagen in a range of mechanical and adhesive properties incorporated with ESCs are being evaluated for directed ESC differentiation into neural lineages. A microfluidic approach would be very efficient for this work allowing for a high throughput method to test cell preference for mechanical and adhesive properties of the material. Each experiment can be consolidated into one device and many replicates can be done at one time making experiments quick and cost effective due to the small amount of reagents necessary in microfluidic devices.

Another application for this system would be to specifically pattern stripes of substrates to separate cells such as astrocytes from neurons after injury. During spinal cord injury, due to the body's inflammatory response, a physical barrier, called a glial scar, is created that prevents neurons from crossing the injury site [11]. Reactive astrocytes are the primary component of the glial scar and chief source of inhibition of growing neurons. Although there are many cell types in the injury site, astrocytes are thought to be the most detrimental because they heavily proliferate after injury and are most often encountered by growth cones [12, 13]. We know from previous work that astrocytes prefer much stiffer substrates then neurons [14] and they are attracted to different adhesive proteins such as vitronectin [15] rather then laminin. Interestingly, astrocytes are growth promoting in some cases [16] and have been shown to assist in axonal regeneration during development and in uninjured tissue as seen in the normal

arrangement of astrocytes in the CNS [17]. Using a 'Y-shaped' microfluidic system we are able to make adjacent 3D stripes with different adhesive and mechanical properties. It is therefore possible to pattern a biomaterial with stripes tailored toward astrocytes adjacent to stripes specific for neurons in order to separate astrocytes and neurons after injury, allowing neurons to grow uninhibited.

Microfluidics/BioMEMs techniques have gained popularity in the last several years as a method for studying cell morphology and migration in stable gradient systems and high throughput assays. Most current research in microfluidic gradients are in 2D systems with some macroscale gradient studies done in 3D. Though 2D experiments can be important for as a first step in understanding cellular migration and differentiation, 3D conditions are more physiologically relevant. BioMEMs devices have several advantages including small reagent volumes, making them cost efficient and shorter reaction times, making the time efficient. Using a microfluidic system we are able to spatially pattern mechanical and adhesive properties in 3D for nerve guidance. The outcome of these experiments can lead to the potential use of biomaterial based gradients in addition to currently used techniques for SCI repair. We plan to test cellular migration of various cell types in 3D but the soft lithography/microfluidic techniques described in this thesis can be used for various patterns including gradients, stripes, and cellular islands and are essentially 'limitless'. We expect that future work with these devices will bring about better understanding of cellular preferences and functions in a physiologically relavant state and lead to improved implantable devices for various tissue engineering applications.

References

1. Chen, S.C., et al., *A novel pH-sensitive hydrogel composed of N,O-carboxymethyl chitosan and alginate cross-linked by genipin for protein drug delivery.* J Control Release, 2004. **96**(2): p. 285-300.
2. Liang, H.C., et al., *Genipin-crosslinked gelatin microspheres as a drug carrier for intramuscular administration: in vitro and in vivo studies.* J Biomed Mater Res A, 2003. **65**(2): p. 271-82.
3. Moffat, K.L. and K.G. Marra, *Biodegradable poly(ethylene glycol) hydrogels crosslinked with genipin for tissue engineering applications.* J Biomed Mater Res B Appl Biomater, 2004. **71**(1): p. 181-7.
4. Hasegawa, K., et al., *Embryonic radial glia bridge spinal cord lesions and promote functional recovery following spinal cord injury.* Exp Neurol, 2005. **193**(2): p. 394-410.
5. Santos-Benito, F.F. and A. Ramon-Cueto, *Olfactory ensheathing glia transplantation: a therapy to promote repair in the mammalian central nervous system.* Anat Rec B New Anat, 2003. **271**(1): p. 77-85.
6. Fouad, K., et al., *Combining Schwann cell bridges and olfactory-ensheathing glia grafts with chondroitinase promotes locomotor recovery after complete transection of the spinal cord.* J Neurosci, 2005. **25**(5): p. 1169-78.
7. Bunge, M.B., *Bridging areas of injury in the spinal cord.* Neuroscientist, 2001. **7**(4): p. 325-39.
8. Piotrowicz, A. and M.S. Shoichet, *Nerve guidance channels as drug delivery vehicles.* Biomaterials, 2006. **27**(9): p. 2018-27.
9. Dodla, M.C. and R.V. Bellamkonda, *Anisotropic scaffolds facilitate enhanced neurite extension in vitro.* J Biomed Mater Res A, 2006. **78**(2): p. 213-21.
10. Dodla, M.C. and R.V. Bellamkonda, *Differences between the effect of anisotropic and isotropic laminin and nerve growth factor presenting scaffolds on nerve regeneration across long peripheral nerve gaps.* Biomaterials, 2008. **29**(1): p. 33-46.
11. Profyris, C., et al., *Degenerative and regenerative mechanisms governing spinal cord injury.* Neurobiol Dis, 2004. **15**(3): p. 415-36.
12. Fawcett, J.W., *Overcoming inhibition in the damaged spinal cord.* J Neurotrauma, 2006. **23**(3-4): p. 371-83.
13. Silver, J. and J.H. Miller, *Regeneration beyond the glial scar.* Nat Rev Neurosci, 2004. **5**(2): p. 146-56.
14. Georges, P.C., et al., *Matrices with compliance comparable to that of brain tissue select neuronal over glial growth in mixed cortical cultures.* Biophys J, 2006. **90**(8): p. 3012-8.
15. Milner, R., et al., *Distinct roles for astrocyte alphavbeta5 and alphavbeta8 integrins in adhesion and migration.* J Cell Sci, 1999. **112 (Pt 23)**: p. 4271-9.
16. Biran, R., M.D. Noble, and P.A. Tresco, *Directed nerve outgrowth is enhanced by engineered glial substrates.* Exp Neurol, 2003. **184**(1): p. 141-52.
17. Davies, S.J., P.M. Field, and G. Raisman, *Regeneration of cut adult axons fails even in the presence of continuous aligned glial pathways.* Exp Neurol, 1996. **142**(2): p. 203-16.

Bibliography

Adams, D. N., E. Y. Kao, et al. (2005). "Growth cones turn and migrate up an immobilized gradient of the laminin IKVAV peptide." J Neurobiol **62**(1): 134-47.

Almog, J., Y. Cohen, et al. (2004). "Genipin--a novel fingerprint reagent with colorimetric and fluorogenic activity." J Forensic Sci **49**(2): 255-7.

Angele, P., J. Abke, et al. (2004). "Influence of different collagen species on physico-chemical properties of crosslinked collagen matrices." Biomaterials **25**(14): 2831-41.

Arora, P. D., N. Narani, et al. (1999). "The compliance of collagen gels regulates transforming growth factor-beta induction of alpha-smooth muscle actin in fibroblasts." Am J Pathol **154**(3): 871-82.

Balgude, A. P., X. Yu, et al. (2001). "Agarose gel stiffness determines rate of DRG neurite extension in 3D cultures." Biomaterials **22**(10): 1077-84.

Behrman, A. L. and S. J. Harkema (2007). "Physical rehabilitation as an agent for recovery after spinal cord injury." Phys Med Rehabil Clin N Am **18**(2): 183-202, v.

Bellamkonda, R., J. P. Ranieri, et al. (1995). "Laminin oligopeptide derivatized agarose gels allow three-dimensional neurite extension in vitro." J Neurosci Res **41**(4): 501-9.

Biran, R., M. D. Noble, et al. (2003). "Directed nerve outgrowth is enhanced by engineered glial substrates." Exp Neurol **184**(1): 141-52.

Blits, B., G. J. Boer, et al. (2002). "Pharmacological, cell, and gene therapy strategies to promote spinal cord regeneration." Cell Transplant **11**(6): 593-613.

Bonner, J. and T. P. O'Connor (2001). "The permissive cue laminin is essential for growth cone turning in vivo." J Neurosci **21**(24): 9782-91.

Borkenhagen, M., J. F. Clemence, et al. (1998). "Three-dimensional extracellular matrix engineering in the nervous system." J Biomed Mater Res **40**(3): 392-400.

Boyden, S. (1962). "The chemotactic effect of mixtures of antibody and antigen on polymorphonuclear leucocytes." J Exp Med **115**: 453-66.

Buettner, H. M. (1994). "Nerve growth dynamics. Quantitative models for nerve development and regeneration." Ann N Y Acad Sci **745**: 210-21.

Bunge, M. B. (2001). "Bridging areas of injury in the spinal cord." Neuroscientist **7**(4): 325-39.

Burdick, J. A., A. Khademhosseini, et al. (2004). "Fabrication of gradient hydrogels using a microfluidics/photopolymerization process." Langmuir **20**(13): 5153-6.

Butler, M. F., Y. F. Ng, et al. (2003). "Mechanism and kinetics of the crosslinking reaction between biopolymers containing primary amine groups and genipin." Journal of Polymer Science Part a-Polymer Chemistry **41**(24): 3941-3953.

Campbell, D. S., A. G. Regan, et al. (2001). "Semaphorin 3A elicits stage-dependent collapse, turning, and branching in Xenopus retinal growth cones." J Neurosci **21**(21): 8538-47.

Cao, X. and M. S. Shoichet (2003). "Investigating the synergistic effect of combined neurotrophic factor concentration gradients to guide axonal growth." Neuroscience **122**(2): 381-9.

Casey, M. L. and P. C. MacDonald (1997). "Lysyl oxidase (ras recision gene) expression in human amnion: ontogeny and cellular localization." J Clin Endocrinol Metab **82**(1): 167-72.

Ceballos, D., X. Navarro, et al. (1999). "Magnetically aligned collagen gel filling a collagen nerve guide improves peripheral nerve regeneration." Exp Neurol **158**(2): 290-300.

Chang, W. H., Y. Chang, et al. (2003). "A genipin-crosslinked gelatin membrane as wound-dressing material: in vitro and in vivo studies." J Biomater Sci Polym Ed **14**(5): 481-95.

Chang, Y., M. H. Lee, et al. (2004). "Acellular bovine pericardia with distinct porous structures fixed with genipin as an extracellular matrix." Tissue Eng **10**(5-6): 881-92.

Chen, S. C., Y. C. Wu, et al. (2004). "A novel pH-sensitive hydrogel composed of N,O-carboxymethyl chitosan and alginate cross-linked by genipin for protein drug delivery." J Control Release **96**(2): 285-300.

Chung, B. G., L. A. Flanagan, et al. (2005). "Human neural stem cell growth and differentiation in a gradient-generating microfluidic device." Lab Chip **5**(4): 401-6.

Corey, J. M., D. Y. Lin, et al. (2007). "Aligned electrospun nanofibers specify the direction of dorsal root ganglia neurite growth." J Biomed Mater Res A **83**(3): 636-45.

Davies, S. J., P. M. Field, et al. (1996). "Regeneration of cut adult axons fails even in the presence of continuous aligned glial pathways." Exp Neurol **142**(2): 203-16.

de Paula, M., G. Goissis, et al. (2005). "Injectable gels of anionic collagen:rhamsan composites for plastic correction: preparation, characterization, and rheological properties." J Biomed Mater Res B Appl Biomater **75**(2): 393-9.

Dertinger, S. K., X. Jiang, et al. (2002). "Gradients of substrate-bound laminin orient axonal specification of neurons." Proc Natl Acad Sci U S A **99**(20): 12542-7.

Dhoot, N. O., C. A. Tobias, et al. (2004). "Peptide-modified alginate surfaces as a growth permissive substrate for neurite outgrowth." J Biomed Mater Res A **71**(2): 191-200.

Dietrich, W. D., K. Chatzipanteli, et al. (2004). "The role of inflammatory processes in the pathophysiology and treatment of brain and spinal cord trauma." Acta Neurochir Suppl **89**: 69-74.

Discher, D. E., P. Janmey, et al. (2005). "Tissue cells feel and respond to the stiffness of their substrate." Science **310**(5751): 1139-43.

Dodla, M. C. and R. V. Bellamkonda (2006). "Anisotropic scaffolds facilitate enhanced neurite extension in vitro." J Biomed Mater Res A **78**(2): 213-21.

Dodla, M. C. and R. V. Bellamkonda (2008). "Differences between the effect of anisotropic and isotropic laminin and nerve growth factor presenting scaffolds on nerve regeneration across long peripheral nerve gaps." Biomaterials **29**(1): 33-46.

Dowell-Mesfin, N. M., M. A. Abdul-Karim, et al. (2004). "Topographically modified surfaces affect orientation and growth of hippocampal neurons." J Neural Eng **1**(2): 78-90.

Drew, B. and C. Leeuwenburgh (2002). "Aging and the role of reactive nitrogen species." Ann N Y Acad Sci **959**: 66-81.

Duan, X., C. McLaughlin, et al. (2007). "Biofunctionalization of collagen for improved biological response: scaffolds for corneal tissue engineering." Biomaterials **28**(1): 78-88.

Dubey, N., P. C. Letourneau, et al. (1999). "Guided neurite elongation and schwann cell invasion into magnetically aligned collagen in simulated peripheral nerve regeneration." Exp Neurol **158**(2): 338-50.

Dubey, N., P. C. Letourneau, et al. (2001). "Neuronal contact guidance in magnetically aligned fibrin gels: effect of variation in gel mechano-structural properties." Biomaterials **22**(10): 1065-75.

Edelman, G. M. and F. S. Jones (1998). "Gene regulation of cell adhesion: a key step in neural morphogenesis." Brain Res Brain Res Rev **26**(2-3): 337-52.

Elkin, B. S., E. U. Azeloglu, et al. (2007). "Mechanical heterogeneity of the rat hippocampus measured by atomic force microscope indentation." J Neurotrauma **24**(5): 812-22.

Enever, P. A., D. I. Shreiber, et al. (2002). "A novel implantable collagen gel assay for fibroblast traction and proliferation during wound healing." J Surg Res **105**(2): 160-72.

Engler, A., L. Bacakova, et al. (2004). "Substrate compliance versus ligand density in cell on gel responses." Biophys J **86**(1 Pt 1): 617-28.

Engler, A. J., M. A. Griffin, et al. (2004). "Myotubes differentiate optimally on substrates with tissue-like stiffness: pathological implications for soft or stiff microenvironments." J Cell Biol **166**(6): 877-87.

Faber-Elman, A., V. Lavie, et al. (1995). "Vitronectin overrides a negative effect of TNF-alpha on astrocyte migration." Faseb J **9**(15): 1605-13.

Fawcett, J. W. (2006). "Overcoming inhibition in the damaged spinal cord." J Neurotrauma **23**(3-4): 371-83.

Fawcett, J. W., R. A. Barker, et al. (1995). "Dopaminergic neuronal survival and the effects of bFGF in explant, three dimensional and monolayer cultures of embryonic rat ventral mesencephalon." Exp Brain Res **106**(2): 275-82.

Flanagan, L. A., Y. E. Ju, et al. (2002). "Neurite branching on deformable substrates." Neuroreport **13**(18): 2411-5.

Forgacs, G., S. A. Newman, et al. (2003). "Assembly of collagen matrices as a phase transition revealed by structural and rheologic studies." Biophys J **84**(2 Pt 1): 1272-80.

Fouad, K., L. Schnell, et al. (2005). "Combining Schwann cell bridges and olfactory-ensheathing glia grafts with chondroitinase promotes locomotor recovery after complete transection of the spinal cord." J Neurosci **25**(5): 1169-78.

Fujikawa, S., Y. Fukui, et al. (1987). "A spontaneous reaction product between genipin and glycine." Tetrahedron Letters **28**(40): 4699-4700.

Gallo, G. and P. C. Letourneau (1999). "Axon guidance: A balance of signals sets axons on the right track." Curr Biol **9**(13): R490-2.

Georges, P. C. and P. A. Janmey (2005). "Cell type-specific response to growth on soft materials." J Appl Physiol **98**(4): 1547-53.

Georges, P. C., W. J. Miller, et al. (2006). "Matrices with compliance comparable to that of brain tissue select neuronal over glial growth in mixed cortical cultures." Biophys J **90**(8): 3012-8.

Ghosh, K., Z. Pan, et al. (2007). "Cell adaptation to a physiologically relevant ECM mimic with different viscoelastic properties." Biomaterials **28**(4): 671-9.
Giannone, G., B. J. Dubin-Thaler, et al. (2004). "Periodic lamellipodial contractions correlate with rearward actin waves." Cell **116**(3): 431-43.
Girton, T. S., T. R. Oegema, et al. (1999). "Exploiting glycation to stiffen and strengthen tissue equivalents for tissue engineering." J Biomed Mater Res **46**(1): 87-92.
Goldner, J. S., J. M. Bruder, et al. (2006). "Neurite bridging across micropatterned grooves." Biomaterials **27**(3): 460-72.
Grados-Munro, E. M. and A. E. Fournier (2003). "Myelin-associated inhibitors of axon regeneration." J Neurosci Res **74**(4): 479-85.
Grimpe, B. and J. Silver (2002). "The extracellular matrix in axon regeneration." Prog Brain Res **137**: 333-49.
Hasegawa, K., Y. W. Chang, et al. (2005). "Embryonic radial glia bridge spinal cord lesions and promote functional recovery following spinal cord injury." Exp Neurol **193**(2): 394-410.
Heller, D. A., V. Garga, et al. (2005). "Patterned networks of mouse hippocampal neurons on peptide-coated gold surfaces." Biomaterials **26**(8): 883-9.
Houle, J. D. and A. Tessler (2003). "Repair of chronic spinal cord injury." Exp Neurol **182**(2): 247-60.
Huang, L. L., H. W. Sung, et al. (1998). "Biocompatibility study of a biological tissue fixed with a naturally occurring crosslinking reagent." J Biomed Mater Res **42**(4): 568-76.
Ito, H., M. Miyazaki, et al. (1998). "Haptotactic migration of pancreatic cancer cells induced by bioactive components in bovine liver extract." J Surg Oncol **68**(3): 153-8.
Itoh, S., I. Yamaguchi, et al. (2003). "Hydroxyapatite-coated tendon chitosan tubes with adsorbed laminin peptides facilitate nerve regeneration in vivo." Brain Res **993**(1-2): 111-23.
Jin, J., M. Song, et al. (2004). "Novel chitosan-based films cross-linked by genipin with improved physical properties." Biomacromolecules **5**(1): 162-8.
Kapur, T. A. and M. S. Shoichet (2004). "Immobilized concentration gradients of nerve growth factor guide neurite outgrowth." J Biomed Mater Res A **68**(2): 235-43.
Knapp, D. M., V. H. Barocas, et al. (1997). "Rheology of reconstituted type 1 collagen gel in confined compression." Journal of Rheology **41**(5): 971-992.
Landis, W. J. and F. H. Silver (2002). "The structure and function of normally mineralizing avian tendons." Comp Biochem Physiol A Mol Integr Physiol **133**(4): 1135-57.
Leach, J. B., X. Q. Brown, et al. (2007). "Neurite outgrowth and branching of PC12 cells on very soft substrates sharply decreases below a threshold of substrate rigidity." J Neural Eng **4**(2): 26-34.
Legg, A. T. and T. P. O'Connor (2003). "Gradients and growth cone guidance of grasshopper neurons." J Histochem Cytochem **51**(4): 445-54.
Letourneau, P. C., M. L. Condic, et al. (1992). "Extracellular matrix and neurite outgrowth." Curr Opin Genet Dev **2**(4): 625-34.

Li Jeon, N., H. Baskaran, et al. (2002). "Neutrophil chemotaxis in linear and complex gradients of interleukin-8 formed in a microfabricated device." Nat Biotechnol **20**(8): 826-30.

Liang, H. C., W. H. Chang, et al. (2003). "Genipin-crosslinked gelatin microspheres as a drug carrier for intramuscular administration: in vitro and in vivo studies." J Biomed Mater Res A **65**(2): 271-82.

Liang, H. C., Y. Chang, et al. (2004). "Effects of crosslinking degree of an acellular biological tissue on its tissue regeneration pattern." Biomaterials **25**(17): 3541-52.

Lin, F., C. M. Nguyen, et al. (2004). "Effective neutrophil chemotaxis is strongly influenced by mean IL-8 concentration." Biochem Biophys Res Commun **319**(2): 576-81.

Liu, B. S., C. H. Yao, et al. (2003). "In vitro evaluation of degradation and cytotoxicity of a novel composite as a bone substitute." J Biomed Mater Res A **67**(4): 1163-9.

Liu, Y. M., C. Jiaa, et al. (1997). "Evaluation of amorphous carbon nitride thin film for magnetic rigid thin film disk by IR spectroscopy." IEEE Transactions on Magnetics **33**(5): 3106-3108.

Lo, C. M., H. B. Wang, et al. (2000). "Cell movement is guided by the rigidity of the substrate." Biophys J **79**(1): 144-52.

Massia, S. P., M. M. Holecko, et al. (2004). "In vitro assessment of bioactive coatings for neural implant applications." J Biomed Mater Res A **68**(1): 177-86.

Mi, F. L. (2005). "Synthesis and characterization of a novel chitosan-gelatin bioconjugate with fluorescence emission." Biomacromolecules **6**(2): 975-87.

Mi, F. L., Y. C. Tan, et al. (2001). "In vitro evaluation of a chitosan membrane cross-linked with genipin." J Biomater Sci Polym Ed **12**(8): 835-50.

Milner, R., X. Huang, et al. (1999). "Distinct roles for astrocyte alphavbeta5 and alphavbeta8 integrins in adhesion and migration." J Cell Sci **112 (Pt 23)**: 4271-9.

Moffat, K. L. and K. G. Marra (2004). "Biodegradable poly(ethylene glycol) hydrogels crosslinked with genipin for tissue engineering applications." J Biomed Mater Res B Appl Biomater **71**(1): 181-7.

Monteiro, G. A., A. V. Fernandes, et al. "Positively and negatively modulating cell adhesion to type I collagen via peptide grafting." (in review).

Nelson, R. D., P. G. Quie, et al. (1975). "Chemotaxis under agarose: a new and simple method for measuring chemotaxis and spontaneous migration of human polymorphonuclear leukocytes and monocytes." J Immunol **115**(6): 1650-6.

Nurminskaya, M. V., B. Recheis, et al. (2002). "Transglutaminase factor XIIIA in the cartilage of developing avian long bones." Dev Dyn **223**(1): 24-32.

Paik, D. C., J. Dillon, et al. (2001). "The nitrite/collagen reaction: non-enzymatic nitration as a model system for age-related damage." Connect Tissue Res **42**(2): 111-22.

Palecek, S. P., J. C. Loftus, et al. (1997). "Integrin-ligand binding properties govern cell migration speed through cell-substratum adhesiveness." Nature **385**(6616): 537-40.

Park, E., A. A. Velumian, et al. (2004). "The role of excitotoxicity in secondary mechanisms of spinal cord injury: a review with an emphasis on the implications for white matter degeneration." J Neurotrauma **21**(6): 754-74.

Pedersen, J. A. and M. A. Swartz (2005). "Mechanobiology in the third dimension." Ann Biomed Eng **33**(11): 1469-90.

Pelham, R. J., Jr. and Y. L. Wang (1998). "Cell locomotion and focal adhesions are regulated by the mechanical properties of the substrate." Biol Bull **194**(3): 348-9; discussion 349-50.

Peyton, S. R. and A. J. Putnam (2005). "Extracellular matrix rigidity governs smooth muscle cell motility in a biphasic fashion." J Cell Physiol **204**(1): 198-209.

Piacentini, M., C. Rodolfo, et al. (2000). ""Tissue" transglutaminase in animal development." Int J Dev Biol **44**(6): 655-62.

Piotrowicz, A. and M. S. Shoichet (2006). "Nerve guidance channels as drug delivery vehicles." Biomaterials **27**(9): 2018-27.

Profyris, C., S. S. Cheema, et al. (2004). "Degenerative and regenerative mechanisms governing spinal cord injury." Neurobiol Dis **15**(3): 415-36.

Quaglino, D., C. Fornieri, et al. (1993). "Extracellular matrix modifications in rat tissues of different ages. Correlations between elastin and collagen type I mRNA expression and lysyl-oxidase activity." Matrix **13**(6): 481-90.

Ranieri, J. P., R. Bellamkonda, et al. (1994). "Spatial control of neuronal cell attachment and differentiation on covalently patterned laminin oligopeptide substrates." Int J Dev Neurosci **12**(8): 725-35.

Ranieri, J. P., R. Bellamkonda, et al. (1995). "Neuronal cell attachment to fluorinated ethylene propylene films with covalently immobilized laminin oligopeptides YIGSR and IKVAV. II." J Biomed Mater Res **29**(6): 779-85.

Ranucci, C. S., A. Kumar, et al. (2000). "Control of hepatocyte function on collagen foams: sizing matrix pores toward selective induction of 2-D and 3-D cellular morphogenesis." Biomaterials **21**(8): 783-93.

Reinhart-King, C. A., M. Dembo, et al. (2005). "The dynamics and mechanics of endothelial cell spreading." Biophys J **89**(1): 676-89.

Richardson, P. M., U. M. McGuinness, et al. (1980). "Axons from CNS neurons regenerate into PNS grafts." Nature **284**(5753): 264-5.

Rosner, B. I., R. A. Siegel, et al. (2003). "Rational design of contact guiding, neurotrophic matrices for peripheral nerve regeneration." Ann Biomed Eng **31**(11): 1383-401.

Saadi, W., S. W. Rhee, et al. (2007). "Generation of stable concentration gradients in 2D and 3D environments using a microfluidic ladder chamber." Biomed Microdevices **9**(5): 627-35.

Saez, A., M. Ghibaudo, et al. (2007). "Rigidity-driven growth and migration of epithelial cells on microstructured anisotropic substrates." Proc Natl Acad Sci U S A **104**(20): 8281-6.

Saneinejad, S. and M. S. Shoichet (1998). "Patterned glass surfaces direct cell adhesion and process outgrowth of primary neurons of the central nervous system." J Biomed Mater Res **42**(1): 13-9.

Santos-Benito, F. F. and A. Ramon-Cueto (2003). "Olfactory ensheathing glia transplantation: a therapy to promote repair in the mammalian central nervous system." Anat Rec B New Anat **271**(1): 77-85.

Schense, J. C. and J. A. Hubbell (2000). "Three-dimensional migration of neurites is mediated by adhesion site density and affinity." J Biol Chem **275**(10): 6813-8.

Schmalenberg, K. E. and K. E. Uhrich (2005). "Micropatterned polymer substrates control alignment of proliferating Schwann cells to direct neuronal regeneration." Biomaterials **26**(12): 1423-30.

Schmidt, C. E., J. Dai, et al. (1995). "Integrin-cytoskeletal interactions in neuronal growth cones." J Neurosci **15**(5 Pt 1): 3400-7.

Schmidt, C. E. and J. B. Leach (2003). "Neural tissue engineering: strategies for repair and regeneration." Annu Rev Biomed Eng **5**: 293-347.

Semler, E. J., C. S. Ranucci, et al. (2000). "Mechanochemical manipulation of hepatocyte aggregation can selectively induce or repress liver-specific function." Biotechnol Bioeng **69**(4): 359-69.

Shreiber, D. I., P. A. Enever, et al. (2001). "Effects of pdgf-bb on rat dermal fibroblast behavior in mechanically stressed and unstressed collagen and fibrin gels." Exp Cell Res **266**(1): 155-66.

Silver, F. H., D. DeVore, et al. (2003). "Invited Review: Role of mechanophysiology in aging of ECM: effects of changes in mechanochemical transduction." J Appl Physiol **95**(5): 2134-41.

Silver, F. H., I. Horvath, et al. (2002). "Mechanical implications of the domain structure of fiber-forming collagens: comparison of the molecular and fibrillar flexibilities of the alpha1-chains found in types I-III collagen." J Theor Biol **216**(2): 243-54.

Silver, F. H., P. B. Snowhill, et al. (2003). "Mechanical behavior of vessel wall: a comparative study of aorta, vena cava, and carotid artery." Ann Biomed Eng **31**(7): 793-803.

Silver, J. and J. H. Miller (2004). "Regeneration beyond the glial scar." Nat Rev Neurosci **5**(2): 146-56.

Socrates, G. (1994). "Infrared Characteristic Group Frequencies - Tables and Charts." New York: John Wiley & Sons;.

Stamenovic, D., S. M. Mijailovich, et al. (2003). "Experimental tests of the cellular tensegrity hypothesis." Biorheology **40**(1-3): 221-5.

Stoltz, J. F. (2004). "Adaptation concept, tissue remodeling, mechanobiology and tissue engineering: a survey." Biorheology **41**(3-4): 155-6.

Sundararaghavan, H. G., G. A. Monteiro, et al. (2008). "Genipin-induced changes in collagen gels: Correlation of mechanical properties to fluorescence." J Biomed Mater Res A.

Sung, H. W., W. H. Chang, et al. (2003). "Crosslinking of biological tissues using genipin and/or carbodiimide." J Biomed Mater Res A **64**(3): 427-38.

Sung, H. W., Y. Chang, et al. (1999). "Mechanical properties of a porcine aortic valve fixed with a naturally occurring crosslinking agent." Biomaterials **20**(19): 1759-72.

Sung, H. W., R. N. Huang, et al. (1998). "Feasibility study of a natural crosslinking reagent for biological tissue fixation." J Biomed Mater Res **42**(4): 560-7.

Sung, H. W., I. L. Liang, et al. (2001). "Stability of a biological tissue fixed with a naturally occurring crosslinking agent (genipin)." J Biomed Mater Res **55**(4): 538-46.

Takami, M. and Y. Suzuki (1994). "Hydrophobic blue pigment formation from phosphatidylgenipin." J Nutr Sci Vitaminol (Tokyo) **40**(5): 505-9.

Tan, J. L., J. Tien, et al. (2003). "Cells lying on a bed of microneedles: an approach to isolate mechanical force." Proc Natl Acad Sci U S A **100**(4): 1484-9.

Tashiro, K., G. C. Sephel, et al. (1989). "A synthetic peptide containing the IKVAV sequence from the A chain of laminin mediates cell attachment, migration, and neurite outgrowth." J Biol Chem **264**(27): 16174-82.

Thompson, D. M. and H. M. Buettner (2006). "Neurite outgrowth is directed by schwann cell alignment in the absence of other guidance cues." Ann Biomed Eng **34**(1): 161-8.

Tolic-Norrelykke, I. M., J. P. Butler, et al. (2002). "Spatial and temporal traction response in human airway smooth muscle cells." Am J Physiol Cell Physiol **283**(4): C1254-66.

Tong, Y. W. and M. S. Shoichet (2001). "Enhancing the neuronal interaction on fluoropolymer surfaces with mixed peptides or spacer group linkers." Biomaterials **22**(10): 1029-34.

Touyama, R., Y. Takeda, et al. (1994). "Studies on the Blue Pigments Produced from Genipin and Methylamine .1. Structures of the Brownish-Red Pigments, Intermediates Leading to the Blue Pigments." Chemical & Pharmaceutical Bulletin **42**(3): 668-673.

Tucker, R. P. (2001). "Abnormal neural crest cell migration after the in vivo knockdown of tenascin-C expression with morpholino antisense oligonucleotides." Dev Dyn **222**(1): 115-9.

Vera-Portocarrero, L. P., C. D. Mills, et al. (2002). "Rapid changes in expression of glutamate transporters after spinal cord injury." Brain Res **927**(1): 104-10.

Wang, S. J., W. Saadi, et al. (2004). "Differential effects of EGF gradient profiles on MDA-MB-231 breast cancer cell chemotaxis." Exp Cell Res **300**(1): 180-9.

Wang, X., X. Li, et al. (2005). "Microtensile testing of collagen fibril for cardiovascular tissue engineering." J Biomed Mater Res A **74**(2): 263-8.

Webb, K., E. Budko, et al. (2001). "Substrate-bound human recombinant L1 selectively promotes neuronal attachment and outgrowth in the presence of astrocytes and fibroblasts." Biomaterials **22**(10): 1017-28.

Whitesides, G. M., E. Ostuni, et al. (2001). "Soft lithography in biology and biochemistry." Annu Rev Biomed Eng **3**: 335-73.

Willerth, S. M. and S. E. Sakiyama-Elbert (2007). "Approaches to neural tissue engineering using scaffolds for drug delivery." Adv Drug Deliv Rev **59**(4-5): 325-38.

Willerth, S. M. and S. E. Sakiyama-Elbert (2008). "Cell therapy for spinal cord regeneration." Adv Drug Deliv Rev **60**(2): 263-76.

Willits, R. K. and S. L. Skornia (2004). "Effect of collagen gel stiffness on neurite extension." J Biomater Sci Polym Ed **15**(12): 1521-31.

Yerramalli, C. S., A. I. Chou, et al. (2007). "The effect of nucleus pulposus crosslinking and glycosaminoglycan degradation on disc mechanical function." Biomech Model Mechanobiol **6**(1-2): 13-20.

Yu, X., G. P. Dillon, et al. (1999). "A laminin and nerve growth factor-laden three-dimensional scaffold for enhanced neurite extension." Tissue Eng **5**(4): 291-304.

Zicha, D., G. A. Dunn, et al. (1991). "A new direct-viewing chemotaxis chamber." J Cell Sci **99 (Pt 4)**: 769-75.

Curriculum Vita

Education:

Rutgers, The University of New Jersey, New Brunswick, NJ August 2008

Ph.D. Biomedical Engineering

Thesis topic: "Modification of collagen scaffold mechanical and adhesive properties for directed and enhanced spinal cord regeneration" (David Shreiber, Advisor (Biomedical Engineering); Bonnie Firestein Co- Advisor (Neuroscience))

The University of Michigan – College of Engineering, Ann Arbor, MI May 2002

B.S.E. Chemical Engineering

Research:

Rutgers, The University of New, New Brunswick, NJ May 2003-Present

Department of Biomedical Engineering

NSF-IGERT Fellow and Graduate Assistant

- Initiated BioMEMs and microfluidic capabilities in laboratory
- Designed and fabricated microfluidic devices used to make gradients in 3D scaffold
- Used finite element modeling for microfluidic network design
- Established research group's capabilities in primary neural cell culture
- Developed methods for culturing cells and immunostaining within microfluidic devices
- Formed new, cross-disciplinary collaborations among groups in Biomedical Engineering, Cell biology and Neuroscience

Ecole Polytechnique Federal De Lausanne, Lausanne, Switzerland June 2006–August 2006

Summer Fellow

- Internship in Laboratory of Regenerative Medicine and Pharmacobiology (Laboratory of Dr. Jeffrey Hubbell)
- Synthesized PEG based polymer biomaterials for use in drug delivery
- Encapsulated iron particles in polymer micelles as potential substrate imaging agent

Peer-reviewed journal articles:

Sundararaghavan, H.G., G.A. Monteiro, N.A. Lapin, Y.J. Chabal, J.R. Miksan, and D.I. Shreiber. *Genipin-induced changes in collagen gels: Correlation of mechanical properties to fluorescence.* J Biomed Mater Res A, 2008.

Sundararaghavan, H.G., G.A. Monteiro, B.L. Firestein, D.I. Shreiber. *Neurite growth in 3D collagen gels with gradients of mechanical properties.* (submitted to Biotechnology and Bioengineering)

Monteiro, G.M., **H.G. Sundararaghavan**, A.V. Fernandes and D.I. Shreiber *Enhancing cell migration in collagen gels by modulating collagen adhesivity.* Tissue Eng. (in Preparation)

Sundararaghavan, H.G., G.A. Monteiro, and D.I. Shreiber. *Directed neurite growth in 3D Gradients of IKVAV and YIGSR grafted collagen gels.* (in Preparation)

Sundararaghavan, H.G., S. Haren, M. Samaan, A. Fox, J. Zahn and D.I. Shreiber, *Microdialysis membrane-sealed microfluidic networks for preserving cell viability in static culture.* (in Preparation)